

## BONDING PROPERTIES OF CFRP STRAND SHEET AND CFRP PLATE ON RC BEAM

リファドリ, バハスアン

<https://doi.org/10.15017/1806976>

---

出版情報：九州大学, 2016, 博士（工学）, 課程博士  
バージョン：  
権利関係：全文ファイル公表済

**BONDING PROPERTIES OF CFRP STRAND  
SHEET AND CFRP PLATE ON RC BEAM**

**CFRP スtrandシートおよび CFRP プレート  
の RC はりに対する付着特性**

**RIFADLI BAHSUAN**

# **BONDING PROPERTIES OF CFRP STRAND SHEET AND CFRP PLATE ON RC BEAM**



A DISSERTATION

Submitted to  
Kyushu University  
in partial fulfillment of the requirements  
for degree of

**Doctor of Engineering**

by

**RIFADLI BAHSUAN**

Civil Engineering Department  
Graduate School of Engineering  
Kyushu University, Japan  
November, 2016

*Bismillahirrahmanirrahim*  
*special dedicated to*  
*My father Alm. Ayahanda Ibrahim Bahsuan*  
*My mother Ibunda Hj. Hindun Bahsuan*  
*My mother in-law Hj. Habibah Dai*  
*Nita Suleman, ST, MT*  
*Marha Adlita Qayla Bahsuan*  
*Marha Rifani Fayza Bahsuan*  
*Marha Narini Zayra Bahsuan*  
*My brothers and sisters*  
*for*  
*the prayers, patience, support, sacrifice, tears and laughter*

## ACKNOWLEDGMENTS

*Alhamdulillahirobbil'alamin.....!*

I take this opportunity to express my most sincere gratitude and special appreciation from the bottom of my heart to my supervisor Professor Shinichi HINO, who has given invaluable guidance, knowledge and most importantly his support and motivation during my graduate study at Kyushu University. Without his time, patient advice and constant encouragement this dissertation would not have been possible. Thank you for his kindness and for accepting me to study in Structural Design Lab.

I would also like to express my special thanks to my Advisory Committee Professor Yoshimi SONODA and Professor Hidenori HAMADA for their valuable suggestion and insightful comments to improve this dissertation quality.

I would like to acknowledge to the Ministry of Research, Technology and Higher Education (Ristek dan Dikti) for a full doctoral scholarship (BLN-Dikti scholarship) and Universitas Negeri Gorontalo (State University of Gorontalo) for giving me the opportunity to continue my doctoral study.

I am deeply indebted to Mr. Shigetada HATAKEYAMA, Mrs. Reiko KATO and Mr. Hiroyuki SHIBATA for their tremendous help, attention, guidance and never ending support as long as I carried out study and research.

I also wish to thank to the Nippon Steel and Sumikin Materials Co. Ltd and SNC Co. Ltd. for their support by providing material in this research. My sincere appreciation is also extended to Dr. Kenji TANIGUCHI and Dr. Atsuya KOMORI from Nippon Steel and Sumikin Materials Co. Ltd, Dr. Kohei YAMAGUCHI from JBEC and Mr. Kazuaki AKAZAWA from SNC Co. Ltd for their discussion and invaluable input for my publications and this dissertation.

I am very grateful for all the Bridge Laboratory members, present and past members, for helping me during study and experiment. Especially for Mr Takahiro OHGI, thank you for working together during specimen preparation and testing. Last but not least, for all Indonesian friends thank to three very memorable year.

Thank you very much everyone.....!

*Fukuoka, November 2016*

*Rifadli Bahsuan*

## ABSTRACT

A lot of reinforced concrete (RC) structures have been required to retrofit or strengthen due to decrease of their loading capacities caused by age, environmental influences, poor design and construction, lack of maintenance, and damage caused by heavy earthquake and so on. Carbon fiber reinforced polymer (CFRP) has been successfully used to retrofitting these RC structures because of its excellent properties. However, there are a number of problems to be solved related to the external composite CFRP-concrete performance.

Therefore, in order to establish more reliable and rational design, the bonding properties of CFRP-concrete interface must be an important task to be evaluated. Related to the bonding properties in this external composite system, some issues are addressed in this study. In this study, both CFRP-concrete bonding test and RC beam test as well as a finite element analysis were carried out to examine the CFRP-concrete bonding properties and the strengthening effect for RC beam. The used types of CFRP are CFRP strand sheet and both high tension and high modulus types of CFRP plate. Also, the variation of adhesive types are epoxy, MMA (methyl methacrylate) and PCM (polymer cement mortar), as well as polyurea soft layer to improve the CFRP plate-concrete bonding behavior. To discuss this matter, this dissertation is divided into six chapters.

**Chapter 1** presents the research background of this study, problem statement, research objective, contribution of research, limitation and the dissertation arrangement as outline of the research.

**Chapter 2** presents the information about FRP, adhesive and the application of CFRP strengthening method to RC members. In other parts of this chapter previous studies related to the FRP/CFRP strengthening methods were described. Some factors, theory of bonding properties and bonding characteristics were also briefly presented. Finally, the issues addressed in this study were also discussed in this chapter.

**Chapter 3** presents the application of CFRP strand sheet strengthening method on RC beams. Three kinds of adhesive materials were used in this experiment. They were epoxy, MMA

(methyl methacrylate) and PCM (polymer cement mortar). Seven RC beams comprising one non-retrofitted beam (specimen N) as a control beam and six retrofitted beams for three kinds of adhesive materials with one layer and two layers of CFRP strand sheet were tested in this study. The dimensions of RC beams specimens were 200mm x 300mm x 2200mm. FEM analysis was performed to confirm the experimental results. The results indicated that all the strengthening with CFRP strand sheet could improve the capacity of RC beam. The failure mode of specimen with CFRP strand sheet strengthening method was found to be highly dependent on the type of adhesive. Epoxy resin, MMA resin and PCM could be recommended as adhesive material to the CFRP strand sheet strengthening method. However, some experimental and FEM analytical results did not show a fairly good agreement. It was found that the bond slip interface model could be required to be corrected.

**Chapter 4** discusses the investigation of bonding behavior of CFRP strand sheet and concrete. Both experiment and analysis were conducted to evaluate the performance of CFRP strand sheet and concrete strengthening method. The bonding test was done based on JSCE-E543-2007. In this test, two kinds of adhesive materials such as MMA and PCM were used. The variation of layers of CFRP strand sheet were one, two and three layers. Three specimens were prepared for each type. The results showed that the typical failure of bonding test was the interfacial failure occurred on only one side of the prism. From the results, MMA specimens showed the average maximum load of two and three layers increased by 17.5% and 30.8%, respectively, compared with the single layer. Meanwhile, PCM specimens showed that there was an increase in average maximum load of 30.7% for two layers compared with the single layer. It can be proved that MMA and PCM were fairly good adhesive material for CFRP strand sheet strengthening method. At the end of this chapter, applications of the bond slip used to the RC beams analysis were tested previously.

**Chapter 5** investigates the bonding properties of the CFRP plate and concrete. This chapter also describes the effect of the bonding behavior on polyurea soft layer for both high tension and high modulus types of CFRP plates. The specimen had a total bonding length of 590mm on both sides in this test. The test results showed that specimens with soft layer had more different failure mode than specimen without soft layer. The polyurea soft layer could enhance significantly the performance of bonding behavior on the high tensile type of CFRP

plate. However, polyurea soft layer did not give sufficient effect on the high modulus type. This was because high modulus type without soft layer specimens had longer effective bond length than used bonding length of specimen itself. At the end of this chapter, a simple equation has been proposed for the rational design.

**Chapter 6** offers conclusion and recommendations for future research.



# TABLE OF CONTENTS

DEDICATION	i
ACKNOWLEDGMENTS	ii
ABSTRACT	iii
TABLE OF CONTENT	vi
LIST OF TABLES	x
LIST OF FIGURES	xi
LIST OF PHOTOS	xiv
CHAPTER	
<b>1. INTRODUCTION</b>	
1.1 Research background	I-1
1.2 Research objective	I-3
1.3 Dissertation outline	I-3
REFERENCES	I-6
<b>2. LITERATURE REVIEW</b>	
2.1 Introduction	II-1
2.2 Fiber reinforced polymer (FRP)	II-1
2.2.1 Codes for FRP test method	II-3
2.2.2 Type of FRP for construction	II-5
2.2.2.1 FRP sheet	II-5
2.2.2.2 FRP grid	II-6
2.2.2.3 FRP strand sheet	II-8
2.2.2.4 CFRP plate	II-8
2.3 Adhesives	II-9
2.4 Strengthening method to RC members	II-12
2.5 Bonding test	II-15
2.5.1 Bond strength	II-16
2.5.2 Failure mode	II-17
2.5.3 Effective bond length	II-18
2.5.4 Local bond-stress slip relationship	II-20
2.5.5 Interfacial fracture energy ( $G_f$ )	II-23
2.6 Related research	II-23
2.7 Issues addressed in this study	II-29
REFERENCES	II-31

### **3. FLEXURAL STRENGTHENING EFFECT OF CFRP STRAND SHEETS ON RC BEAMS**

3.1 Introduction	III-1
3.2 Research objective	III-2
3.3 Materials properties	III-2
3.4 The use of adhesive for strengthened RC beams	III-3
3.5 Test set up	III-5
3.6 Test results and discussion	III-6
3.6.1 Failure mode	III-6
3.6.2 Loading stages	III-11
3.6.3 Load and displacement	III-12
3.6.4 Load and strain of CFRP strand sheet	III-13
3.7 Finite Element Analysis for Flexural Strengthening of CFRP Strand Sheets on RC Beams	III-15
3.7.1 Idealization of FEM analysis	III-15
3.7.2 FEM results and verification	III-16
3.7.2.1 Crack pattern	III-16
3.7.2.2 Load and displacement	III-18
3.7.2.3 Load and strain of CFRP strand sheet	III-18
3.8 Conclusive remarks	III-19
REFERENCES	III-20

### **4. BONDING BEHAVIOR OF CFRP STRAND SHEET AND CONCRETE WITH MMA AND PCM ADHESIVE**

4.1 Introduction	IV-1
4.2 Research objective	IV-3
4.3 Test set up	IV-3
4.4 The use of adhesive and specimen manufacturing process	IV-6
4.5 Test result and discussion	IV-9
4.5.1 Failure mode	IV-9
4.5.2 Maximum load, bond strength and interfacial fracture energy	IV-10
4.5.3 Strain distribution of CFRP strand sheet	IV-13
4.5.4 Effective bond length	IV-16
4.5.5 Local bond stress-slip relationship	IV-18
4.5.6 Load-total slip relationship	IV-21
4.6 Finite element analysis of bonding behavior between CFRP strand sheet and concrete	IV-22

4.7 Verification of finite element model with experimental results	IV-24
4.7.1 Strain distribution	IV-24
4.7.2 Maximum load	IV-25
4.7.3 Effective bond length	IV-25
4.8 Verification of CFRP strand sheet strengthened RC beams with the local bond stress slip relationship	IV-27
4.9 Conclusive remarks	IV-29
REFERENCES	IV-30

## **5. BONDING BEHAVIOR OF CFRP PLATE AND CONCRETE WITH AND WITHOUT POLYUREA SOFT LAYER**

5.1 Introduction	V-1
5.2 Research objective	V-2
5.3 Material properties	V-3
5.4 Specimen preparation	V-5
5.4.1 With soft layer specimen	V-5
5.4.2 Without soft layer specimen	V-6
5.5 Test program	V-7
5.6 Result and discussion	V-10
5.6.1 Failure mode	V-10
5.6.2 Strain distribution	V-11
5.6.2.1 <i>CFRP plate high tension type</i>	V-11
5.6.2.2 <i>CFRP plate high modulus type</i>	V-13
5.6.2.3 <i>Strain distribution at the maximum load</i>	V-14
5.6.3 Maximum load and CFRP plate stiffness relationship	V-15
5.6.4 Bond stress-slip relationship	V-16
5.6.5 Interfacial fracture energy ( $G_f$ )	V-19
5.6.6 Effect of polyurea soft layer for experiment result	V-21
5.7 Finite element analysis of CFRP plate and concrete bonding behavior	V-22
5.7.1 Idealization	V-22
5.7.2 Modelling of material and interface	V-23
5.7.3 Verification of FEM analysis with experiment results	V-23
5.7.3.1 <i>Maximum load</i>	V-24
5.7.3.2 <i>Strain Distribution</i>	V-24
5.7.3.3 <i>Total load and total slip at the loaded-end relationship</i>	V-25
5.7.3.4 <i>Local bond stress distribution</i>	V-26
5.7.4 The simulation of the FEM model	V-27

5.7.4.1 <i>Specimen with polyurea soft layer</i>	V-27
5.7.4.2 <i>Specimen without polyurea soft layer</i>	V-36
5.8 Conclusive remarks	V-39
REFERENCES	V-41
<b>6. CONCLUSIONS AND RECOMMENDATION</b>	
6.1 Conclusion	VI-1
6.2 Recommendation	VI-2

## LIST OF TABLES

<b>Table No</b>		<b>Page</b>
Table 2.1	Typical FRP properties	II-2
Table 3.1	Mechanical properties of adhesive (MPa)	III-3
Table 3.2	Mechanical properties of CFRP strand sheet	III-3
Table 3.3	Mechanical properties of steel reinforcement (MPa)	III-3
Table 3.4	Experiment load results (MPa)	III-11
Table 4.1	Mechanical properties of CFRP strand sheet	IV-6
Table 4.2	Mechanical properties of adhesive (MPa)	IV-6
Table 4.3	Results of bond test	IV-10
Table 4.4	The Popovics's equation parameter	IV-20
Table 4.5	Experimental and FEM load results	IV-27
Table 5.1	CFRP Plate material properties	V-4
Table 5.2	Concrete material properties (MPa)	V-4
Table 5.3	Material property of adhesive and soft layer (MPa)	V-5
Table 5.4	Specimen identity and experimental results	V-9
Table 5.5(a)	The parameter and results of laboratory specimen (experimental and FEM analysis) for with soft layer specimen	V-29
Table 5.5(b)	The parameter and results of simulation specimens (FEM analysis) for with soft layer specimen	V-30
Table 5.6(a)	The parameter and results of laboratory specimen (experimental and FEM analysis) for without soft layer specimen	V-34
Table 5.6(b)	The parameter and results of simulation specimens (FEM analysis) for without soft layer specimen	V-35

## LIST OF FIGURES

<b>Figure No</b>		<b>Page</b>
Fig. 1.1	Shipment quantity of carbon fiber per year	I-1
Fig. 1.2	Flowchart of present work	I-5
Fig. 2.1	FRP Grid Typically	II-7
Fig. 2.2	Structure of Grid Crossing	II-7
Fig. 2.3	Bonding test specimen	II-16
Fig. 2.4	Determine point in the strain distribution for effective bond length	II-19
Fig. 2.5	Effective bond length	II-20
Fig. 2.6	Interface behavior of shear specimen	II-21
Fig. 2.7	Typical local bond stress-slip relationship	II-21
Fig. 3.1	Cross section of CFRP strand sheet strengthened RC beams	III-4
Fig. 3.2	RC beams specimen detail (Unit: mm)	III-5
Fig. 3.3	Total load versus mid-span deflection	III-13
Fig. 3.4	Total load versus strain of CFRP strand sheet at mid-span	III-14
Fig. 3.5	Schematic of FEM element	III-14
Fig. 3.6	Constitutive law of concrete	III-16
Fig. 3.7	Specimen crack pattern of experimental and FEM analysis results	III-17
Fig. 3.8	Total load–mid-span deflection relationship of experimental and FE analysis	III-18
Fig. 3.9	Total load–mid-span strain of CFRP strand sheet	III-19
Fig. 4.1	Stress-strain relationship of reinforcing materials	IV-2
Fig. 4.2	Geometry for bonding test specimen	IV-4
Fig. 4.3	Cross-section of material CFRP strand sheet	IV-7
Fig. 4.4	Maximum load results of MMA specimen	IV-12
Fig. 4.5	Maximum load results of PCM specimen	IV-12
Fig. 4.6	Average results of average bond stress	IV-13
Fig. 4.7	Average results of interfacial fracture energy	IV-13
Fig. 4.8	MMA 1 layer strain distribution of FE analysis and experimental results	

		IV-14
Fig. 4.9	MMA 2 layers strain distribution of FE analysis and experimental results	IV-14
Fig. 4.10	MMA 3 layers strain distribution of FE analysis and experimental results	IV-15
Fig. 4.11	PCM 1 layer strain distribution of FE analysis and experimental results	IV-15
Fig. 4.12	PCM 2 layer strain distribution of FE analysis and experimental results	IV-15
Fig. 4.13	Point used to determine the effective bond length	IV-17
Fig. 4.14	Effective bond length (mm)	IV-17
Fig. 4.15	Local bond stress-slip relationship by Popovics's equation for one layer MMA	IV-19
Fig. 4.16	Load-total slip relationship for MMA specimen	IV-20
Fig. 4.17	Load-total slip relationship for PCM specimen	IV-21
Fig. 4.18	Idealization and typical finite element me	IV-23
Fig. 4.19	Constitutive law of concrete	IV-24
Fig. 4.20	Comparison of the maximum load by FE model and experimental results	IV-26
Fig. 4.21	Comparison of the effective bond length by FE model and experimental results	IV-26
Fig. 4.22	Load and midspan deflection of specimen MMA1	IV-28
Fig. 4.23	Total load and CFRP strand sheet strain at midspan of specimen MMA1	IV-28
Fig. 5.1	Detail of specimen bonding method	V-8
Fig. 5.2	Specimen detail	V-8
Fig. 5.3	Cross section A-A	V-8
Fig. 5.4	Strain distribution of CFRP plate high modulus type	V-12
Fig. 5.5	Strain distribution of CFRP plate high modulus type	V-13
Fig. 5.6	Strain distribution at maximum load	V-15
Fig. 5.7	Maximum load –CFRP plate stiffness relationship	V-16
Fig. 5.8	Local bond stress-slip relationship	V-19

Fig. 5.9	Interfacial fracture energy-CFRP plate relationship of experimental results	V-20
Fig. 5.10	Effect of soft layer for each of CFRP plate stiffness	V-21
Fig. 5.11	Idealization of the finite element analysis	V-22
Fig. 5.12	Constitutive law of concrete	V-23
Fig. 5.13	Comparison of the maximum load by FE model and experimental results	V-24
Fig. 5.14	Comparison between experiment and FEM analysis strain distribution	V-25
Fig. 5.15	Comparison between experimental and FEM load-total slip	V-25
Fig. 5.16	Comparison between experimental and FEM internal stress distribution at the maximum load	V-26
Fig. 5.17	Effective bond length (EBL)	V-28
Fig. 5.18	$l_e \text{ plate}$ vs $E_p t_p$	V-31
Fig. 5.19	$P_{max}$ vs $E_p t_p$	V-32
Fig. 5.20	$\alpha$ vs $l_b/l_e \text{ plate}$	V-33
Fig. 5.21	Calculated prediction vs Experimental and FEM analysis results for specimen with soft layer	V-33
Fig. 5.22	$l_e \text{ plate}$ vs $E_p t_p$	V-36
Fig. 5.23	$P_{max}$ vs $E_p t_p$	V-37
Fig. 5.24	$\alpha$ vs $l_b/l_e \text{ plate}$	V-38
Fig. 5.25	Calculated prediction vs Experimental and FEM analysis results for specimen without soft layer	V-39



## LIST OF PHOTOS

<b>Photo No</b>		<b>Page</b>
Photo 2.1	CPRP Sheets	II-5
Photo 2.2	CFRP grid	II-7
Photo 2.3	CFRP strand sheet	II-8
Photo 2.4	Shear strengthening by CFRP grid and PCM	II-13
Photo 2.5	Seismic retrofitting of high piers	II-14
Photo 2.6	Rapid retrofitting method for Okayama Bridge	II-14
Photo 3.1	RC beam test	III-6
Photo 3.2	Crack pattern and failure condition of specimens	III-10
Photo 3.3	Failure detail of specimen PCM2	III-11
Photo 3.4	Photograph of crack pattern specimen	III-17
Photo 4.1	CFRP strand sheet	IV-2
Photo 4.2	Specimens for bonding test	IV-4
Photo 4.3	Specimen during bonding test set	IV-5
Photo 4.4	The manufacturing process of MMA specimen	IV-8
Photo 4.5	The manufacturing process of PCM specimen	IV-8
Photo 4.6	Typical failure model of MMA specimen	IV-9
Photo 4.7	Typical failure model of PCM specimen	IV-10
Photo 5.1	CFRP plate	V-3
Photo 5.2	Primer and polyurea putty	V-4
Photo 5.3	Primer and epoxy putty	V-4
Photo 5.4	The making process of specimen with soft layer	V-6
Photo 5.5	The making process of specimen without soft layer	V-7
Photo 5.6	Experiment setting up	V-8
Photo 5.7	Failure types of specimen	V-11

# CHAPTER 1

## INTRODUCTION

---

### 1.1 Research background

Rapid development in construction world has produced various innovations in the reinforced concrete science. The most important things in the use of reinforced concrete are change in their use, new design standards, deterioration due to corrosion in the steel caused by exposure to an aggressive environment and accident events such as earthquakes. In such circumstances there are two possible solutions: replacement or strengthening/retrofitting. Overall structure replacement might have determinate compensation such as high cost, a lot of labor and environmental impact. Therefore strengthening/retrofitting become the wisest solutions to solve that problem <sup>(1.1)</sup>.

Since the late 80's the application of fiber reinforced polymer (FRP) reinforcement for concrete has been steadily increasing. Especially after the late 90's the FRP sheet (or continuous fiber sheet) has been applied in many cases for seismic retrofitting, upgrading and durability retrofitting.

Carbon fiber reinforced polymer (CFRP) external bonding, one of the types FRP strengthening method, becomes commonly used for strengthening and retrofitting of both concrete and steel structure. **Fig. 1.1** shows carbon fiber shipping quantity from manufacturer in Japan in periods from 1991 to 2014 in metric tons for all area of application <sup>(1.2)</sup>.

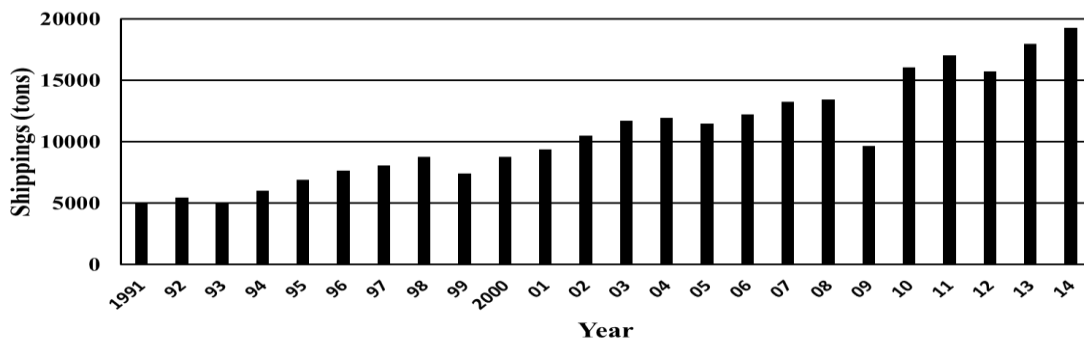


**Fig. 1.1** Shipment quantity of carbon fiber per year <sup>(1.2)</sup>

Many issues related to the structural performances of CFRP strengthened RC elements have been studied. With the development of the technology of upgrading existing concrete structures by using externally bonded, a number of issues related to the structural behavior after upgrading have been studied during the past decade. The mechanism of interface bond between CFRP and concrete adjacent is to be the most interesting to study. The bonding interface is relatively weak in comparison with the neighboring material in the whole of upgrade system<sup>(1,3)</sup>. Previous researcher had tried various ways to understand bonding interface performance and behavior. Numerous research programs have been performed in the last three decades to investigate the CFRP–concrete bonding characteristics such as bond strength and effective bond length etc.

Among the challenges that are still to be taken up in application of CFRP strengthening method for concrete is to improve the performance of the composite CFRP-concrete system, including the function of keeping the integrity and durability of composite system. Therefore, a lot of researches that aims to gain a good understanding on the behavior of the CFRP-concrete bonding characteristics are a prerequisite for achieving more reliable but rational design.

In this study, the experiment was conducted to observe the behavior of CFRP-concrete bonding characteristics by using a variety of adhesive. Two types of CFRP used in this study, they are CFRP strand sheet and CFRP plate consist of high modulus type and high tension type, were examined in this research. As adhesive, MMA, PCM, epoxy and polyurea soft layer material were used to investigate behavior of bonding interface between CFRP and concrete. Then followed by applications of bonding method to the RC beams were evaluated. Furthermore, a finite element analysis is developed in order to verify and to give complete picture from the experiment results. Finally, the effectiveness of each bonding method was evaluated to conclude this study.

Through this research, the contribution expected from this study are as follows;

- Review the application of MMA and PCM as adhesive on the fundamental properties of CFRP strand sheet-concrete interface, including maximum load, average bond stress, effective bond length, interfacial fracture energy, internal bond stress and slip.
- Can inform the comparison of performance of CFRP plate strengthening method with polyurea soft layer and without polyurea soft layer.

- Develop an implementation design of the use of CFRP plate strengthening method with polyurea soft layer as adhesive. analyzed
- Asses the application of CFRP strand sheet strengthening method on RC beams with variation types of adhesive.

Hopefully by conducting this research, it can be something useful and beneficial for construction technology in general.

It can be noted that this study is limited the behavior of concrete structures strengthening by using externally bonded of CFRP strand sheet and CFRP plate. Long term behavior and environment effect are not discussed in this research. Only static load and simply supported RC beams are applied in experiment.

## 1.2 Research objective

The purpose of this research is to evaluate the effectiveness of CFRP bonding method in the RC members. The main focus of this study is firstly to identify the influencing parameter of the CFRP bonding performance, next, to assess the effects of parameter affecting, such as type of CFRP, thickness or layer, type of adhesive, etc. Then, to propose a new simple equation that can be applied to the local behavior with the same condition and strengthening method on RC members. A general condition of RC beams with external strengthening was not considered in this study although some results of this research can be applied.

## 1.3 Dissertation outline

**Fig.1.2** illustrates the dissertation arrangement which is composed of six chapters as follows;

**Chapter 1** describes the backgrounds, problem statement, the objectives, contribution and limitation of this study.

**Chapter 2** presents literature review related to information of FRP for construction in Japan, strengthening/retrofitting methods, type of FRP and various types of adhesive and basic theory of FRP strengthening in correlation with current situation and the issue to be addressed in this study.

**Chapter 3** examines the effect of CFRP strand sheet strengthening for bending on RC beams with various types of adhesive, such as, epoxy, MMA (Methyl methacrylate)

and PCM (Polymer Cement Mortar) with variations of layers number. Then, a finite element analysis was used to analyze strengthening effect of CFRP strand sheet on RC beams.

**Chapter 4** addresses the bonding behavior of CFRP strand sheet and concrete with various type of adhesive (MMA and PCM) with variations of layers number. To investigate the bonding behavior, experimental results and finite element analysis were analyzed. To obtain the objective of this research, a double lap shear pull out type bond test was conducted. The bonding test was done by adopting the JSCE-E543 –2007, about test method for bonding properties of continuous fiber sheet to concrete.

**Chapter 5** discusses polyurea soft layer effect on the bonding between CFRP plate and concrete. The aim of this study was to obtain the results of bonding performance between CFRP plate, both high tension and high modulus type, and concrete for with and without polyurea soft layer condition and to evaluate the bonding characteristics including, maximum load, bond stress, interfacial fracture energy ( $G_f$ ) and to determine the effective bond length with various thickness of CFRP plate. To make investigation completely, the finite element analysis was conducted for a comparison with experimental results. At the end of this chapter, the new simple equation will be proposed for application of this strengthening method.

**Chapter 6** presents the conclusion of the results obtained from Chapter 3 to Chapter 5. Some recommendations will be recommended for future work.

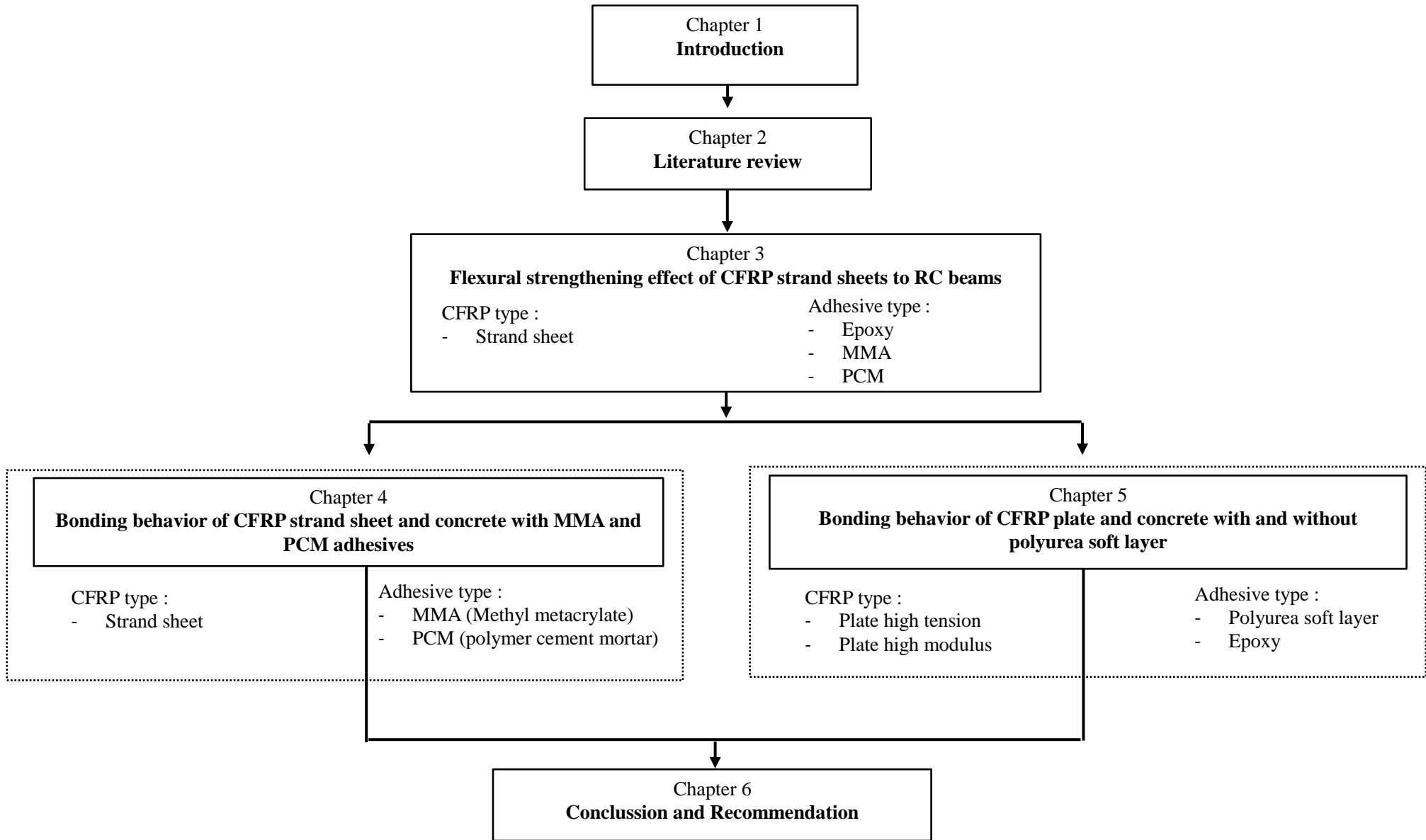


**Fig. 1.2** Flowchart of present work

## REFERENCES

- 1.1 Obaidat Y.T., “Structural Retrofitting of Concrete Beams Using FRP – Debonding Issues” Doctoral Thesis, Lund University, 2011
- 1.2 The Japan Carbon Fiber Manufacturers Association
- 1.3 Dai J.G. and Ueda T., “Interface Bond between FRP Sheets and Concrete Substrate: Properties, Numerical Modelling and Roles in Member Behavior” Prog. Struct. Engng. Mater 7 : John Wiley and Sons, 27-43, 2005

## CHAPTER 2

### LITERATURE REVIEW

---

#### 2.1 Introduction

Fiber reinforced polymer (FRP) have been used for many years in the aerospace, automotive, sport, environment, electronics, medical and construction industry. In the construction industry, FRP can be used for strengthening of existing structure that have vulnerable condition. The vulnerability can occur due to age factor, environmental influence, poor design, lack of maintenance, change of structure function and damage caused by events such as earthquake, tsunami, fire and others. These materials are becoming popular for strengthening of existing structure. The upgrading of existing structure has attracted great attention of researchers for over a decade.

In general, there are two ways for FRP application in construction area. The first application involves the use of FRP bars instead of steel reinforcing bars or pre-stressing strands in concrete structures. The second application, which is the focus of this thesis, is to retrofit structural members with external application of FRP.

#### 2.2 Fiber reinforced polymer (FRP)

In Japan, there are many variation of types and forms related FRP as construction materials, including FRP reinforcement bars (or continuous fiber reinforcement) for concrete and steel structures, FRP shapes and concrete reinforced with short fiber (or fiber reinforced concrete), as well, the types of fiber material forming are carbon, glass, aramid, and other organic fibers such as polyacetal fiber (PAF) and polyester fiber such as polyethylene terephthalate (PET).

FRP is a composite material that consists of high strength material fiber embedded in a polymeric resin. The type of fiber that is often used in the fabrication of FRP is carbon, then called carbon fiber reinforced polymer (CFRP), aramid (aramid fiber reinforced polymer, ARFP) and glass (glass fiber reinforced polymer, GFRP). A comparison of the typical FRP properties is shown in **Table 2.1**. Obviously, these value can vary for each of manufacturers.



**Table 2.1** Typical FRP properties <sup>(2.1)</sup>

Type of Fiber	Tensile Strength (MPa)	Elasticity Modulus (GPa)	Elongation (%)	Specific Density
Carbon: high strength	4300-4900	230-240	1.9-2.1	1.80
Carbon: high modulus	2740-5490	294-329	0.7-1.9	1.78-1.81
Carbon: ultra-high modulus	2600-4020	540-640	0.4-0.8	1.91-2.12
Aramid	3200-3600	124-130	2.4	1.44
Glass	2400-3500	70-85	3.5-4.7	2.60

*Carbon fibers* are applied for high performance composites and described by high value of stiffness and strength but they are not very sensible to creep and fatigue and exhibit negligible loss of strength in the long term. The precursors is a modern technology of production of carbon fibers based on the thermal decomposition in absence of oxygen of organic substances. The most popular precursors are polyacrylonitrile and rayon fibers. Fibers are stabilized first, through a thermal treatment inducing a preferential orientation of their molecular structure, then they undergo a carbonization process in which all components other than carbon are eliminated. The process is completed by a graphitization during which, as the word indicate, the fibers are crystallized in a form similar to graphite. Fibers with carbon content higher than 99% are sometime called graphite fibers <sup>(2.1)</sup>.

*Aramid fibers* are organic fibers, made of aromatic polyamides in an extremely orientated form. Introduced for the first time in 1971 as “Kevlar”, these fibers are distinguished for their high tenacity and their resistance to manipulation. They have a strength and stiffness between glass and carbon fibers. This kind of fibers undergoes degradation under sunlight, with a loss of strength of up to 50%. They can also be sensitive to moisture. They exhibit creep and are fatigue sensitive. The technology of fabrication is based on the extrusion at high temperature of the polymer in a solution and subsequent rapid cooling and drying. The synthesis of polymer is done before the extruding equipment by using very acid solutions. It is finally possible to apply a thermal orientation treatment to improve the mechanical characteristics <sup>(2.1)</sup>.

*Glass fibers* are widely used in the naval industry for the fabrication of composites with medium to high performance. They are characterized by high strength. Glass is made

mainly of silica (SiO<sub>2</sub>) in tetrahedral structure (SiO<sub>4</sub>). Aluminium and other metal oxides are added in different proportions to simplify processing or modify some properties. The technology of production is based on the spinning of a batch made essentially of sand, alumina and limestone. The components are dry mixed and melted at 1260 °C. Fibers are originated from the melted glass. Glass fibers are less stiff than carbon and aramid fibers and are sensitive to abrasion. Due to the latter care must be used when manipulating fibers before impregnation. This kind of fibers exhibit non negligible creep and are fatigue sensitive <sup>(2.1)</sup>.

It can be noted that the technology development in this field over the years allow the FRP properties is evolving towards better and better. Although these fiber materials have relatively high of both modulus of elasticity and tensile strength however they possess elongation (ultimate strain) only from 0.5% to 4.5 %, considerably small compared to the ultimate strain of common steel (up to 20%). In recent years, the application of high elongation organic fibers, approximately 10 % of ultimate strain, with the small modulus of elasticity has been studied. The use of large fiber breaking elongation possible to improve ductility of the structure.

#### 2.2.1 Codes for FRP test method <sup>(2.2)</sup>

There are two codes for test method of FRP, the first is for new concrete structures (Research Committee on Continuous Fiber Reinforcing Materials 1997; Editorial Committee on Concrete Reinforced with Continuous Fiber Reinforcement 1995) and second is for upgrading of existing concrete structures (Research Committee on Upgrading of Concrete Structures with Use of Continuous Fiber Sheet 2001). Next, the two codes are introduced following:

- (1) Recommendation for design and construction of concrete structures using continuous fiber reinforcing materials (Research Committee on Continuous Fiber Reinforcing Materials 1997)

The recommendation for design and construction of concrete structures using continuous fiber reinforcing materials can be used to the FRP bars available in Japan, which are carbon and aramid bars (round/rectangular rods, strands and braids) and carbon, aramid and glass grids. The recommendations application is prepared in accordance with JSCE's Standard Specifications for Concrete Structures and introduces new design

formulas, such as those for shear strength of linear members and anchorage length.

At the same time, JSCE published related standards. They are Quality Specifications for Continuous Fiber Reinforcing Materials, which specify the material properties of FRP reinforcements and the following test methods:

- Test method for tensile properties of continuous fiber reinforcing materials.
- Test method for flexural tensile properties of continuous fiber reinforcing materials.
- Test method for creep failure of continuous fiber reinforcing materials.
- Test method for long-term relaxation of continuous fiber reinforcing materials.
- Test method for tensile fatigue of continuous fiber reinforcing materials.
- Test method for coefficient of thermal expansion of continuous fiber reinforcing materials by thermo-mechanical analysis.
- Test method for performance of anchorages and couplers in pre-stressed concrete using continuous fiber reinforcing materials.
- Test method for alkali resistance of continuous fiber reinforcing materials.
- Test method for bond strength of continuous fiber reinforcing materials by pull-out testing.
- Test method for shear properties of continuous fiber reinforcing materials by double plane shear.

- (2) Recommendations for upgrading of concrete structures with use of continuous fiber sheets (Research Committee on Upgrading of Concrete Structures with Use of Continuous Fiber Sheet 2001)

Both column and beam retrofit with use of carbon and aramid fiber sheets can apply the recommendations for upgrading of concrete structures with use of continuous fiber sheets. Column retrofit means seismic retrofit. The recommendations were prepared based on Guidelines for Retrofit of Concrete Structures – Draft – (JSCE Working Group on Retrofit Design of Concrete Structures in Specification Revision Committee 2001) in which performance-based concept is accepted.

In the Recommendations verification methods for safety are provided by newly proposed prediction methods of flexural strength, shear strength and ductility. In the flexural strength prediction, interfacial fracture energy concept is applied, while debonding is considered in the shear strength prediction. Next, the subsequent test

methods as standard were presented:

- Test method for tensile properties of continuous fiber sheets.
- Test method for overlap splice strength of continuous fiber sheets.
- Test method for bond properties of continuous fiber sheets to concrete.
- Test method for bond properties of continuous fiber sheets to steel plate.
- Test method for direct pull-out strength of continuous fiber sheets with concrete.
- Test method for tensile fatigue strength of continuous fiber sheets.
- Test method for accelerated artificial exposure of continuous fiber sheets.
- Test method for freeze-thaw resistance of continuous fiber sheets.
- Test method for water, acid and alkali resistance of continuous fiber sheets.



**Photo 2.1** CFRP Sheets <sup>(2,3)</sup>

## 2.2.2 Type of FRP for construction

### 2.2.2.1 FRP sheet

As FRP materials for repairing and strengthening of existing concrete structures, FRP sheets such as carbon fiber sheet (CFRP sheets) (**Photo 2.1**) and aramid fiber sheet are widely used in Japan. In this method, the dry continuous fiber sheet is bonded to concrete surface using room temperature curing resin and impregnated with the same resin at the same time. After curing, FRP is formed on the concrete surface. In recent years, this

method has also been applied for repairing and strengthening of corroded steel structures (2.3).

Three types of carbon fiber sheets are as follows; high strength, high modulus, and middle modulus type. The unidirectional FRP sheet which arranged carbon or aramid fiber in one direction is mainly used for strengthening of concrete structures. Number of plies, the types of the sheet, and types of the fiber are determined according to the design calculation. Epoxy putty is widely used as the adhesive between FRP and concrete. In addition, MMA (Methyl methacrylate) putty is sometimes used because of excellent curing characteristics such as low temperature curing and rapid-curing (2.3).

#### 2.2.2.2 FRP grid

FRP grid is a continuous fiber reinforcing material consisting of high-performance continuous fibers such as glass, carbon, and aramid. All of the fibers are impregnated with resin of high resistance to chemical agents and formed into FRP grids. This material has many useful characteristics, such as light weight, high strength, and is free from rust and corrosion. The characteristics of FRP grid are as follows :

- The use of high-performance continuous fibers gives extremely high strength of the axial bar and the FRP grid crossing. This ensure bond and anchorage of FRP grid to concrete.
- As the FRP grid crossing are in the same plane as the axial bars, concrete coverage can be reduced and the amount of concrete can be saved.
- Since FRP grid has low specific gravity at 1.3- 1.7, it is light and can be formed into any shapes required on site as well as a flat surface. Thus, it can improve work productivity.

Three types of FRP grid namely CFRP, GFRP, and AFRP are commercially available with different combinations of fiber types. **Fig. 2.1** shows photograph of several types of FRP grid. Flat panel and curved panel are commercially available. At the grid crossing of FRP grid, fibers are laminated alternately as shown in **Fig. 2.2**, adequate strength is provided by constraint effect of fibers in addition to the adhesive strength of matrix resin (2.3). **Photo 2.2** shows CFRP grid which has been ready to use for strengthening of RC members.



**Fig. 2.1** FRP Grid Typically <sup>(2.3)</sup>

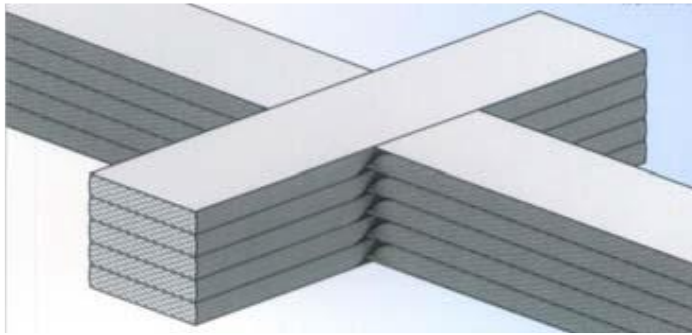


**Fig. 2.2** Structure of Grid Crossing <sup>(2.3)</sup>



**Photo 2.2** CFRP Grid

### 2.2.2.3 FRP strand sheet

Strand sheet, can be made of carbon or aramid, is produced by a very thin filaments material with a diameter of about 5-10micrometer from 3000 to 24.000 strands that are collected into one and become a strand. Each strand impregnated with a resin such as polymeric thermo-hardening resins, a strand has a diameter of about 0.5 to 2.0mm which was by heating in an electric furnace. It can be seen in **Photo 2.3**, the strand sheet is made out of fine CFRP strands which are individually impregnated with resin and hardened. Hundreds of these strands are arranged horizontally in 1m width and woven with thread to make it into a sheet form <sup>(2.4)</sup>.

Following is the characteristic of the strand sheet: it has a high strength with and a light weight and also has only one direction strengthening, suitable for structural beam. FRP strand sheet can be used without impregnation of adhesive into the concrete and can produce a thinner construction. It allows the overlap splice, less possibility of air bubble occurrence in the interface area.



**Photo 2.3** CFRP strand sheet

### 2.2.2.4 CFRP plate

Unidirectional CFRP plates are usually established by the pultrusion process. Fibers are drawn off in a carefully controlled pattern through a resin bath which impregnates the fibers bundle. They are then pulled through a mold which consolidates the fibers-resin combination and forms the required shape. The mold is heated which sets and cure the resin, allowing the completed composite to be drawn off by reciprocating clamps or a tension device. The process enables a high proportion of fibers (generally

about 65%) to be incorporated in the cross section. Hence in the longitudinal direction, relatively high strength and stiffness are achieved. Because most, if not all, of the fibers are in the longitudinal direction, transversal direction strength will be very low <sup>(2.1)</sup>.

Plates formed have a thickness of 1-2 mm and have a variation in widths, typically between 50 and 100 mm. As pultrusion is a continuous process, very long lengths of material are available. Thinner material is provided in the form of a coil, with a diameter of about 1m. It can be easily cut to length on site using a common guillotine. Typically plates have a fiber volume fraction of 55 %, and can incorporate 10% fibers to improve the handling strength. The lengths of the plate produced are up to 12m, with a thickness being tailored to the particular application. The widths up to 1.25m have been produced and the thickness up to 30mm <sup>(2.1)</sup>.

### **2.3 Adhesives**

There are many types of adhesive that is often used in research. The properties are also highly variable and highly dependent on the manufacture. However, the important properties of adhesive is shear stiffness. The shear stiffness,  $K_a$ , is shear modulus of adhesive,  $G_a$ , divided by adhesive layer thickness,  $t_a$  ( $K_a = G_a/t_a$ ). The shear stiffness can influence the behavior of a retrofitted beam and the failure mode. Some researchers reported that the beam load capacity decreases slightly with increasing shear stiffness of adhesive <sup>(2.5), (2.6)</sup>. This is due to the fact that a high shear stiffness value of the adhesive increases the rate of stress transfer between FRP and concrete, which leads to stress concentrations in the interface, which will increase the risk of debonding at lower load more than expected.

Following are some types of adhesive used in this study;

#### *Epoxy putty*

Epoxy putty is widely used as the adhesive between FRP and concrete. In application, epoxy putty is made by mixture of two compounds, resin and hardener. Curing process is begin when the resin is mixed with certain catalyst. The curing process is the process when the molecular chains react at the active chemical. This process produce the exothermic reaction. The mixing between resin (epoxide group) and hardener (catalyst) that arise from this combination is able to cross-linkage of polymer. This combination



determine the stiffness and the strength of epoxy adhesive.

Epoxy adhesive can be used to various kinds of material and their properties are dependent upon the specific chemistry and the existing cross-linkage of the system. Some of the important performance of the epoxy adhesive include exceptional chemical and heat resistance, excellent adhesion and water resistance as well as satisfactory mechanical and electrical insulating properties. In the RC beams field application, prior to apply epoxy adhesive, epoxy primer is needed for surface preparation.

#### *Methyl methacrylate (MMA) putty*

MMA (Methyl methacrylate) putty is cured by a reaction called radical polymerization. Compared with epoxy resin, MMA is suitable for low temperature, wet environment and have a faster time for construction. The advantages of this characteristics are the execution work during the winter and the cold climates, the time limit for traffic construction and a lot of work to be done.

Methacrylic resin used in the continuous fiber reinforcement construction method is a resin material by polymerizing. The repeating units called several monomers comprising methyl methacrylate (MMA) is contiguous chemically bonded. This MMA putty can be used as dental filler, optical material such as a lens, in the civil engineering and construction field, transparent acrylic plate, floor coverings, has been widely used in paving materials and the like.

#### *Polymer cement mortar (PCM)*

The concept of mixing the polymer and the mortar is not something new. In 1932, the patent of pavement material in accordance with natural rubber latex blended in the UK has been publish.

The polymer admixture, is a material that is mixed into concrete and mortar that is intended their properties, is also referred to as a "polymer for cement admixture (polymer for cement modifier)". The mixing of concrete, mortar and the polymer admixture is called polymer cement concrete (polymer modified concrete, PMC, referred to polymer cement concrete, or PCC) and polymer cement mortar (polymer modified mortar, PMM, referred to polymer cement concrete, PCM)

### *Polyurea putty*

Polyurea is a type of elastomer (an elastomer is a polymer with viscoelasticity and very weak inter-molecular forces, generally having low Young's modulus and high failure strain compared with other materials) that is derived from the reaction product of an isocyanate component and a synthetic resin blend component through step-growth polymerization. The isocyanate can be aromatic or aliphatic in nature. It can be monomer, polymer, or any variant reaction of isocyanates, quasi-prepolymer or a prepolymer. The prepolymer, or quasi-prepolymer, can be made of an amine-terminated polymer resin, or a hydroxyl-terminated polymer resin <sup>(2.7)</sup>.

Polyurea and polyurethane are copolymers used in the manufacture of spandex, which was invented in 1959. Polyurea was originally developed to protect tabletop edges which led to the development of two-component polyurethane and polyurea spray elastomers took place in the 1990s by Mark S Barton and Mark Schlichter US 5534295 patent. Its fast reactivity and relative moisture insensitivity made it useful for coatings on large surface area projects, such as secondary containment, manhole and tunnel coatings, tank liners, and truck bed liners. Excellent adhesion to concrete and steel is obtained with the proper primer and surface treatment. They can also be used for spray molding and armor. Some polyureas reach strengths of 6000psi (40MPa) tensile and over 500% elongation making it a tough coating. The quick cure time allows many coats to be built up quickly <sup>(2.7)</sup>.

Broekaert (2002) <sup>(2.8)</sup> described in his report that polyurea holds a unique position in the coatings industry as well as in the polyurethane coatings industry. The new developments both for the raw material and the application equipment have enlarged the application portfolio considerably. The important advantages of polyurea spray coatings are their reactivity, water insensitivity, low temperature curing and their unique physical and chemical properties.

Some of the advantages of polyurea is as follows <sup>(2.9)</sup>;

- Easily applied and self-priming on most surfaces: metal, wood, concrete, fabric, etc.
- High resistant to extreme environmental conditions such as heat, cold, chemicals, radiology and aging (approved for 75 years).
- Seamless & Waterproof

- No solvents, No VOC's, No odor.
- Easily decontaminated / high polymer surface.
- Low Level Radiation Barrier.
- In combination with radiation shielding technologies, increased shielding against Alpha-, Beta-, X- and Gamma rays is achieved.
- Robotic systems can be applied for execution purposes.
- Anti-corrosion.
- Hydrophobic.
- Flexible: bridges cracks and expands and contracts with substrate.
- Fast application time / Minimal downtime (sets in seconds).
- Excellent abrasion resistance.
- Easy maintenance.
- High Impact resistant.
- High tensile strength.
- High elongation & hardness (Structural reinforcement).
- Resistant to many chemicals

#### 2.4 Strengthening method to RC members

Recently, retrofit materials with FRP is being used for a large variety of application such as box culvert, bridge pier , bridge slab overlays, aqueduct tunnel and for building member. Generally, the strengthening of RC members is required for structural that have experienced declining in capacity due to poor design, environment influences, change of function, and damage caused by events such as earthquake, fire and others.

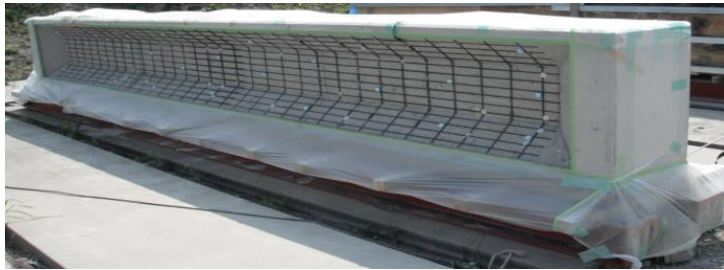
The objective of strengthening may be one or a combination of several such as : to increase axial, flexural or shear load capacities, to increase ductility of columns mainly for improved seismic performance, to increase stiffness for reduced deflections under service and design loads, to increase remaining fatigue life <sup>(2.10)</sup>.

Following are some applications of FRP that was used as a structure strengthening;  
*Shear strengthening by CFRP grid spraying PCM concrete* <sup>(2.11)</sup>

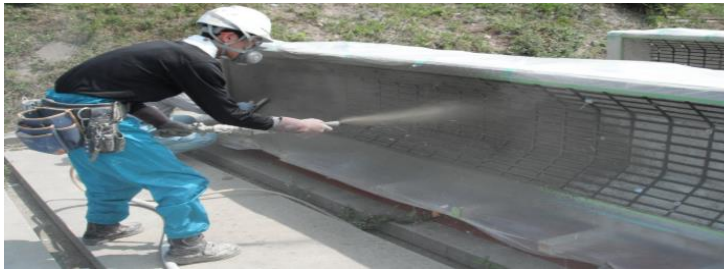
**Photo 2.4(a) ~ (c)** show shear strengthening of RC beam by CFRP grid spraying by PCM method. The benefits of this method are that it is unnecessary to drill the haunch, increased thickness amount is also thin, and corrosion resistance.



(a) RC beams



(b) CFRP grid installation



(c) Spraying by PCM

**Photo 2.4** Shear strengthening by CFRP grid and PCM

*Seismic retrofitting of bridge piers* <sup>(2.12)</sup>

**Photo 2.5** shows seismic retrofitting of RC high piers of express high way with using CFRP sheets. This 60m high RC pier had hollow circular cross section to minimize self-weight. The longitudinal reinforcement was curtailed at several levels according to the old design specification.



**Photo 2.5** Seismic retrofitting of high piers <sup>(2.12)</sup>

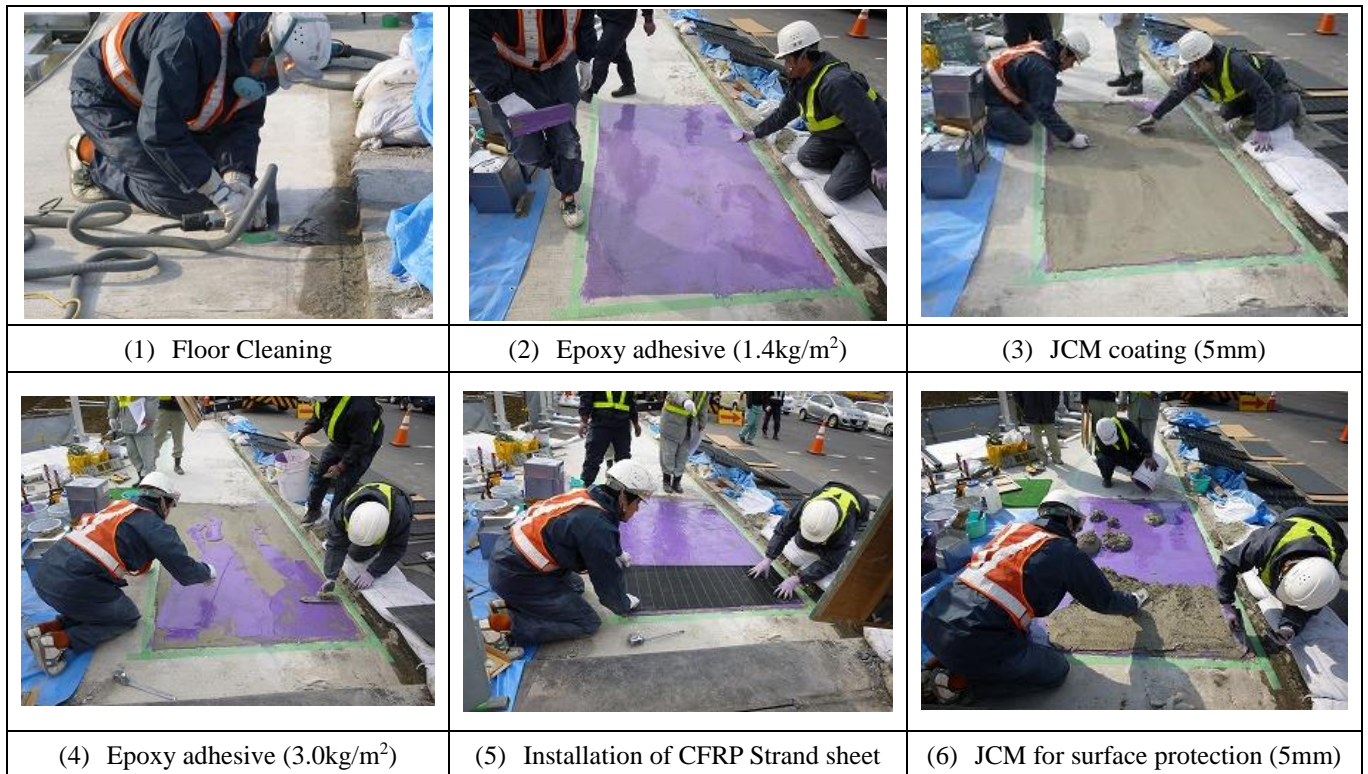


**Photo 2.6** Rapid retrofitting method for Okayama Bridge <sup>(2.13)</sup>

### *Rapid retrofitting method of bridge deck* <sup>(2.13)</sup>

The work that require quick time in construction without a long treatment time has been applied by using CFRP strand sheet in the bridge retrofitting. By using this retrofitting method was possible to be able to use the adhesive before JCM becomes hard. It was obviously making the time of construction become short. After installation, it was possible to carry out deck waterproofing and pavement restoration in about three hours of curing time. Since the surface finishing was JCM, it was no matter for adhesion of waterproofing or asphalt pavement. In these circumstances, it is possible to approximately 20m<sup>2</sup> construction per one day. **Photo 2.6** shows the actual construction of bridge in Okayama Prefecture.

### **2.5 Bonding test** <sup>(2.14)</sup>

Some specimen types used in the bonding test between FRP laminates and concrete can be seen in **Fig. 2.3(a) ~ (d)**. **Fig. 2.3(a)** shows a test specimen preparation to get the bond strength using a tile or similar methods have been performed. This is known as direct tensile test. But, it was difficult to precisely describe the bonding characteristics of the FRP-concrete composite system.

**Fig. 2.3(b)** show one alternative that has been widely used as the solution to solve this problem. This method, was adopted in this research, consists of a prism with a notch at the center and was reinforced with FRP laminates on both faces. The shortcomings of this method is acting force's eccentricity in experiments due to inaccuracies when specimen preparation. This test model is known as double lap shear pullout test.

**Fig. 2.3(c)** shows single lap shear pullout test specimen. The objective of this test is to remove the acting force's eccentricity in experiments when using laminates in both faces on the double lap pullout test. **Fig. 2.3(d)** shows the bending test type. This test is proposed to estimate the bending. This test specimen consists of two prisms reinforced at the center with FRP laminates. Large numbers of experiments have been performed by various researchers. But the amount of variability with regards to type of tests performed, materials used, curing conditions, surface preparation of concrete and FRP material properties is very high.

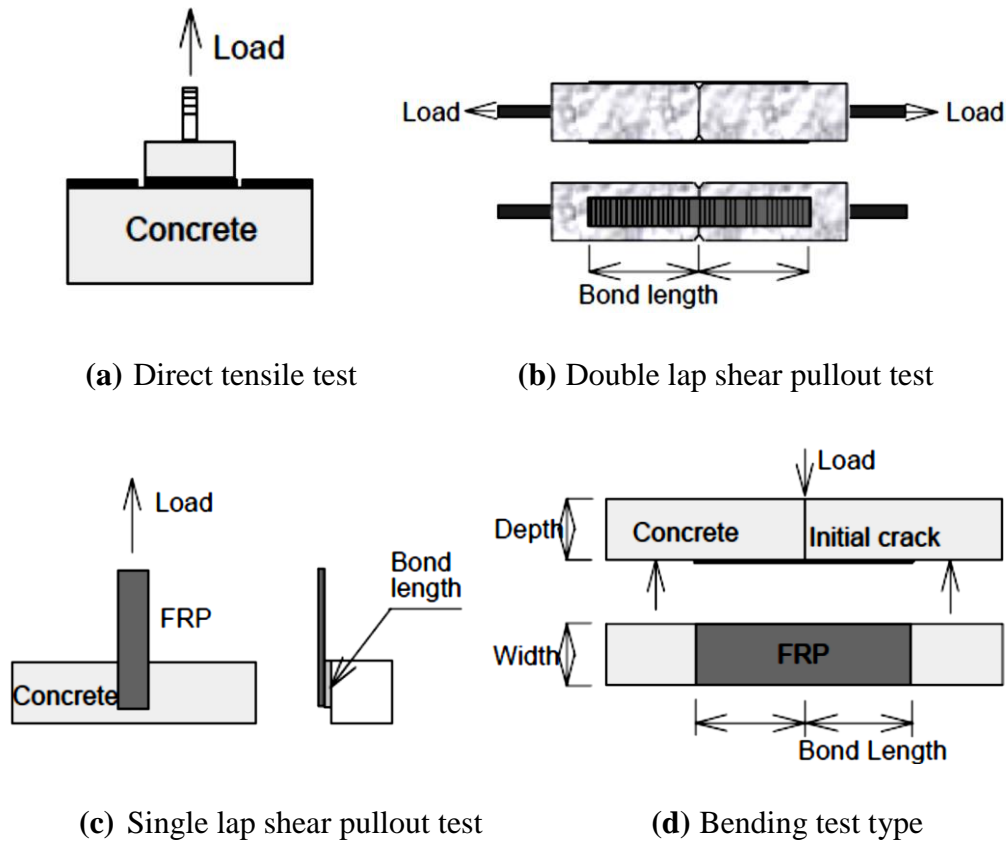


**Fig. 2.3** Bonding test specimen <sup>(2.14)</sup>

### 2.5.1 Bond strength

Most of the FRP failure shown that debonding has occurred at the interface of concrete adhesive with some concrete cover separation and depends on bond strength. It has been proven that bond strength is affected by concrete strength. Most of the research showed that an increase in ultimate load related with concrete strength. Their proposed a linier proportion such as  $f'_c{}^{1/2}$ ,  $f'_c{}^{2/3}$ ,  $f'_c{}^{1/5}$  and  $f'_c{}^{0.19}$ . However, their assumption is based on few experimental data, so there is no conclusion could be drawn on the bond strength and concrete strength relationship.

Beside the concrete strength, the bond strength is affected also by the surface preparation methods. Two concrete surface preparations: water jet and ordinary sander had been studied by Yoshizawa et al. <sup>(2.15)</sup>. Water jet on the concrete surface yielded the highest bonding strength (about 37% higher than the sander) was conclusion of this

experiment. Toutanji and Ortiz <sup>(2.16)</sup> reported in their experiment that the water jet method was found to exhibit a bonding load 60-75% higher than the ordinary sanding method for surface preparation. There are many more studies in correlation with surface preparation, however, water jet (hydro-demolition) and sand blasting are the best surface preparation methods for an effective FRP bond to concrete.

As mention in section 2.3 that bond strength is also influenced by adhesive properties. As the adhesive is softer, the bond strength is stronger <sup>(2.5), (2.6)</sup>. In recent numerical study, Benyoucef et al <sup>(2.17)</sup> showed increasing the thickness of the adhesive layer can decrease significantly in the peak interfacial stress and can increase the bond strength. Its result relates to the shear stiffness,  $K_a$ , as mention in section 2.3 ( $K_a = G_a/t_a$ ). So, it can be said that the shear stiffness of adhesive can influence the bond strength of composite laminate.

Yoshizawa et al <sup>(2.18)</sup> revealed that the maximum load increased with the FRP stiffness increased. Similar results were found by Nakaba et al <sup>(2.14)</sup> and de Lorenzis et al <sup>(2.19)</sup>. In connection with the effect of bonding length, there are many study have been done. The result of the experiment that had been conducted by Brosens and Van Gemert <sup>(2.20)</sup> showed that the fracture load increase with bonding length increase. While, the mean shear strength decrease with the bonding length was a conclusion resulting from Bizindavyi and Neale <sup>(2.21)</sup>. But these results were denied by De Lorenzis et al <sup>(2.19)</sup>, they reported that the bonding length did not affect the bond failure the bond failure load. This results is more reasonable through the notion of an existing effective bonding length.

Finally, it can be concluded that the bond strength of FRP laminate to concrete is influenced by concrete strength, surface preparation of concrete, adhesive properties (adhesive shear stiffness), FRP type and FRP stiffness. The bonding length do not affect on the bond strength if the bonding length exceed the existing effective bonding length.

### 2.5.2 Failure Mode

Pham and Mahaidi (2007) reported in their publication <sup>(2.22)</sup> that both for single and double shear tests, there are five possible different failure mode for an FRP bonded to concrete. The five possible failure mode are

- (1) Interfacial debonding failure

This mode is most commonly observed. The failure surface is in the concrete a few



millimeter beneath to the concrete adhesive surface. A concrete prism may also be pulled out near the loaded end.

- (2) Shear or tension failure of concrete  
The main crack of this mode is into the concrete block. This mode tends to occur only when the bonding length is relatively short.
- (3) FRP tensile rupture  
This mode can occur if the FRP cross-sectional area is very small
- (4) Adhesive failure  
The cohesion failure through the adhesive became the main feature on this failure mode.
- (5) FRP delamination  
FRP delamination has also been reported, where delamination path may bridge across the adhesive layer and penetrates into the concrete.

The last three modes are rare, especially for normal strength concrete, of which the shear strength is much lower compared than that of the adhesive and FRP.

### 2.5.3 Effective bonding length

Many researchers have studied the effect of bonding length. The research results show that when the bonding length increase beyond a certain extent the bond strength do not increase any further. Researchers have defined this length as the effective bonding length. Tension in concrete is transferred to FRP sheets mainly through shear stresses in the adhesive in a short length near the applied load. As the load increases, cracking near the applied load shifts the active bond zone to a new area further away from the loading point, indicating that only part of the bond is effective. This part is called the effective bonding length (effective bonding length). The definition of effective bonding length used is different for different researchers <sup>(2.10), (2.23)</sup>.

Currently, many methods were used to evaluate the effective bonding length. The effective bonding length can be defined as a length over which majority of bond stress maintained. The effective bonding length of the FRP takes the entire load to a certain level at which localized debonding/delamination occurs, causing the effective bonding length to shift to another active bonding zone. This phenomenon continued until the FRP was completely debonding from the concrete. In other words, when delamination occurs in the

vicinity due to fracture of concrete surface, the active zone is shifted to a new zone. This phenomenon is repeated until delamination propagates completely <sup>(2.10), (2.13), (2.23) (2.24)</sup>.

**Fig. 2.4** shows one of the way used to estimate the effective bonding length used by Sugiyama (2011) <sup>(2.25)</sup>. The first is estimate the effective bond area on the strain distribution diagram on the maximum load. Then, the next step is determining two points that results the steepest gradient on the distribution. Maximum stress is decided by **Eq. (2.1)**. The last is calculate the effective bonding length by **Eq. (2.2)**. **Fig.2.4** shows how to specify the used points to determine the effective bonding length.

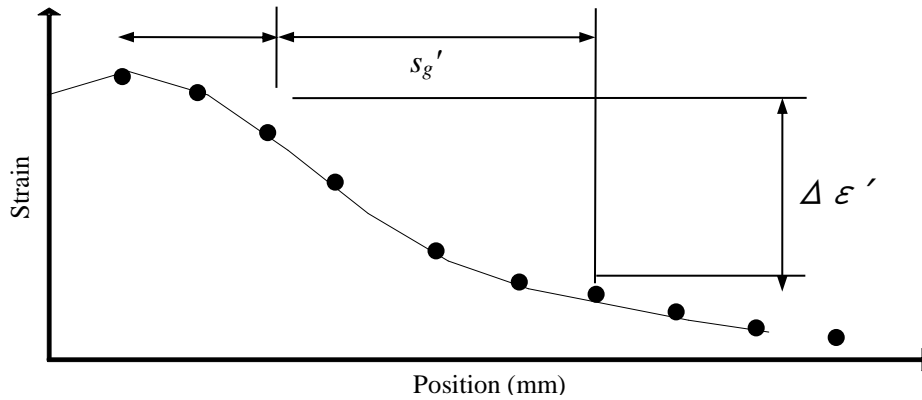


**Fig.2.4** Determine point in the strain distribution for effective bonding length <sup>(2.25)</sup>

$$\tau_{max} = \frac{\Delta\varepsilon \cdot E_f \cdot A_f}{S_g \cdot b} \quad (2.1)$$

$$l_e = \frac{P_{max}}{2\tau_{max} \cdot b} \quad (\text{for double shear test}) \quad (2.2.a)$$

$$l_e = \frac{P_{max}}{\tau_{max} \cdot b} \quad (\text{for single shear test}) \quad (2.2.b)$$

Where,

- $\tau_{max}$  = the maximum bond strength (MPa)
- $l_e$  = the effective bonding length (mm)
- $\Delta\varepsilon$  = difference strain at a steepest area
- $E_f$  = tensile modulus of CFRP strand sheet (MPa)

- $A_f$  = area of CFRP strand sheet ( $\text{mm}^2$ )  
 $S_g$  = interval of strain at steepest area (mm)  
 $b$  = average width of CFRP strand sheet (mm)

It is also determined herein that the effective bonding length is the distance between two points that correspond to 10% of the maximum local bond stress. This way tends to be used by many researchers to determine the effective bonding length ( $l_e$ ) (2.2), (2.10), (2.14), (2.23), (2.24). **Fig. 2.5** shows graphically how to determine the effective bonding length of this method.

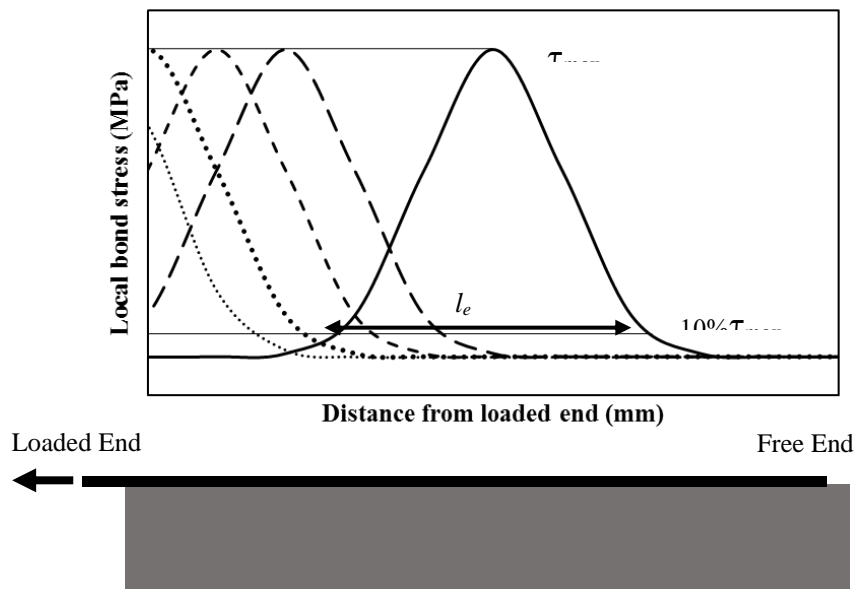


**Fig.2.5** Effective bonding length

#### 2.5.4 Local bond stress-slip relationship

An important step toward understanding bond behavior is to have an assumption for local bond stress-slip relationship. Many researchers show different results the local bond-slip relationship – linear and nonlinear model. This curve is determined by the material properties of FRP, adhesive and concrete that can control the bond properties as a whole (2.10), (2.14). The bond-slip model shows the relationship of the shear (bond) stress and slip at the bonded interface. As shown in **Fig. 2.6**, the major characteristic components

of finitely small interface units in the bond-slip model are maximum shear stress, slip, and fracture energy. The bond-slip model can be expressed by the nonlinear distribution of shear stress, which occurs along the bonded interface for different loading stages. Therefore, it is possible to predict the debonding failure of CFRP by comparing the shear stress and slip. However, the bond-slip model can be successfully used as the appropriate model to derive the governing equation that expresses the failure mechanisms of the bonded interface <sup>(2.26)</sup>.

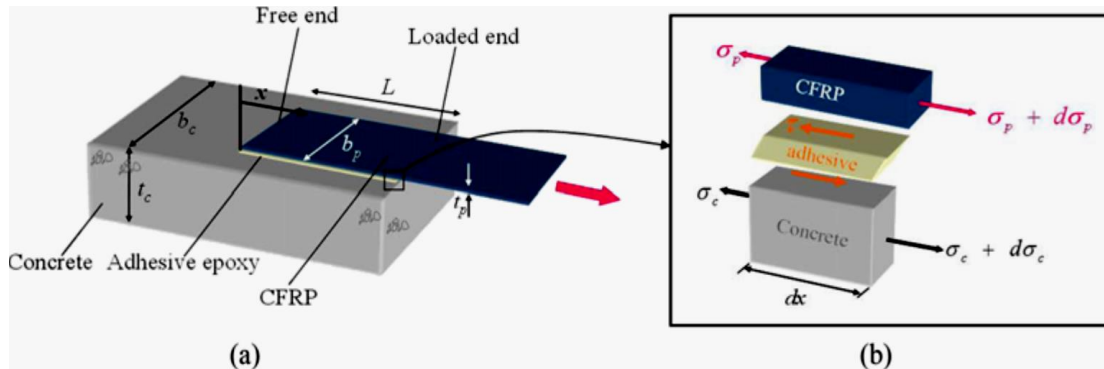


**Fig. 2.6** interface behavior of shear specimen <sup>(2.26)</sup>

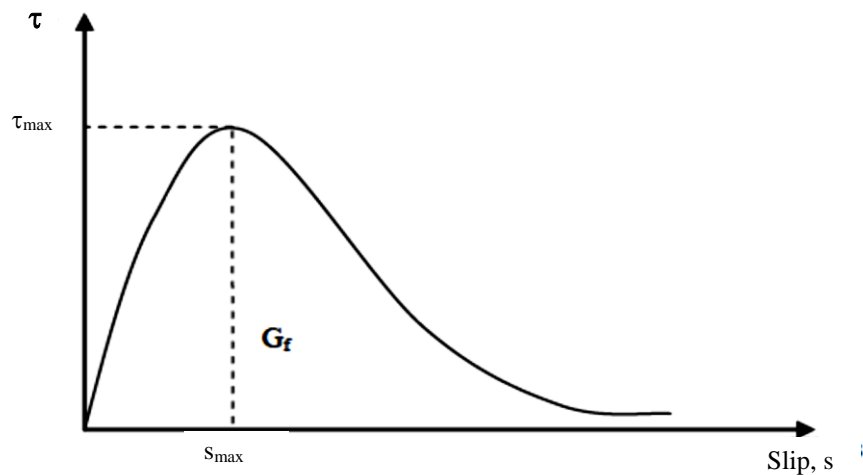


**Fig. 2.7** Typical local bond stress-slip relationship

A local-slip curve describes the relation between shear stress and slip at a point in the bond layer. There are many local bond-slip models suggested by various researchers to predict interface behavior. For example, the configuration of bond stress-slip

relationship, including bilinear, cut off, tensile softening type and Popovics's type have been proposed. The general shape of a typical bond-slip curve is shown in **Fig. 2.7**. In order to obtain the local bond stress-slip relationship, the average bond stress of section  $i$  is calculated the following equation:

$$\tau_{b,i} = \frac{(\varepsilon_{f,i} - \varepsilon_{f,i-1})t_f E_f}{\Delta x} \quad (2.3)$$

Where,

$\tau_{b,i}$  = average bond stress between the section  $i$  and  $i-1$  from free end (MPa).

$\varepsilon_{f,i}$  = strain of FRP at the section  $i$ .

$t_f$  = thickness of FRP (mm).

$E_f$  = elastic modulus of CFRP (MPa).

$\Delta x$  = strain gages interval (mm).

Local slip or slip is caused by the strain differences between CFRP plate and concrete. However, due to the stiffness of the concrete is very large, the concrete strain can be neglected. Next, to simplify analysis, the free end slip can be approximately as zero. The slip can be calculated by the following equation:

$$s_i = \frac{\Delta x}{2} (\varepsilon_0 + 2\sum_{j=1}^{i-1} \varepsilon_j + \varepsilon_i) \quad (2.4)$$

Where,

$s_i$  = slip between FRP and concrete corresponding with average bond stress between section  $i$  and  $i-1$  from free end (mm).

$\varepsilon_0$  = FRP strain at the free end.

$\varepsilon_{i,j}$  = strain on CFRP plate.

After calculating all data, local bond stress versus slip was plotted in a graph for each interval of strain gauge on each specimen. The most widely used approach in term of local bond stress-slip relationship is Popovics's equation <sup>(2.14), (2.22), (2.27), (2.28), (2.29)</sup>. Popovich's equation was utilized to represent the local bond stress and slip relationship, shown as follows:

$$\frac{\tau}{\tau_{max}} = \frac{s}{s_{max}} \frac{n}{(n-1) + (s/s_{max})^n} \quad (2.5)$$

Where,

- $\tau_{max}$  = maximum local bond stress (MPa)  
 $s_{max}$  = slip at  $\tau_{max}$  (mm)  
 $n$  = constant

### 2.5.5 Interfacial fracture energy ( $G_f$ )

Interfacial fracture energy is defined as the area below the local bond stress-bond slip curve. Yuan et al. <sup>(2.30)</sup> proposed that the maximum bond strength is a function of the interfacial fracture energy and FRP stiffness. Interfacial fracture energy has been clearly defined by the theory of fracture mechanics and it can be used in the bond equations without any deviations.

Dai and Ueda <sup>(2.5)</sup> reported that the interfacial fracture energy is almost same a constant value regardless of FRP type or FRP stiffness. The effects of the adhesive layer shear stiffness on interfacial fracture energy have been also reported, in which the increase of interfacial fracture energy with decreasing shear stiffness of adhesive layers.

Based on energy or force equilibrium method and the assumption of concrete prism stiffness is very large compared to FRP stiffness, interfacial fracture energy can be calculated by **Eq. (2.6)** <sup>(2.5), (2.31)</sup> as follows:

$$G_f = \frac{P_{max}^2}{8b^2 E_f t} \quad (\text{for double lap shear test}) \quad (2.6.a)$$

$$G_f = \frac{P_{max}^2}{2b^2 E_f t} \quad (\text{for single lap shear test}) \quad (2.6.b)$$

Where,

- $G_f$  = interfacial fracture energy (N/mm or MPa.mm)  
 $P_{max}$  = maximum load (N)  
 $E_f$  = elastic modulus of CFRP (MPa)  
 $t$  = thickness of FRP (mm)  
 $b$  = width of FRP (mm)

## 2.6 Related research

Lots of experiments have been performed by various researchers. But the amount

of variability with regards to type of tests performed, materials used, curing conditions, surface preparation of concrete and FRP material properties is very high.

Chajes et al. 1996 <sup>(2.32)</sup> did the experiment using single lap shear pull out tests with constant bonded lengths with variations in adhesive type, surface preparation and concrete strengths. By changing the water/cement ratio the concrete compressive strength were varied from 24.13 to 44.82 MPa. This experiments used variation of tensile strength from four different types of adhesives from Sika Corp. and Lord Corp. They were Sikadur 32 Hi-Mod, Sikadur 31 Hi-Mod gel, Tyrite 7500 and Fusor 320/322. The surface preparations used were grinding and mechanical abrasion. The conclusion of these were that the bond performance was affected by adhesive/epoxy used, surface preparation and concrete compressive strength.

Maeda et al. 1997 <sup>(2.33)</sup> carried out double lap shear pull out tests wherein the concrete strength and FRP stiffness were varied. From the effective bonding length equation developed it was shown that as the stiffness of FRP increases effective bonding length also increases which was contrary to all the other models proposed before.

Bizindavyi et al. 1999 <sup>(2.34)</sup> carried out the single lap shear pull out tests with variations types of FRP laminates. Glass-fiber reinforced polymers (GFRP) and carbon-fiber reinforced polymers (CFRP) were used in this study. The tensile strength for GFRP specified was 472 MPa and for CFRP was 1014 MPa with the low modulus of elasticity. The maximum strain that can be approximated form strain distribution was to be  $8000\mu\epsilon$  at the loaded end and the effective bonded length was 160 mm with the failure mode was FRP rupture. But from the modulus of elasticity specified for CFRP to be 75.7 GPa resulted that the effective bonding length varied from 135 mm to 280 mm and from 120 mm to 320 mm for GFRP 1 ply and 2 ply laminate, respectively. The failure at the concrete beneath the shearing line as the failure mode were considered.

De Lorenzis et al. 2001 <sup>(2.19)</sup> conducted flexure tests with variation in the bonding length and thickness of FRP along with concrete strength and concrete surface preparation were varied to study bond characteristics. The results shown that the surface preparation, concrete compressive strength and thickness of FRP affected the bond strength. By the using of a linear bond stress-slip relationship could be seen the reasonable agreement of test results.

Nakaba et al. 2001 <sup>(2.14)</sup> performed double lap shear pull out tests with variation in

FRP type (CFRP, CFRP high stiffness and AFRP), concrete strength, mortar and putty layer on the low concrete strength. The low strength concrete series was important aspect with the effect of putty thickness on the bond strength in which two specimens compared, with putty layer and without putty layer. From this aspect could be concluded that putty thickness did not have an effect on the bond behavior. The effective bonding length was defined to be the distance between two points that corresponds to 10% of the maximum bond stress. Hence the actual effective bonding length values were estimated from the graph of strain distribution. In this research, a local bond stress-slip relationship was proposed based on Popovics's equation, which represents a good agreement with experiment results. The others conclusion from this research were: the maximum load and effective bonding length increase as the stiffness of FRP also increase and maximum local bond stress was not influenced by the type of FRP, but increase as concrete compressive increases.

Dai et al. 2002<sup>(2.35)</sup> undertook single lap shear pull out tests with FRP sheets were bonded to concrete with a wet layup bonding system. The width of bonding was kept constant at 100 mm. During the pull out test procedures, the displacement control loading system was applied. During the test also the pull out forces and the slip at the loaded end can be measured accurately through load cell and LVDT, as a result, the relationship between the strain of FRP sheets and slip at loaded end, as an important parameter in this experiment, can be obtained. Variations were made in the type of adhesive and FRP used. The microscope was used to measure the thickness of the adhesive layer after failure. After analysis of the local bond stress-slip relationship, large variation was seen and hence a model to calculate shear stress-slip relationship was proposed. It was also observed that the thickness and properties of the adhesive layer greatly affects the interfacial fracture energy ( $G_f$ ) and appropriate experimental data was studied and a relationship between shear stress and fracture energy was deduced. The interfacial fracture energy was also affected by the strength of concrete ( $f_c'$ ) and the stiffness of adhesive ( $G_d/t_a$ ) and FRP stiffness ( $E_f t_f$ ). Hence all these affecting factors were incorporated in the fracture energy equation. It was also shown that interfacial fracture energy was hardly affected by FRP stiffness to a large extent but was affected most by adhesive mechanical properties followed by concrete compressive strength. Experimental results show that with the decreasing of the adhesive shear stiffness, the interfacial fracture energy ( $G_f$ ) and



interfacial ductility can be improved. On the other hand, the maximum bond stress increases and the interfacial ductility decreases slightly with increasing of the FRP stiffness.

Yuan et al. 2004 <sup>(2.36)</sup> performed the single lap shear pull-push tests of FRP plate to concrete bonded joint with an analytical solution. As a results, the solution provides a a complete theoretical basis for understanding full range load-displacement behavior of FRP to concrete bonded joints.

72 specimens were tested with single lap shear pull out tests with variations in bonded length of laminates, height of concrete free edge and widths of laminate and concrete undertaken by Yao et al. 2005 <sup>(2.37)</sup>. There were failure mode resulting from this experiment; concrete debonding, interface debonding and concrete prism failure. To have an effect on the bond strength, the bonding length and ratio of FRP width to concrete width have been quoted but the effect of concrete free edge on the bond strength was yet unclear.

Sharma et al. 2006 <sup>(2.38)</sup> carried out single lap shear pull out tests on steel, aluminum, GFRP and CFRP plates. The results of effective bonding length were reported for the set of experiments performed. Variation in material properties of the laminates along with width ratio  $\beta$  and the bonded length were undertaken. The stiffness and width of laminate, compressive strength of concrete and the width ratio  $\beta$  affected the bond strength and effective bonding length were some of this study conclusion.

Boschetto et al. 2006 <sup>(2.39)</sup> tested 24 specimens with double lap shear pull out tests but only 14 effective bonding length values were reported because the failure mode in these specimens was shearing in concrete. The CFRP plates used were varied along with the concrete strength. Variation in the number of plies was also used to get different effect of stiffness of the plates. It was not easy to understand whether the active bond zone or that of the distance from the loaded end when the strain becomes negligible.

Double lap shear pull out tests with variations in surface preparation techniques, sand blasting and water-jet and type of FRP were undertaken by Toutanji et al. 2007 <sup>(2.40)</sup>. The failure was seen in the concrete adjacent to the FRP. The bond strength results with water jetting was higher than with sand-blasting one. A bond strength model was also proposed. Another set of tests were also carried out with variations in stiffness of CFRP sheets and concrete compressive strength by Toutanji et al. Existing models compared with experimental results and it was concluded that models with effective bonding length

in the equation of bond strength gives better predictions.

Double lap shear pull out tests with concrete under static and fatigue loading were carried out by Iwashita et al. 2007 <sup>(2.41)</sup>. The concrete surface was treated with sand paper before bonding of FRP in the tests. The three specimens under static loading were evaluated and all three failed due to different modes of failure. This study considered the failure mode with shearing in concrete. The effective bonding length was defined as the distance from the pre-crack to the position where 97% of the strain value was reached. The values used in this study were calibrated approximately as the distance up to a point where the strain becomes zero.

Ko and Sato 2007 <sup>(2.42)</sup> conducted three experimental variable include i.e.: type of FRP (aramid, carbon and polyacetal), layers (single and double layers), loading hysteresis (monotonic and cyclic model 1 and 2) for 54 specimen. Numerical analysis were also performed to examine the validity of the model and compared well overall the experiment results.

Ceroni et al. 2010 <sup>(2.43)</sup> tested the sample of single lap shear pull out tests with CFRP bonded on one side and applying compressive force to the concrete member and pulling the laminate. CFRP sheet glued in transverse direction to the shear reinforcement, CFRP bar as NSM reinforcement and CFRP fan were three types of CFRP end anchorages used in this experiments. To prevent debonding at the ends, two steel plates were attached. It was observed that debonding occurred along with concrete separation in most cases having no end anchorages. The linear reduction in the failure load was caused by the reduction in CFRP width. Double layers were more effective for lower widths. The bonded lengths did not affect failure load as the lowest bonded length used was 100 mm.

Double lap shear pull out tests with variability in FRP stiffness, bonded lengths and temperature and curing conditions had been undertaken by Ferrier et al. 2010 <sup>(2.44)</sup>. The tests found that curing conditions do not have an effect on the bond strength if the ambient temperature was above 5°C, although a change in failure mode can be observed.

Zhou et al. 2010 <sup>(2.45)</sup> made analytical model of the bond slip relationship for FRP concrete interface. This model was applicable to both long and short bonding length. The conclusion from this research were the bond-slip response with an infinite bonding length was unique and does not vary along the bond face but this conclusion is not applicable when the bonding length is shorter than effective bonding length.

The experiment about the size effect of RC beams strengthened in shear with CFRP strips have been tested by Godat et al 2010<sup>(2.46)</sup>. The three test series have been performed to confirm it condition. The three series were for large, medium and small beam size include U-shape and completely shape. The experimental program consists of seven beams of various sizes grouped. A nonlinear FEM analysis was developed to model the behavior of the CFRP shear strengthened beams. The results confirms that the contributions of the CFRP strips were higher in the smaller specimen.

Arazoe et al 2013<sup>(2.47)</sup> have performed research about bonding characteristics and strengthening effect of CFRP strand sheet with polyurethane soft layer. The use of soft layer was intended to improve the bonding behavior of CFRP strand sheet. By putting soft layer between epoxy adhesive and concrete could make the effective bond layer become longer. Obviously, it could enhance the bonding strength of laminate. The bonding test of this research used double lap shear pull out test based on JSCE<sup>(2.31)</sup> with two kinds of CFRP strand sheet (high tension type and high modulus type). The following results were obtained from the bonding test were; for high tension type, soft layer specimen can increase the maximum load compared than no soft layer specimen and show different in failure mode; for high modulus type, the maximum load and failure mode was almost same for both soft layer and no soft layer specimen. It can be seen that the effective bonding length of this specimen was yet unclear. Meanwhile, the effects of soft layer for RC strengthening can be described as follows the failure mode for soft layer specimen was splitting failure while peeling failure was typical failure mode for no soft layer specimen. Soft layer can raise the maximum load and produce longer displacement.

Arai et al 2013<sup>(2.48)</sup> conducted a study of bonding properties of CFRP strand sheet using polyurea soft layer at elevated temperature. Specimen of this research test has a longer specimen than previous with single lap shear pull out tests. The length of this specimen was 700mm. The temperatures were set at 23<sup>0</sup>C as reference temperature, 50<sup>0</sup>C and 70<sup>0</sup>C as comparison. The finite element analysis have been done to confirm the experimental results. As a result the fracture energy of 50<sup>0</sup>C and 70<sup>0</sup>C soft layer specimen were 0.95 and 0.38, respectively, compared than fracture energy of standard temperature.

Arazoe et al 2014<sup>(2.49)</sup> carried out bonding properties and flexural behavior of CFRP strand sheet with soft layer system. The lap shear pull out tests were done for bonding test with specimens have a length of 500mm and a width of 100mm. The result

from bonding test showed that maximum load of soft layer specimen increased around three times than no soft layer specimen with different failure mode. Besides that, fracture energy of soft layer specimen was enhanced until five times than no soft layer specimen. The results from flexural test of RC beams could be described that the specimen with polyurea had higher maximum load and deflection than no soft layer specimen. The failure mode of soft layer was splitting failure of the beam cover, whereas peeling failure was failure mode for no soft layer specimen.

## **2.7 Issued addressed in this study**

As was stated in the literature review that the bond strength of FRP laminate to concrete is affected by concrete strength, surface preparation of concrete, adhesive properties (adhesive shear stiffness), FRP type and FRP stiffness, and also bonding length. However, the bond strength do not increase if the bonding length exceed the existing effective bonding length.

In this study a laboratory test and a finite element analysis were carried out to examine the bonding test between CFRP and concrete and the strengthening RC beam. This research focuses mainly on the interface bond, including its evaluation, FEM modelling and influence on RC member behavior.

Types of CFRP used in this study are CFRP strand sheet, high tension and high modulus type of CFRP plate. While the type of adhesive used are epoxy, MMA (methyl methacrylate) and PCM (polymer cement mortar), as well as application of polyurea soft layer which has small tensile modulus to find out the CFRP plate-concrete bonding behavior.

**Chapter 3** discusses strengthening effect of CFRP strand sheet with various types of adhesive on the RC beams. This strengthening method used three types of adhesive namely epoxy, MMA and PCM. Meanwhile, **Chapter 4** and **Chapter 5** describe of bonding behavior of CFRP and concrete, to obtain the objective the double lap shear pull out test was conducted. **Chapter 4** discusses the bonding behavior of CFRP strand sheet and concrete with MMA and PCM adhesives by varying the amount of layers. **Chapter 5** examines the bonding behavior of CFRP plate-concrete interface. This chapter is intended to clarify the effect of putting a polyurea soft layer between usual adhesive (epoxy) and concrete. The types of CFRP plate used in this study are high tension and high modulus

type with thickness variation of each CFRP plate type.

## REFERENCES

- 2.1 De Cicco F., “Numerical Analysis the Debonding of FRP Flexural Reinforcement of RC Members” Ph.D Dissertation, University of Naples “Federico II”, 2008.
- 2.2 Ueda T., “FRP for Construction in Japan” In: Joint Seminar on Concrete Engineering, Mongolia, 2005.
- 2.3 Kobayashi A., Hidekuma Y. and Saito M. “Application of the FRP for Construction as High Durability Materials in Japan” Proc. US-Japan Workshop on Life Cycle Assessment of Sustainable Infrastructure Materials, Sapporo, Japan, 2009.
- 2.4 Kobayashi A., Sato Y. and Takahashi Y, ”Basic Characteristics of FRP Strand Sheet and Flexural Behavior of RC Beams Strengthened with FRP Strand Sheet” Proc. of APFIS, Seoul Korea, 2009.
- 2.5 Dai J. G. and Ueda T., “Local Bond Stress Slip Relations for FRP Sheet-Concrete Interface” In: FRPRCS-6, Fibre Reinforced Polymer Reinforcement for Concrete Structures, Singapore (2003).
- 2.6 Lu X.Z., Teng J.G. and Jiang J. J. “Bond-slip model for FRP sheets/plates bonded to concrete” J. Engineering Structure, 27, 920-937, 2005.
- 2.7 Web site, <https://en.wikipedia.org/wiki/Polyurea>.
- 2.8 Broekaert M., “Polyurea Spray Coatings-The Technology and Latest Development” not published, Copyright © 2002 Huntsman International LLC. All rights reserved. 01-2002.
- 2.9 Nippon Coating International Ltd. “Polyurea Coating Technologies and Solutions” not published.
- 2.10 Athawale P. “Analysis of Factors Affecting Effective Bond Length for FRP Composite Laminate Externally Bonded to Concrete Substrate” Master Thesis, Texas Tech University, 2012.
- 2.11 Guo R., Yamaguchi K., Hino S. and Miyano N., “Shearing Capacity for RC Beam with Haunch Retrofitted by CFRP GRID Spraying PCM Shotcrete” Proc. of the 6th International Conference of Asian Concrete Federation, Seoul, Korea, 2014.
- 2.12 Osada K., Yasima N., Terada K. and Ikeda S., “ Seismic Retrofitting of Reinforced Concrete High Piers with Carbon Fiber Sheets” Concrete research and technology, JCI, Vol. 11, No.3, pp. 39-48 (2000) , (in Japanese).
- 2.13 Bahsuan R., Hino S. and Komori A., “Flexural Strengthening Effect of CFRP

- Strand Sheet to RC Beams with Various Types of Adhesive” Proc. of the 2nd Makassar International Conference on Civil Engineering, Makassar, Indonesia, 2015.
- 2.14 Nakaba K., Kanakubo T., Furuta T. and Yoshizawa H., “Bond Behavior between Fiber-Reinforced Polymer Laminates and Concrete” ACI Structural Journal, V98, No. 3, 2001.
  - 2.15 Yoshizawa H, Myojo T, Okoshi M, Mitzukoshi M, Kliger HS, "Effect of Sheet Bonding Condition on Concrete Members Having Externally Bonded Carbon Fiber Sheet," Proceedings of the 4th Materials Engineering Conference, Materials for the New Millennium, V. 2. 1996, pp. 1608-16.
  - 2.16 Toutanji H, Ortiz G, "The effect of surface preparation on the bond interface between FRP sheets and concrete members," Composite Structures, V. 53, No. 4. 2001, pp. 457-62.
  - 2.17 Benyoucef S, Tounsi A, Adda Bedia EA, Meftah SA, "Creep and Shrinkage Effect on Adhesive Stresses in RC Beams Strengthened with Composite Laminates," Composites Science and Technology, V. 67, No. 6. 2007, pp. 933-42.
  - 2.18 Yoshizawa H, Wu Z, Yuan H, Kanakubo T, "Study on FRP-Composite Interface Bond Performance," Journal of Materials, Concrete Structures and Pavements of JSCE, V. 662, No. 49. 2000, pp. 105-19.
  - 2.19 De Lorenzis L, Miller B, Nanni A, "Bond of fiber-reinforced polymer laminates to concrete," ACI Materials Journal, V. 98, No. 3. , pp. 256-64, 2001.
  - 2.20 Brosens K, Van Gemert D, "Anchoring Stresses between Concrete and Carbon Fibre Reinforced Laminates," Proceedings of the 3rd International Symposium (FRPRCS-3), Non-metallic (FRP) Reinforcement for Concrete Structures, V. 1. 1997, pp. 271 - 8.
  - 2.21 Bizindavyi L, Neale KW, "Transfer lengths and bond strengths for composites bonded to concrete," Journal of Composites for Construction, V. 3, No. 4. 1999, pp. 153-60.
  - 2.22 Pham H. B., Mahaidi R. “Modelling of CFRP-Concrete Shear-lap Tests” Construction and Building Material, 21, pp. 727-35, 2007.
  - 2.23 Ueda T. and Dai J., “Interface Bond between FRP Sheets and Concrete Substrate: Properties, Numerical Modelling and Roles in Member Behavior” Prog. Struct.

- Engg. Mater. 7, 27-43, 2005.
- 2.24 Mongi B.O., et all “Effective Bond Length of FRP sheet externally bonded to concrete” International Journal of Concrete Structure and Material Vol. 3 No. 2, pp 127 –31, Dec. 2009.
- 2.25 Sugiyama “Bonding Properties of RC Member Using CFRP Grid and CFRP Strand Sheet Strengthening Method” Master Thesis, Kyushu University, 2011. (In Japanese)
- 2.26 Woo S. K., Kim J.H., Byun K. J. and Song Y.C., “Bond-slip Parameter Determination Procedure of RC Flexure Member Strengthened with Prestressed CFRP Plates” KSCE Journal Civil of Engineering 17(1), pp 179-191, 2013.
- 2.27 Popovics S. “A Numerical Approach to Complete Stress-Strain Curve of Concrete” Cement and Concrete Research, Vol. 3, pp 583-559, 1973.
- 2.28 Guo Z. G., Cao S. Y., et. all “Experimental Study on Bond Stress-Slip Behavior Between FRP Sheets and Concrete” Proc. International Symposium on Bond Behavior of FRP in Structures, Hongkong, December 2005.
- 2.29 Kanakubo T., Furuta T., Fukuyama H. “Bond Strength between Fiber Reinforced Polymer and Concrete” In: FRPRCS-6, Fibre Reinforced Polymer Reinforcement for Concrete Structures, Singapore, 2003.
- 2.30 Yuan H., Teng J. G. , Seracino R., Wu Z. S. , Yao J., "Full-Range Behavior of FRP-to-Concrete Bonded Joints" Engineering Structures, V. 26, No. 5 , pp. 553-65, 2004.
- 2.31 Japan Society of Civil Engineering (JSCE); 'Standard specification for concrete and structure, test method and specification' (May 2007).
- 2.32 Chajes M.J., Finch W.W., Januszka T.F. and Thomson T.A., "Bond and force transfer of composite material plates bonded to concrete," ACI Structural Journal, V. 93, No. 2. , pp. 208-17, 1996.
- 2.33 Maeda T, Asano Y, Sato T, Ueda T, Kakuta Y, "A Study on Bond Mechanism of Carbon Sheet," Proceedings of the 3rd International Symposium (FRPRCS-3), Non-metallic (FRP) Reinforcement for Concrete Structures, Sapporo, Japan,, V. 1. pp 7, 1997.
- 2.34 Bizindavyi L. and Neale K. W., "Transfer lengths and bond strengths for composites bonded to concrete," Journal of Composites for Construction, V. 3, No. 4. pp. 153-60. 1999.



- 2.35 Dai J.G., Sato Y. and Ueda T, "Improving the Load Transfer and Effective Bond Length for FRP Composites Bonded to Concrete," Proceedings of Japan Concrete Institute, V. 24, No. 2. , pp. 1423-8, 2002.
- 2.36 Yuan H, Teng JG, Seracino R, Wu ZS, Yao J, "Full-range behavior of FRP-to-concrete bonded joints," Engineering Structures, V. 26, No. 5 , pp. 553-65, 2004.
- 2.37 Yao J, Teng JG, Chen JF, "Experimental study on FRP-to-concrete bonded joints," Composites Part B-Engineering, V. 36, No. 2, pp. 99-113, 2005.
- 2.38 Sharma S. K., Ali M. S. M., Goldar D and Sikdar PK, "Plate-concrete interfacial bond strength of FRP and metallic plated concrete specimens," Composites Part B-Engineering, V. 37, No. 1, pp. 54-63, 2006.
- 2.39 Boschetto G, Pellegrino C, Tinazzi D, Modena C, "Bond Behaviour between FRP Sheets and Concrete: an Experimental Study," Proceedings of the 2nd International Congress, FIB, Naples, Italy, June 2006 CD-Rom, paper ID: 10-12. 2006.
- 2.40 Toutanji H., Saxena P., Zhao L.Y. and Ooi T., "Prediction of interfacial bond failure of FRP-Concrete surface," Journal of Composites for Construction, V. 11, No. 4, pp. 427-36, 2007.
- 2.41 Iwashita K, Wu ZS, Ishikawa T, Hamaguchi Y, Suzuki T, "Bonding and debonding behavior of FRP sheets under fatigue loading," Advanced Composite Materials, V. 16, No. 1, pp. 31-44, 2007.
- 2.42 Ko H. and Sato Y., "Bond Stress-Slip Relationship between FRP Sheet and Concrete under Cyclic Load" Journal of Composite for Construction, Vol. 11, No. 4, pp. 419-426, 2007.
- 2.43 Ceroni F, Pecce M, "Evaluation of Bond Strength in Concrete Elements Externally Reinforced with CFRP Sheets and Anchoring Devices," Journal of Composites for Construction, V. 14, No. 5, pp. 521-30, 2010.
- 2.44 Ferrier E., Quiertant M., Benzarti K. and Hamelin P., "Influence of the properties of externally bonded CFRP on the shear behavior of concrete/composite adhesive joints," Composites Part B-Engineering, V. 41, No. 5, pp. 354-62, 2010.
- 2.45 Zhou Y. W., Wu Y. F. and Yun Y., "Analytical modeling of the bond slip relationship at FRP-concrete interface for adhesively-bonded joint" Composite: Part B, No. 41, pp 423-433, 2010.
- 2.46 Godat A., Qu Z., Lu X. Z., Labossiere P., Ye P., Neale K.W., "Size effects for

reinforced concrete beams strengthened in shear with CFRP strips” Journal of composite for construction, Vol. 14., No. 3., pp 260-271, 2010.

- 2.47 Arazoe M., Sato Y., Takahashi Y., Kobayashi A., “Bonding Characteristics and Strengthening Effect of Strand Sheet with Soft Layer” (not publish paper), 2013.
- 2.48 Arai T., Arazoe M., Sato Y., “ A Study on Bonding Property of CFRP Strand Sheet using Polyurea Soft Layer at Elevated Temperatures” (not publish paper), 2013.
- 2.49 Arazoe M., Kobayashi A., Takahashi Y., Sato Y., “Bonding and Flexural Behaviors of RC Members with CFRP Strand Sheets-Polyurea Soft Layer System” Proceeding of the 7th International Conference on FRP Composite in Civil Engineering CICE 2014, Vancouver, Canada, August 2014.

## CHAPTER 3

### FLEXURAL STRENGTHENING EFFECT OF CFRP STRAND SHEET ON RC BEAMS

---

#### 3.1 Introduction

As a flexural strengthening for existing concrete member, CFRP strand sheet bonding method has become a popular technique all over the world. This technique can be carried out while the structure is still in use. This material does not suffer from corrosion problem, and most of their mechanical and physical properties are better than those of steel <sup>(3.1)</sup>. In this strengthening method, the performance of the CFRP strand sheet to concrete interface in providing an effective stress transfer is of crucial importance <sup>(3.2)</sup>.

From similar studies related to CFRP strand sheet was known that the behavior of RC beam reinforced beams which are strengthened are influenced by several parameters. The parameters have been studied by Godat et al. <sup>(3.3)</sup>, who conducted research on the effect of size for the CFRP strip strengthened RC beams in shear capacity. The effect of shear reinforcement models and techniques have been studied by Zhang et al. <sup>(3.4)</sup>. In addition, a complete behavior between the FRP and the concrete has been discussed by the Yuan et al. <sup>(3.2)</sup> between the experimental results with a theoretical analysis.

To investigate the behavior and all parameters of the strengthened beams, a finite element analysis can be used. However, experimental results are required to validate the numerical predictions <sup>(3.3)</sup>. Most of the previous studies using numerical prediction showed that having not assumed perfect bonding between FRP and concrete generally produces erroneous predictions on the maximum load capacity and stress levels (Al-Mahaidi et al. <sup>(3.5)</sup>, Santhakumar et al. <sup>(3.6)</sup>, Elyasin et al. <sup>(3.7)</sup>). In general, many studies have found that the model for the interfacial behavior between the FRP and the concrete is not able to accurately predict debonding. The bond performance between the FRP and the concrete may directly influence the stress transfer and the cracking behavior, whereas the presence of concrete cracks would cause high stress concentration or debonding between the FRP and the concrete and influence the bonding performance <sup>(3.8)</sup>.

The method of strengthening with a CFRP strand sheet has some advantages such

as excellent corrosion resistance, thinness, low weight, easier and faster in construction time, and adjustable application processing method of concrete. Besides those, it can be used without impregnating adhesive material into the concrete and has a low possibility of air bubble occurrence in the interface area between CFRP strand sheet and concrete. The strengthening method using CFRP strand sheet can ensure a wide bonding area with equal reinforcing resulting excellent reinforcing effect for improving the debonding resistance and application of at lap joint also is possible. Next, an application of strengthening method of CFRP strand sheet on RC members with various types of adhesive will be discussed in this chapter.

### **3.2 Research objective**

The overall aim of this research was to examine the suitability of CFRP strand sheet for externally bonded strengthening of RC beams subjected to static loading. The following objectives of this research have been established:

- To understand the failure modes of strengthened RC beams by CFRP strand sheet method with various types of adhesive.
- To study the flexural strengthening effect of CFRP strand sheet to RC beams with various types of adhesive.
- To evaluate the numerical analysis of strengthened RC beams by CFRP strand sheet with various types of adhesive.

### **3.3 Material properties**

This study used three types of adhesive namely epoxy, methyl methacrylate (MMA), and polymer cement mortar (PCM). Epoxy putty is commonly used as a standard adhesive in the use of FRP. MMA putty is a quick-hardening adhesive can also be used in low-temperature conditions. MMA putty can be used after two hours of installing. PCM consists of polymer-emulsion, cement, and sand, is used for wet surfaces. It can be applied for waterways or tunnel structures. PCM consists of polymer, cement and sands. **Table 3.1** shows the mechanical properties of the adhesive. The properties of CFRP strand sheet and adhesives were obtained from the manufacturer. High tension type of CFRP strand sheet was used in this study. For more detail, its mechanical properties can be viewed in **Table 3.2**.

**Table 3.1** Mechanical properties of adhesive (MPa)

Type	Epoxy	MMA	PCM
Compressive Strength	78.3	79.0	11.3
Compressive Modulus	3,970	2,500	4,800
Tensile Strength	35.8	43.0	4.8
Flexural Strength	58.8	71.0	6.5
Lap-share Strength	25.8	22.0	-

**Table 3.2** Mechanical properties of CFRP strand sheet

Type	High- tension type
Tensile Strength (MPa)	3,400
Lap-share Strength (MPa)	245,000
Design Thickness (mm)	0.333
Unit Weight (g/m <sup>2</sup> )	600

**Table 3.3** Mechanical properties of steel reinforcement (MPa)

Mechanical properties	Steel reinforcement		
	Dia. 10mm	Dia. 13mm	Dia. 19mm
Elasticity modulus		200,000	
Tensile strength	548	551	559
Yield strength	376	395	407

The mechanical properties of concrete used in this study were 49.8MPa, 4.23MPa, and 33,800MPa for compressive strength, tensile strength and modulus elasticity, respectively. Then, **Table 3.3** presents mechanical properties of steel reinforcement in RC beam. Deformed bars of 19mm in diameter were used as tension reinforcement, 10mm in diameter were used as compression reinforcement, and stirrups as shear reinforcement have a diameter of 13mm.

### 3.4 The use of adhesive for strengthened RC beams

**Fig. 3.1(a)** and **Fig. 3.1(b)** are the cross-section of CFRP strand sheet strengthening method using epoxy putty as an adhesive for both one and two layers. The process of implementation can be explained as follows; epoxy putty prepared was coated on the concrete, then followed by attaching process of CFRP strand sheet. CFRP strand

sheet was placed while under pressure to be evenly distributed. After it was done, the next layer was coated in the same way.

**Fig. 3.1(a)** and **Fig. 3.1(b)** also illustrate in brief the cross section of strengthening types used MMA as an adhesive for both one and two layers. The stages of implementation are as follows; prepared the primer material, then given evenly on the CFRP strand sheet and the surface of the concrete beam. Next, sprinkled MMA material on the concrete surface. Then the CFRP strand sheets were attached to the concrete surface while pressed in order to be uniformly distributed, after it was done, did overcoat for the next layer. In this study, the use of epoxy putty and MMA putty was about 2.5kg/m<sup>2</sup>.

The use of PCM as an adhesive in retrofitting methods can be seen in the cross-section in **Fig. 3.1(c)** and **Fig. 3.1(d)**. The steps of application areas follows; after prepared PCM mixed with the water, spread thinly on the surface of concrete beams. Subsequently, CFRP strand sheet was attached with on the whole surface and was pressed such that the filling could be evenly distributed, then, followed by the next layer. Finally, CFRP strand sheet was covered with the PCM until designed thickness. In this research, PCM, for surface protection, had a thickness of 10mm from CFRP strand sheet layer.

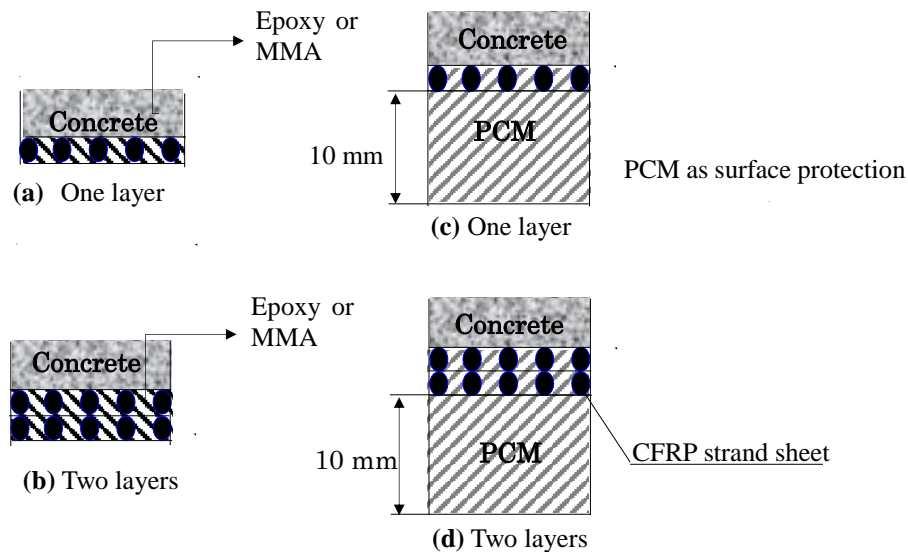


**Fig. 3.1** Cross section of CFRP strand sheet strengthened RC beams

### 3.5 Test set up

Seven RC beams comprising one non-retrofitted beam (specimen N) as control beam and six retrofitted beams for three kinds of adhesive with one layer and two layers of CFRP strand sheet have been tested in this study. Detail of the experimental program can be seen in **Fig.3.2. Detail A** in **Fig.3.2** explains the position of the CFRP strand sheet for the two-layer specimen. To avoid stress concentration at the end of the beam, the CFRP strand sheet was shortened by 25mm for the next layer.

All the beams were four-point loading flexural bending test with two equal loads applied symmetrically about the center of concrete beams that had a span of 2.2m with two small rollers as supports with a distance of 1.6m. The load was applied by a hydraulic jack and measured by a load cell. Deflection control was used in all the tests and deflection measurements were taken at the mid-span of the beam. The fifteen strain gauges were located 100mm on each CFRP strand sheet, four on the steel reinforcement (two for tension rebar and two for compression rebar), and one on the top of the concrete in the mid-span. **Photo 3.1** shows the situation of beam test.

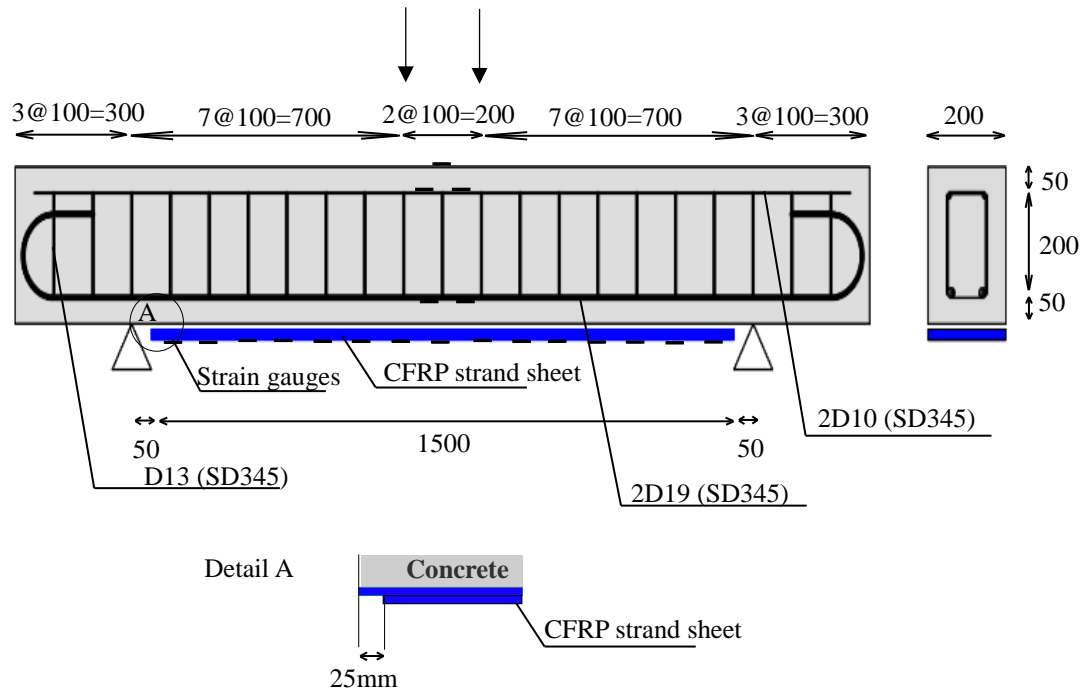


**Fig. 3.2** RC beams specimen detail (unit: mm)



**Photo 3.1** RC beam test

### **3.6 Test results and discussion**

#### **3.6.1 Failure mode**

The failure situation for all specimen until the ultimate loading can be seen in **Photo 3.2(a) ~ (g)**.

Specimen N: crack occurred in some place, especially at the center of the beam. The failure type was bending compression failure (**Photo 3.2(a)**).

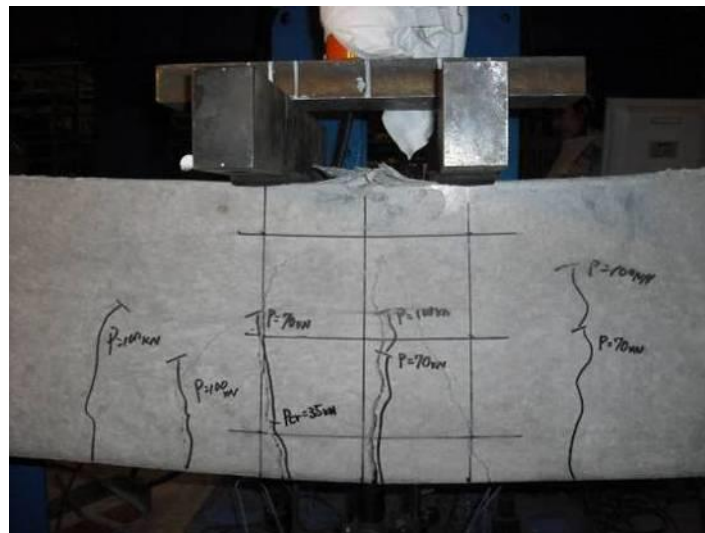
Specimen with epoxy adhesive: cracks spread along the CFRP strand sheet laminate area. The failure was started at the CFRP strand sheet end due to the stress concentration and ends up with debonding propagation inwards. The large crack happened along the tensile rebar area. At the interface between concrete and CFRP strand sheet area, the part of the concrete surface existing is attached to the strand sheet. The failure mode is CFRP interfacial debonding and the concrete cover separation failure. **Photo 3.2(b)** shows failure mode for specimen Epoxy1 (one layer of CFRP strand sheet) and **Photo 3.2(c)** shows failure mode for specimen Epoxy2 (two layers of CFRP strand sheet).

Specimen with MMA adhesive: cracks were distributed along the CFRP strand sheet area. Cracks were started from under loading point along tensile bar when the load is small. The number of cracks is less than beam specimen with epoxy adhesive. A little part of concrete surface existing is attached to the CFRP strand sheet at the interface



between concrete and CFRP strand sheet area. The failure mode is mid-span debonding initiated by a flexural crack. The failure mode of specimen with MMA as adhesive for CFRP strand sheet one layer (specimen MMA1) and two layers (specimen MMA2) can be seen in **Photo 3.2(d)** and **Photo 3.2(e)**, respectively.

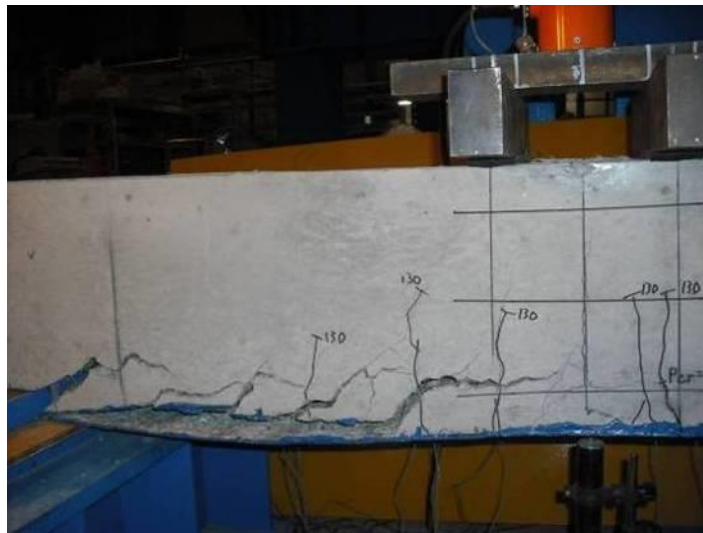
Specimen with PCM adhesive: cracks were distributed in the range of 600mm from beam center. Cracks were started from under loading point along the tensile bar. At the interface between concrete and CFRP strand sheet area, a little part of concrete surface existing is attached to the CFRP strand sheet. The failure mode is peeling off the CFRP and the concrete and bending failure. **Photo 3.2(f)** and **Photo 3.2(g)** show the failure mode of specimen with PCM as adhesive for one layer (specimen PCM1) and two layers (PCM2) of CFRP strand sheet, respectively.



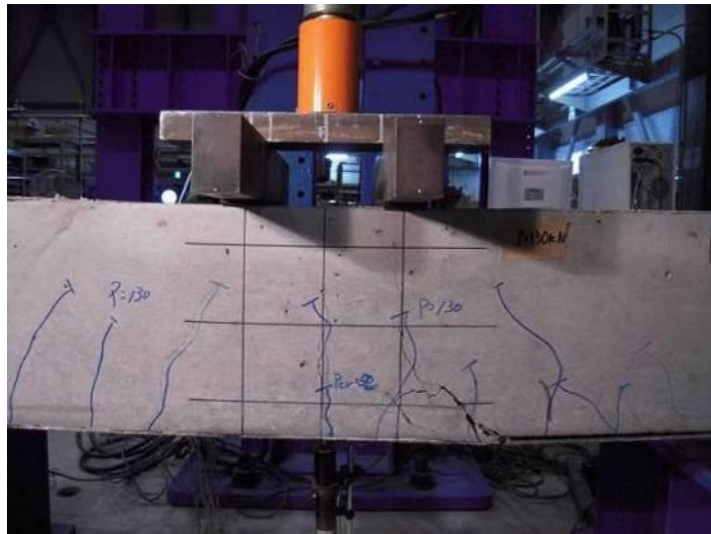
a. Specimen N



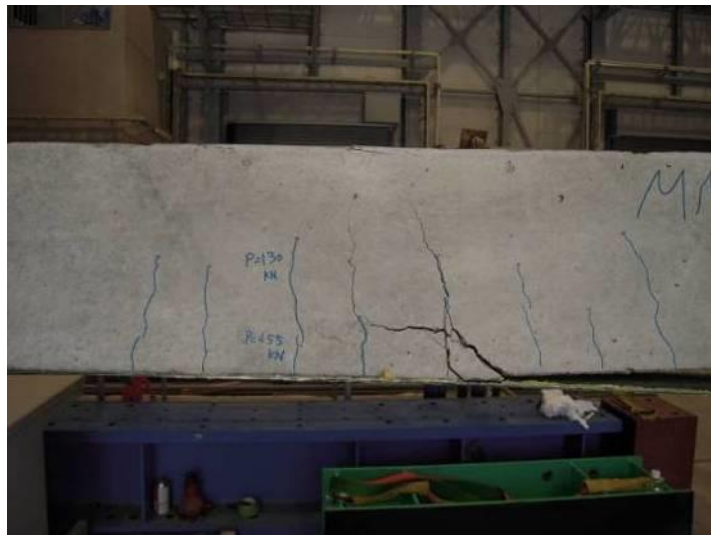
b. Specimen Epoxy1



c. Specimen Epoxy2



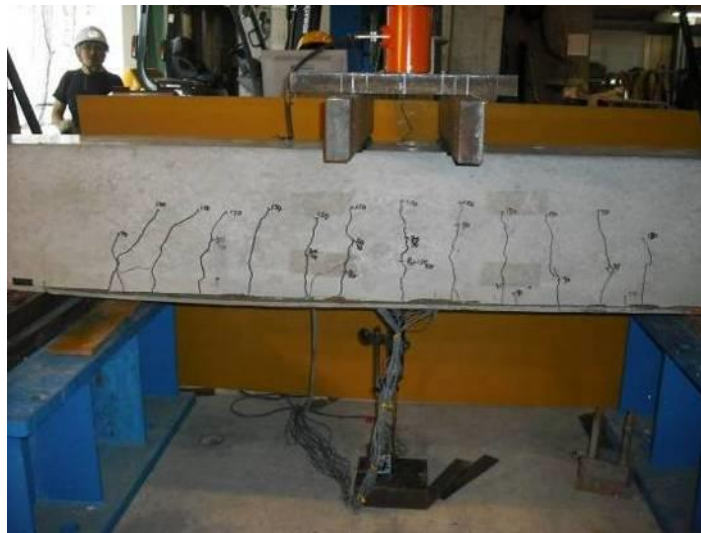
d. Specimen MMA1



e. Specimen MMA2



f. Specimen PCM1



g. Specimen PCM2

**Photo 3.2** Crack pattern and failure condition of specimens



**Photo 3.3** Failure detail of specimen PCM2

**Table 3.4** Experimental and FEM load results

Spec.	Layers numbers.	Experimental results			FEM analysis results	$P_{max.}$ Exp./FEM
		$P_{crack}$ (kN)	$P_{yield}$ (kN)	$P_{max.}$ (kN)	$P_{ultimate}$ (kN)	
N	-	39.8	131	165	155	1.06
Epoxy1	1	50.4	191	278	257	1.08
Epoxy2	2	55.0	236	295	269	1.09
MMA1	1	50.1	205	255	245	1.04
MMA2	2	55.3	216	272	265	1.03
PCM1	1	40.1	171	223	195	1.14
PCM2	2	35.1	191	201	220	0.91

### 3.6.2 Loading stages

The experimental results for each loading stage are given in **Table 3.4**. There were three stages loading can be observed, that is, crack load, yield load, and ultimate load. The results showed an increase in almost all stages of loading. When in the crack state, there was an increase in almost the crack load. For the epoxy adhesive, an increase in crack load was 27% and 38% for the Epoxy1 and Epoxy2 beam, respectively, compared with the control beam (specimen N). For specimen with the MMA adhesive, the results were 26%

and 39% for the MMA1 and MMA2, respectively, higher than the control beam (specimen N). Meanwhile, for PCM1, there was the almost same result with the specimen N. On the other hand, for the PCM2, a decrease in crack load occurred compared with the specimen N. It was possible that initial crack has happened prior to loading on the PCM2.

From **Table 3.4** can be seen that all strengthened beams with CFRP strand sheet have an increase in capacity of yield load compared to the specimen N at the yield loading stage. These showed that an increase of 46% and 80% in the yield load occur for the Epoxy1 and Epoxy2, respectively. For the MMA adhesive, there was an increase of 56% and 65% for the MMA1 and MMA2, respectively. For the PCM adhesive, an increase of 31% and 46% occurred in the PCM1 and PCM2, respectively. It means that the CFRP strand sheet and the adhesives could delay the reinforcing steel to experience yield.

**Table 3.4** also describe the results of maximum load for each specimen. An increase in capacity was observed 46% and 80% of the normal beam for Epoxy1 and Epoxy2, respectively. For MMA adhesive, an increase of 55% and 65% in ultimate over the control beam for MMA1 and MMA2, respectively. For the beam with PCM adhesive, there was an increase of 35% and 22% for PCM1 and PCM2, respectively.

It could be noted that although there is an increase in maximum load but the use of one layer of CFRP strand sheet (PCM1) is more effective than two layers (PCM2) for PCM adhesive. This is different from the assumption that increasing the number of layers will increase the capacity of the beam. This may be caused by the PCM has low shear strength so the interface layer between CFRP strand sheets not effective to resist the existing shear stress and decreases the capability of existing composite mechanisms at the maximum load. Based on this case, the use of CFRP sheet strand more than one layer is not recommended to use PCM adhesive. **Photo 3.3** shows the failure detail of specimen PCM2.

### 3.6.3 Load and displacement

**Fig. 3.3** shows the relationship between total load and mid-span deflection of the specimen. In general, it may be noted that after the maximum load was achieved, the load will decrease closer to the yield load on the specimen N. It means that the specimens show ductile behavior before failure, so it may be able to absorb the energy well and can avoid the occurrence of a sudden collapse.

Prior to the crack occurrence in the center of the beam, the stiffness of the curve showed almost same result compared control beam (specimen N) and strengthened beams, but there were some differences in the term of curve stiffness after the crack. The stiffness of strengthened beams tend to remain but the specimen N stiffness declining slowly. The Epoxy2 had the highest stiffness after the crack occurrence until the maximum load, followed by MMA2, MMA1, and Epoxy1, respectively. While, among strengthened beams, PCM1 and PCM2 showed decline slightly greater stiffness after the crack occurrence.

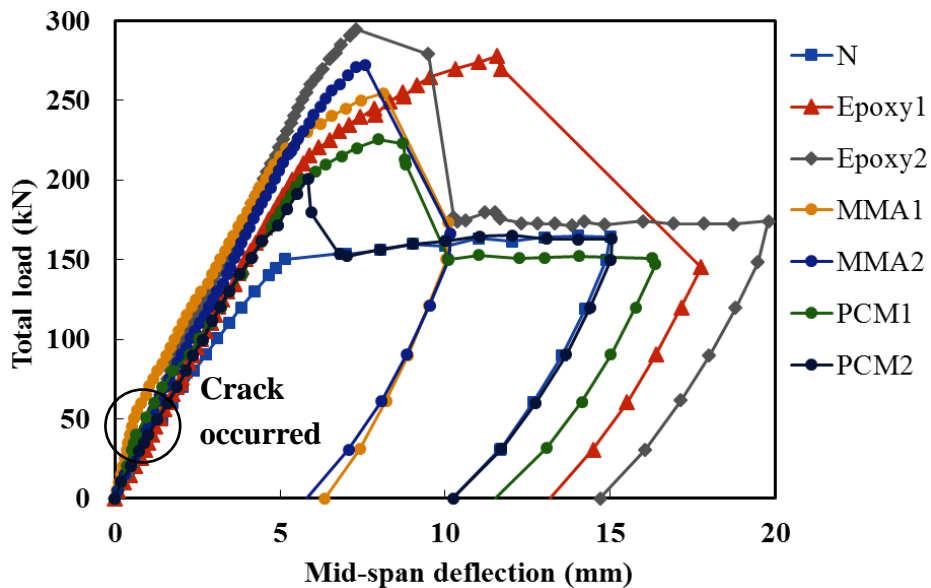


**Fig. 3.3** Total load versus mid-span deflection

#### 3.6.4 Load and strain of CFRP strand sheet

Load and strain of CFRP strand sheet at the mid-span is shown in **Fig. 3.4**. It can be seen that the first crack occurred on the surface of the beam at about 40–55kN (as can see in **Table 3.4**), an exception in the specimen PCM2 (35kN). It also confirmed that the initial crack occurred in the specimen PCM2.

After crack, Epoxy1 and MMA1 had a decrease significantly of the slope curve, but after around the load of 70kN, gained strain hardening until the load of 210kN. Then, the curve decreases again until the maximum load achieved. This behavior differs with Epoxy2, MMA2, PCM1, and PCM2. After crack, the reduction in slope curve was not too

big with the Epoxy2 had a largest ultimate strain.

The maximum ultimate strain that could be reached was around  $7000\mu$  for both the Epoxy1. Next, ultimate strain for the specimen MMA1 was around  $6000\mu$ , and followed by the Epoxy2 was around  $4500\mu$ . In addition, the other specimens had ultimate strain around  $2500\mu$ . It can be seen that CFRP strand sheet's ultimate strain (about  $13500\mu$ ) can never be reached. So, although epoxy, MMA, and PCM, as an adhesive in this strengthening method, could improve the capacity of the RC beam, it is not able to maximize the strength of the CFRP strand sheet.

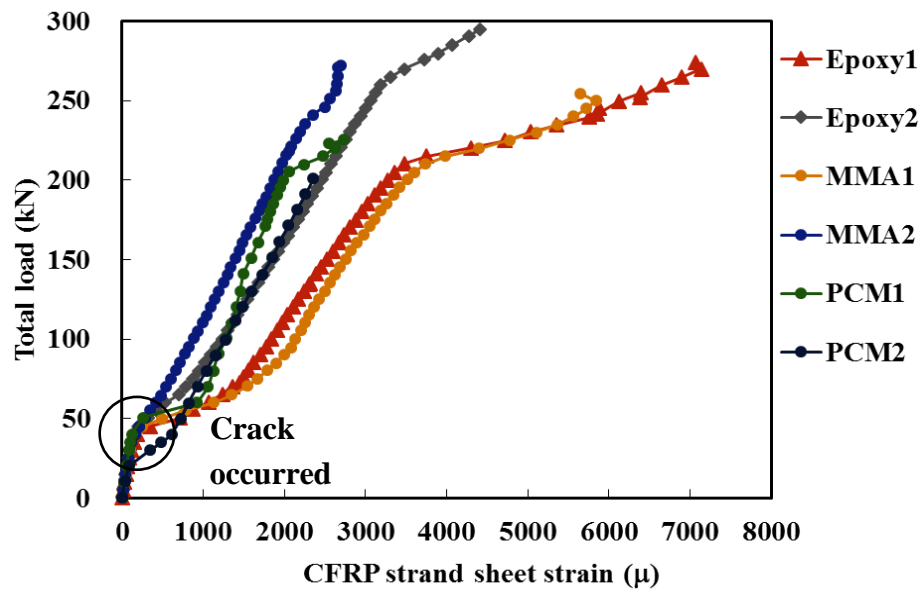


Fig. 3.4 Total load versus strain of CFRP strand sheet at mid-span

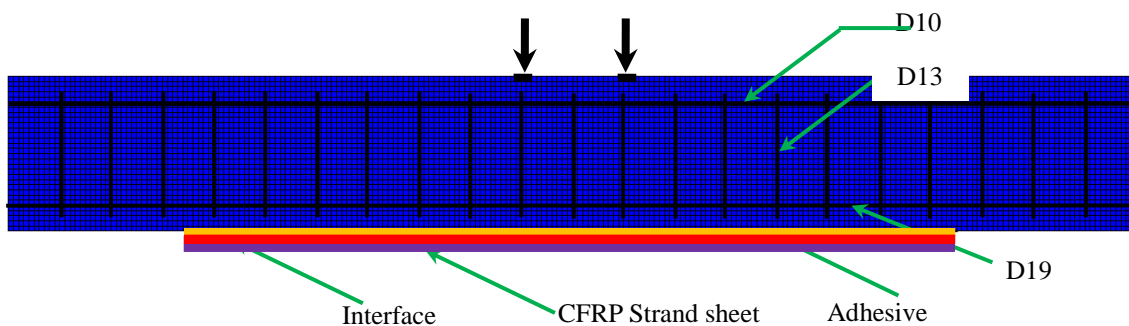


Fig. 3.5 Schematic of FEM element



### 3.7 Finite Element Analysis for Flexural Strengthening of CFRP Strand Sheet on RC Beams

This section will be verified FEM analysis of CFRP sheet strand using PCM as an adhesive. The results of the further analysis will be verified with the results of experiments that had been conducted on specimens N, specimen PCM1 and specimen PCM2.

#### 3.7.1 Idealization of FEM analysis

**Fig. 3.5** shows the schematic of FEM element. FEM analysis in this paper was done by using a two-dimensional FE analysis using DIANA program (version 9.4.3)<sup>(3.9)</sup>. Next will be explained the model of each material used in this FEM analysis.

The CFRP strand sheet was modeled by using truss element L2TRU. From the DIANA's Element Library<sup>(3.9)</sup>, The L2TRU is a two-node directly integrated (1-point) truss element which may be used in one-, two- and three-dimensional modeling with a basic variable for displacement,  $u_x$ . The CFRP strand sheet was considered as a full elastic material in compression and brittle material in tension. The CFRP strand sheet areas are 66.66mm<sup>2</sup> for one layer and 133.33mm<sup>2</sup> for two layers.

The concrete and the PCM were modeled by applying a four-node quadrilateral linear plane stress element (Q8MEM). Each element has eight degrees of freedom with two displacements ( $u_x$  and  $u_y$ ) at each node<sup>(3.9)</sup>. Concrete and PCM were applied to a rotating crack model with a thickness of 200mm.

A non-linear tension softening proposed by Hordijk<sup>(3.10)</sup> as shown in **Fig. 3.6(a)** was applied to the stress-strain relationship of concrete and PCM in tension area. This relationship uses the expression provided by CEB-FIP Model Code 90<sup>(3.11)</sup>. The area under stress and strain curve is given by  $G_{fc}/h$ , where  $G_{fc}$  is the fracture energy or energy required to spread a tensile crack of unit area and  $h$  is the crack bandwidth related to the area of the concrete element. Based on CEB-FIP Model Code 90, the fracture energy was computed to be 0.083N/mm for concrete and 0.029N/mm for PCM. **Fig. 3.6(b)** shows the behavior of concrete and PCM in the compression area. The behavior was applied to the model proposed by Thorenfeldt, et al.<sup>(3.12)</sup>.

The idealization of reinforcement used bar elements. All the reinforcement materials were applied in terms of the yield condition of Von Misses as an ideal plasticity material.

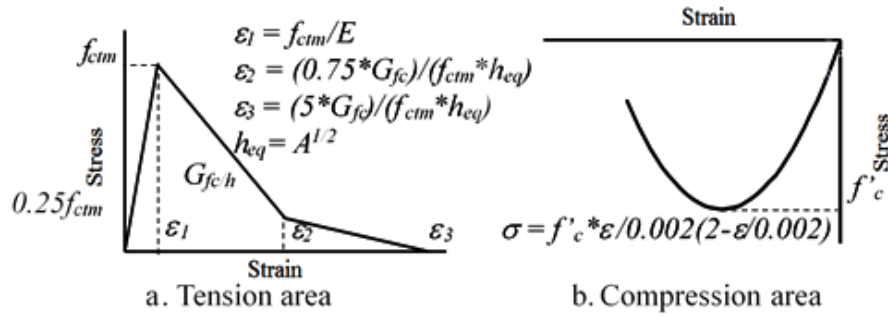


**Fig. 3.6** Constitutive law of concrete

Interface between of concrete and strand sheet was modeled using L8IF. L8IF is a model of the interface element that has a four-node based on linear interpolation between two lines in a two-dimensional configuration <sup>(3.9)</sup>. The interface layer was assumed to be 0.5 mm in thickness with a total perimeter of 320 mm for one layer and 640 mm for two layers of CFRP strand sheet. The linier relationship of bond stress-slip relationship is 1000 N/mm<sup>3</sup> and 1 N/mm<sup>3</sup> for normal and shear stiffness modulus, respectively <sup>(3.13)</sup>.

### 3.7.2 FEM Results and Verification

The bonding between CFRP strand sheet and concrete with PCM as an adhesive is extremely important in order to achieve high mechanical properties in the composite action. It is an often critical point to use the composite material. FEM analysis was carried out to compare and confirm with the experimental test.

#### 3.7.2.1. Crack Pattern

From **Fig. 3.7(a) ~ (c)** and **Photo 3.4(a) ~ (c)** show the specimen failure modes (crack patterns) from both experimental and FEM analysis result. The failure modes of the strengthened beams with CFRP strand sheet are the result of debonding at the interface of concrete beams and CFRP strand sheet. This means that the tensile strength of CFRP strand sheet has not been achieved. The figures show a similar appearance between experiment and FEM analysis results. It means that FEM results captures the crack pattern reasonably well.

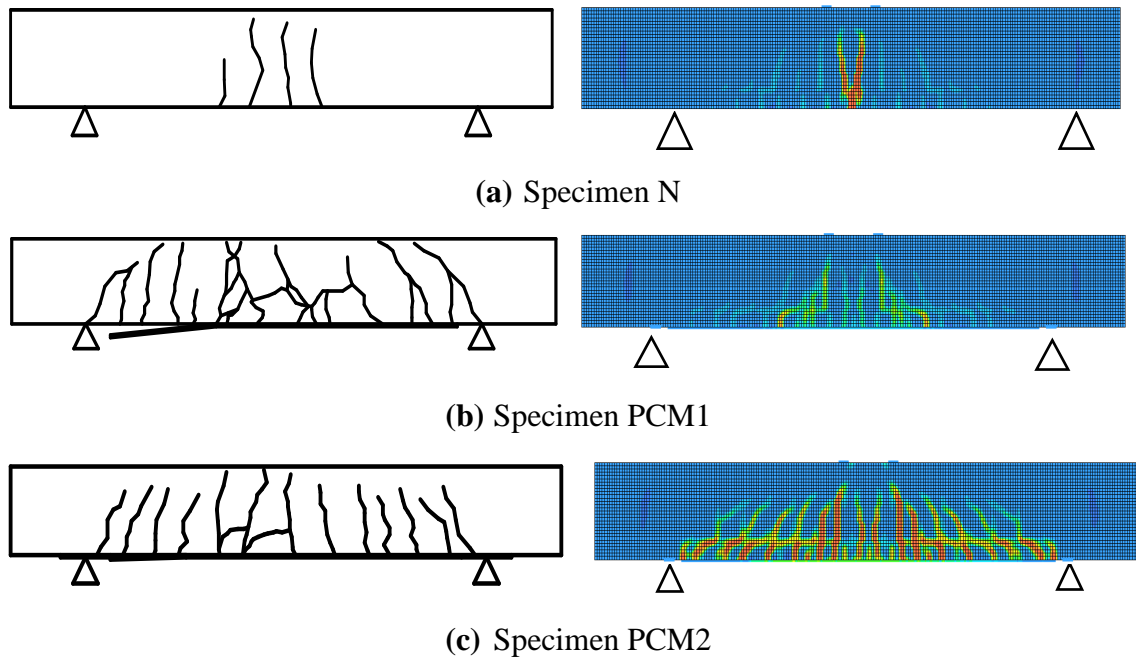


**Fig. 3.7** Specimen crack pattern of experimental and FEM analysis results



(a) Specimen N



(b) Specimen PCM1



(c) Specimen PCM2

**Photo 3.4** Photograph of crack pattern specimen

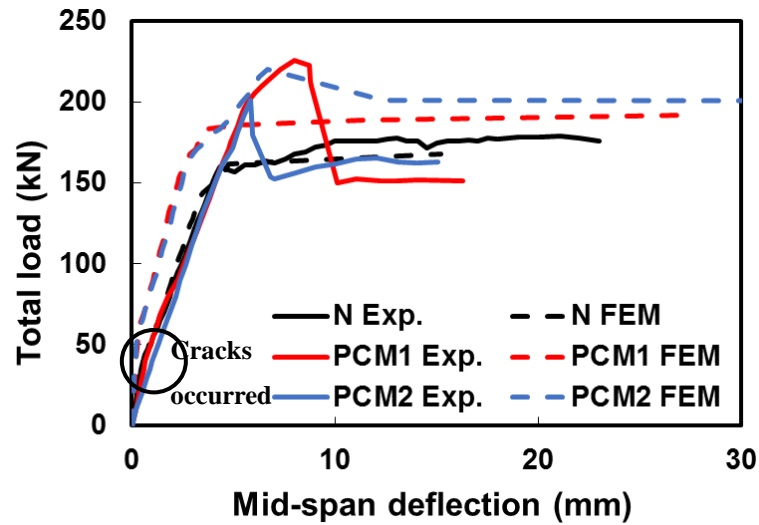


**Fig. 3.8** Total load–mid-span deflection relationship of experimental and FE analysis

#### 3.7.2.2. Load and displacement

Comparison between such total load and mid-span deflection based on both experimental results and FEM analysis results are shown in **Fig. 3.8**. After crack occurred, the stiffness of FEM results are slightly higher than those observed, but generally, the comparisons show a fairly satisfactory agreement. However, it can be seen that the stiffness of strengthened RC beams seems a little differences compared with the test result this indicates that the interface material must be corrected.

#### 3.7.2.3. Load and strain of CFRP strand sheet

Comparison with the mid-span CFRP strand sheet strain for both the experimental and the FEM analysis results is shown in **Fig. 3.9**. It can be seen that a slightly good agreement, except in experimental results of the specimen PCM2. It was due to initial crack was happened before test loading (as described in the previous section). The relationship shows a similar stiffness, however, at higher load, there is a little differences.

In general, the present FEM model was inadequate for predicting the behavior of the strengthened RC beams due to poor in interface modelling.

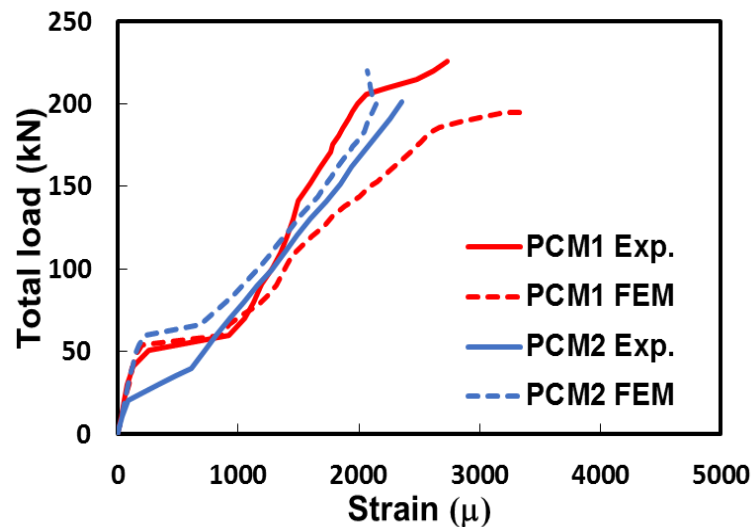


Fig. 3.9 Total load–mid-span strain of CFRP strand sheet

### 3.8 Conclusive remarks

In the present study, in order to carry out a study on reinforcing the effect of the CFRP strand sheet in the case of using a variety of adhesive, it was carried out the beam test. The resulting findings are as follows;

1. The failure mode of the specimen with CFRP strand sheet strengthening was highly dependent on the type of adhesive. Specimen with epoxy adhesive tend to experience CFRP interfacial debonding and concrete cover separation failure. Meanwhile, the specimen with MMA adhesive had a failure at mid-span initiated by a flexural crack. CFRP strand sheet strengthened RC beams that used PCM as adhesive have peeling off with the concrete separation as the failure mode.
2. Epoxy putty, MMA putty, and PCM can be applied as adhesive to the CFRP strand sheet strengthening method on RC beams. It could be seen that all strengthened RC beams increase in all loading stage.
3. The load displacement of all strengthened RC beams showed that after the maximum load was achieved, the total load will be decreased dramatically closer to the yield load on the specimen N. This can be understood that the specimens showed ductile behavior before failure and could avoid the occurrence of a sudden collapse.
4. The FEM analysis was performed to examine the experiment test model validity nevertheless the interface material model must be corrected.

## REFERENCES

- 3.1 Rahimi, H. and Hutchinson, A., “Concrete Beams Strengthened with Externally Bonded FRP Plates” *J. Composite for Construct*, Vol. 5 (1), 2001, pp.44-56.
- 3.2 Yuan, H., Teng, J. G., Seracino, R., Wu, Z. S. and Yao, J., “Full-range Behavior of FRP-to-Concrete Bonded Joints,” *J. Engg. Struc.* 26 (5), Elsevier, 2004, pp.553–565.
- 3.3 Godat. A., Qu. Z., Lu. X. Z., Labosieere. P., Ye. L. P., Neale. K. W., “Size Effect for Reinforced Concrete Beams Strengthened in Shear with CFRP Strips,” *J. Comp. for Cons.* Vol.14 No.3 ASCE, June 2010, pp. 260–271.
- 3.4 Zhang. Z., Tzu. C., “Shear Strengthening of Reinforced Concrete Beams Using Carbon Fiber Reinforced Polymer Laminates,” *J. Comp. for Cons.* Vol.9 No.2. ASCE, April 2005, pp 158–169.
- 3.5 Al-Mahaidi, R., Lee, K., and Taplin, G., “Behavior and Analysis of RC T-beams Partially Damaged in Shear and Repaired with CFRP Laminates,” *Structural congress and Expositon*, P. C. Chang, ed., ASCE, Washington, D. C, Proc., May 2001, pp. 1–8.
- 3.6 Santhakumar, R., Chandrasekaran, E., and Dhanaraj, R.,”Analysis of Retrofit Reinforced Concrete Shear Beam Using Carbon Fiber Composites,” *Electron. J. Struct. Eng.*, 4, 2004, pp. 66–74.
- 3.7 Elyasian, I., Abdoli, N., and Ronaph, H. R.,” Evaluation of Parameter Effective in FRP Shear Strengthening of RC Beams Using FE Method,” *Asian Journal of Civil Engineering (Building and Housing)*, 7(3), 2006, pp 249–257.
- 3.8 Niu, H. and Wu, Z., “Effects of FRP-Concrete Interface Bond Properties on the Performance of RC Beams Strengthened in Flexure with Externally Bonded FRP Sheets” *J. of Materials in Civil Engineering*, Vol 18 (5), 2006, pp. 723-31.
- 3.9 TNO DIANA, “DIANA User’s Manual Version 9.4.3” 1st edition, Delft, The Netherlands (November 2010).
- 3.10 D. A. Hordijk DA; “Local Approach to Fatigue Concrete, Delft University of Technology, (1991).
- 3.11 Comite Euro-International du Beton, “CEB-FIB Model Code 1990,” London, Great Britain; Thomas Telford, 1991.
- 3.12 E. Thorenfeldt, A. Tomaszewics, and J. J. Jensen,; “Mechanical Properties of

High-Strength Concrete and Application in Design, Proc. Symposium Utilization of High-Strength Concrete, Stavanger, Norway (1987)”

- 3.13 Muelman, E., “ Combining Existing Independent Seismic Reinforcing Methods for Clay Brick Masonry” Master Thesis, Delft Technology University, 2016
- 3.14 Bahsuan, R., Yamaguchi, K. and Hino, S., “Experiment and Analysis on Bonding Properties of CFRP Strand Sheet and Concrete,” Memoirs of the Faculty of Engineering, Kyushu University, Vol. 75, No. , July 2015

## CHAPTER 4

### **BONDING BEHAVIOR OF CFRP STRAND SHEET AND CONCRETE WITH MMA AND PCM ADHESIVE**

---

#### **4.1 Introduction**

Many innovations have been carried out for strengthening reinforced concrete structures. Strengthening is required for structural elements in which its strength have been declining due to age, environmental influences, poor design, lack of maintenance, change of function and damage caused by events such as earthquakes and others.

FRP (Fiber Reinforced Plastics) is proposed as a solution for solving this problem, despite having a fairly expensive price. FRP has many advantages such as corrosion resistance, high tensile strength, durability, good fatigue resistance, lighter specific gravity, easy and fast in application, as well as adjustable processing method of concrete. FRP is a composite material that consists of high strength material fiber embedded in a polymeric resin. The type of fiber that is often used in the fabrication of FRP is carbon, then called Carbon Fiber Reinforced Plastics (CFRP), aramid (Aramid Fiber Reinforced Plastics, ARFP) and glass (Glass Fiber Reinforced Plastics, GFRP). **Fig. 4.1** shows a comparison between CFRP, AFRP and GFRP composites, and reinforcing steel in the stress-strain relationship diagram. It can be seen that CFRP is 7 to 8 times stronger than reinforcing steel.

It is worth noting that bonding behavior plays an important role in reinforcing design by using FRP materials as externally strengthening. Recently, many studies have been carried out to find out the bonding behavior between concrete and FRP <sup>(4.1), (4.2), (4.3), (4.4), (4.5), (4.6), (4.7), (4.8)</sup>, but only a few have been discussed about bonding behavior between CFRP strand sheet and concrete. Numerical prediction of the previous study showed that there was no sufficient assumption regarding the bonding behavior and generally produced erroneous predictions on the ultimate load capacity and stress levels.



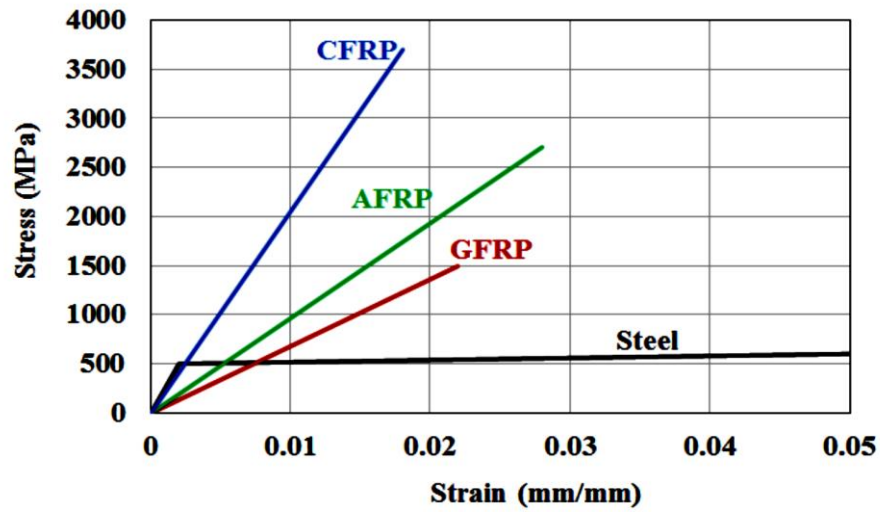


**Fig. 4.1** Stress-strain relationship of reinforcing materials

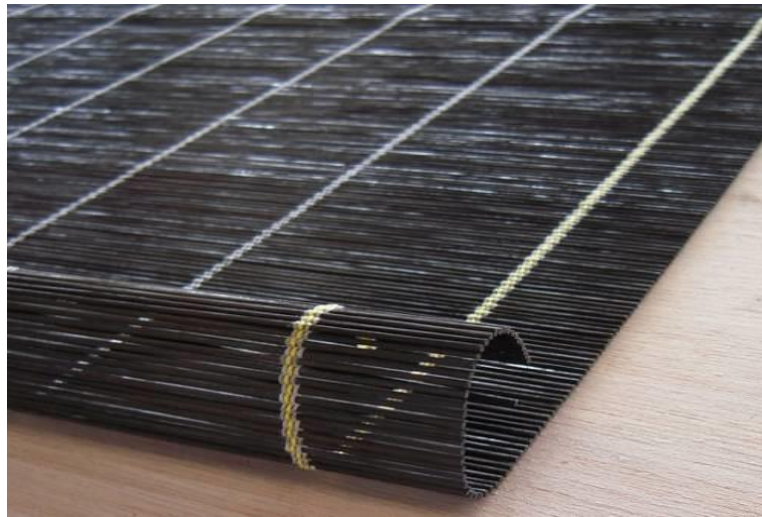


**Photo 4.1** CFRP strand sheet

CFRP strand sheet, as shown in **Photo 4.1**, is one of CFRP interface bonding system that has been recently developed. CFRP strand sheet has only one direction strengthening and is suitable for the structural beam. Some advantages in the utilization of CFRP strand sheet model compared to conventional sheet model are, CFRP strand sheet can be used without impregnating of adhesive material into the concrete and less possibility of air bubble occurrence in the interface area between CFRP strand sheet and

concrete.

This chapter discusses the bonding behavior of CFRP strand sheet and concrete by both experimental and finite element investigation. This research used two types of adhesive namely MMA (methyl methacrylate) and PCM (polymer cement mortar) with variation in numbers of the layer.

## **4.2 Research objective**

The objective of this study is to evaluate the bonding properties of the interface between CFRP strand sheet and adjacent concrete, including adhesive, with MMA and PCM as adhesive. To reach the general purposes, the following specific objectives have been determined as follows;

- To investigate the failure mode or the fracture mode from the specimen with MMA and PCM as adhesive.
- To compare the bonding properties of the specimen with MMA and PCM as adhesive.
- To present a simple analytical way for the local bond-slip relationship based on the strain distribution and then is fitted with by Popovich equation for the specimen with MMA and PCM as an adhesive.
- To verify the experimental results through FEM analysis.

## **4.3 Test set up**

To obtain the objective of this research, a double lap shear pull out bonding test was conducted <sup>(4.9)</sup>. The bonding test was done based on JSCE-E543 –2007 <sup>(4.10)</sup>, about test method for bonding properties of continuous fiber sheet to concrete. In this test method, CFRP strand sheets were bonded to concrete on the both sides of the specimen. The specimens of this research are shown in **Fig. 4.2(a) ~ (c)** and **Photo 4.2**. They were made three for each of sample. The sample were one, two, three layers of CFRP strand sheet for MMA adhesive and one, two layers of CFRP strand sheet for PCM adhesive. The bonding test specimen size 100mm x 100mm x 620mm with two CFRP strand sheets were bonded on two opposite sides of the specimen which have a width of 50mm.

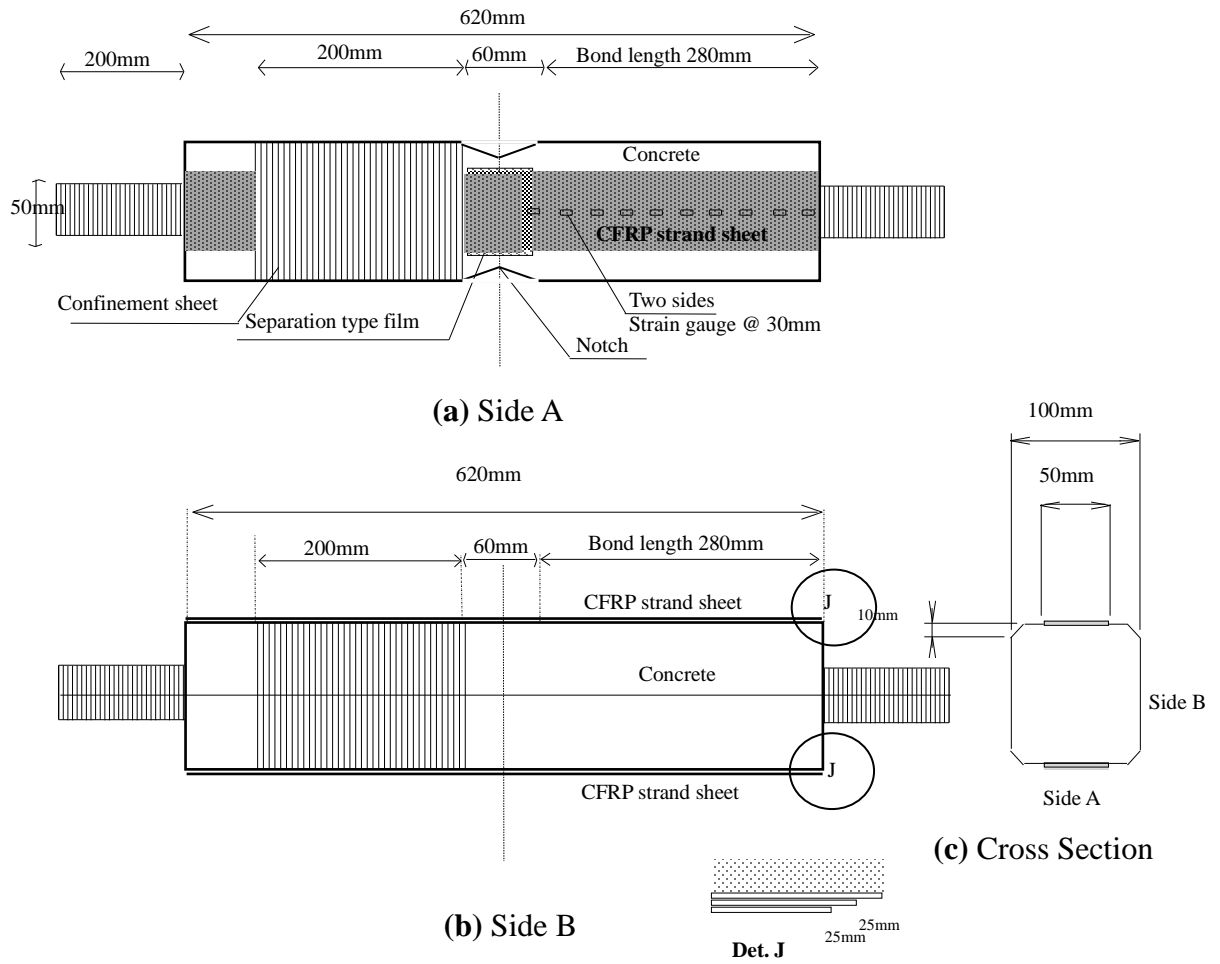


**Fig. 4.2** Geometry for bonding test specimen

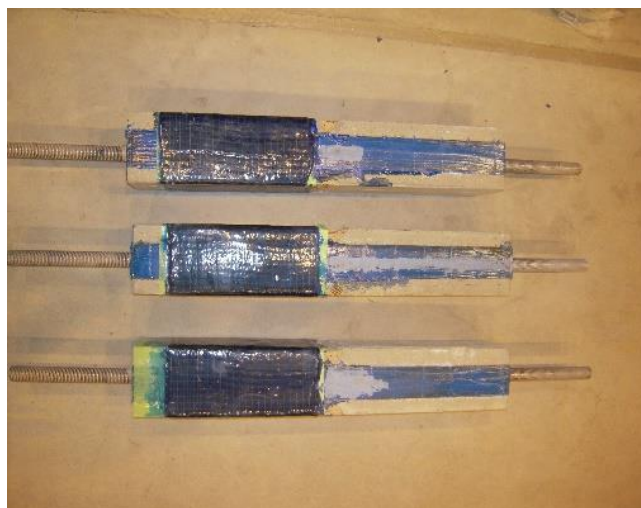


**Photo 4.2** Specimens for bonding test



**Photo 4.3** Specimen during bonding test

There were two notches at the center of the prism that made at the time of concrete casting. To pull out the specimen, there were two steel bars embedded into the concrete that also had no connection. So, the specimen was divided into two parts. One part of the specimen was given a confinement sheet (as shown in **Fig. 4.2**). This means that during the test, after the crack at the center of prism happened, the two parts of prisms were connected only with the CFRP strand sheet and the failure occurred only on the opposite confined part area, where strain gauges were set up. The total bonding length of CFRP strand sheet were 280mm on the both sides, the strain gauge had a distance of 30mm. CFRP strand sheet at the center of the prism. At the loaded end area of CFRP strand sheet near the center of the prism, there were unbonded areas. In these areas were placed separation type film between the CFRP strand sheet and concrete. It was intended to avoid failure at the loaded end area.

To avoid stress concentration, at free end area of specimen that had two or three layers, the upper layer was made shorter than the previous layer by 25mm (**Fig. 4.2 Det. J**). Monotonic static loading test method was carried out in this investigation. A universal testing machine with a capacity of 1000kN was used, as shown in **Photo 4.3**. The increase rate of the load was approximately 5kN per minute and the strain gauge was recorded at 1kN of load increment.

High tensile strength of CFRP strand sheet type was used in this study. **Table 4.1** captures the CFRP strand sheet mechanical properties. The properties of CFRP strand

sheet were obtained from the company. Furthermore, the compressive strength and the elasticity modulus of concrete used in this study were 37.1 MPa and 26,900 MPa, respectively.

**Table 4.1** Mechanical properties of CFRP strand sheet

Type	High-Strength Type
Tensile Strength (MPa)	3,400
Tensile Modulus (MPa)	245,000
Design thickness (mm)	0.333
Unit Weight (g/m <sup>2</sup> )	600

**Table 4.2** Mechanical properties of adhesive (MPa)

Type	MMA	PCM
Compressive Strength	79.0	11.3
Compressive Modulus	2,500	4,800
Tensile Strength	43.0	2.4
Flexural Strength	71.0	6.5
Lap-share Strength	22.0	-

#### 4.4 The use of adhesive

**Table 4.2** shows the mechanical properties of the adhesive. The properties of adhesive were obtained from the manufacturer. MMA is a quick-drying adhesive can also be used in low-temperature conditions. The MMA can be used after two hours of installation. PCM is used for wet surfaces. In this study, the use of MMA adhesive was about 2.5 kg/m<sup>2</sup>. PCM, for surface protection, had a thickness of 10 mm from CFRP strand sheet layer.

*MMA (methyl methacrylate)*

**Fig. 4.3(a) ~ (c)** illustrate briefly about retrofitting types that were used MMA as an adhesive for 1 to 3 layers. Stages of implementation are as follows; prepared the primer material, then given evenly on the CFRP strand sheet and the surface of the concrete beam. Next, sprinkled MMA material on the concrete surface. Then, the CFRP strand sheets were attached to the concrete surface while pressed in order to be spread evenly after was done, did overcoat for the next layer.

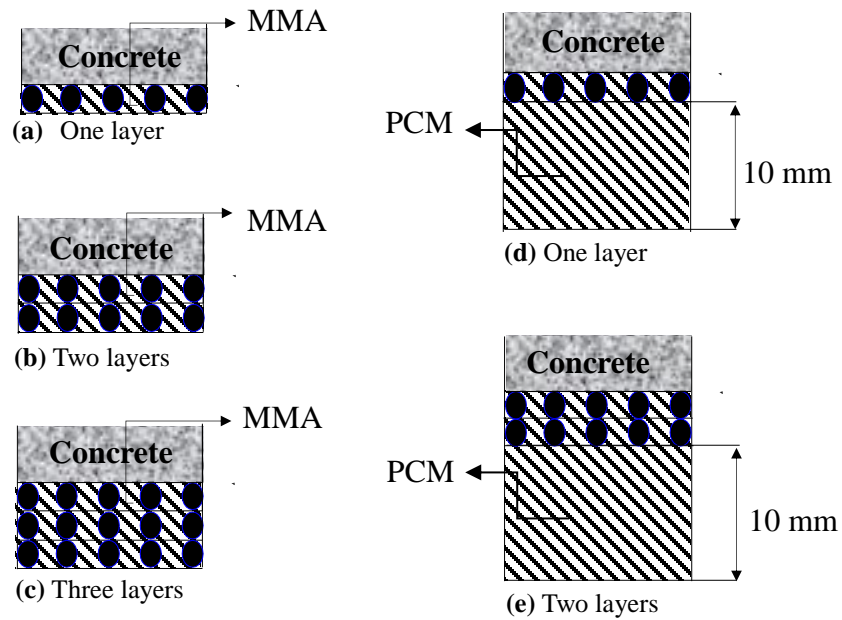


**Fig. 4.3** Cross-section of material CFRP strand sheet

*PCM (polymer cement mortar)*

The use of PCM as an adhesive in retrofitting methods can be seen in the cross-section in **Fig. 4.3(d)** and **Fig. 4.3(e)**. Stages of implementation are as follows; after prepared PCM mixed with the water, then spread thinly on the surface of concrete beams. Subsequently, CFRP strand sheet was attached on the whole surface and pressed such that the impregnation could be evenly distributed. After that, followed by the next layer. Finally, CFRP strand sheet was covered with the PCM until designed thickness (10mm).

For more details, the manufacturing of MMA specimen and PCM specimen can be seen in **Photo 4.4** and **Photo 4.5**, respectively.

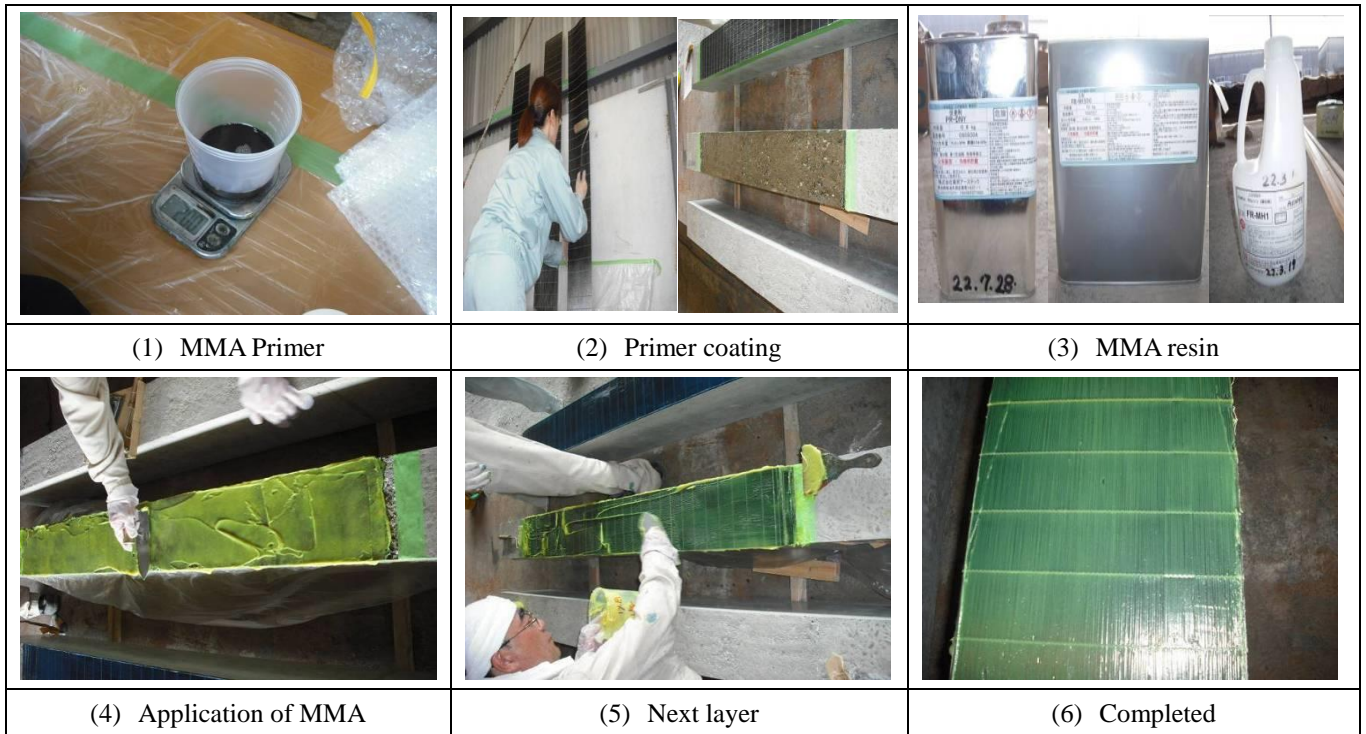


**Photo 4.4** The manufacturing process of MMA specimen

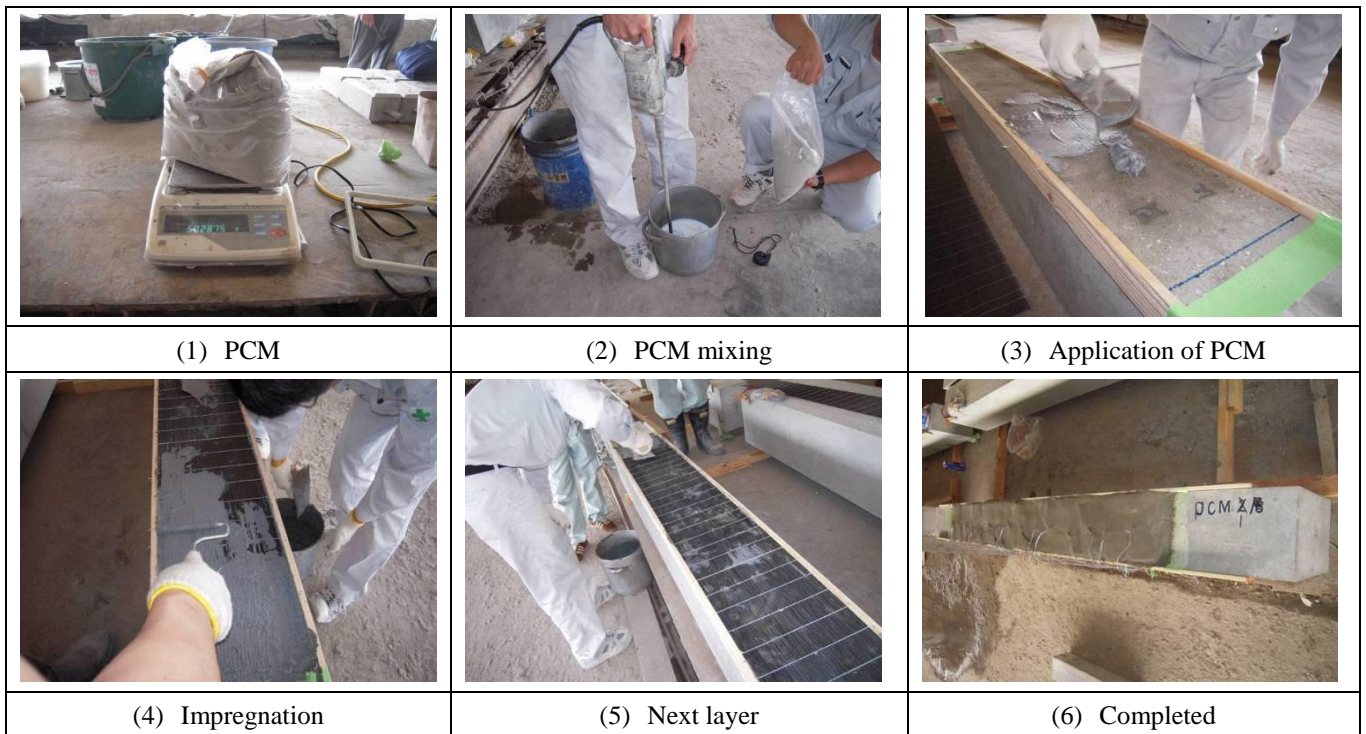


**Photo 4.5** The manufacturing process of PCM specimen

## 4.5 Test results and discussion

### 4.5.1 Failure mode

Pham and Mahaidi (2007) <sup>(4.8)</sup> stated that there is five possibility failure mode as described in the previous chapter, as follows; interfacial debond failure, shear or tension failure on concrete, FRP tensile rupture, adhesive failure and FRP delamination. In addition, JSCE –E543 –2007 confirmed that there are two categories for test specimen failure; (a) the interfacial failure, which is a debonding failure between surface CFRP strand sheet and concrete, and (b) base material failure, which is the CFRP strand sheet reaches its ultimate strength.

All the specimen collapsed due to peeling off the CFRP strand sheet from concrete. The typical failure of bonding test is shown in **Photo 4.6(a)** and **Photo 4.6(b)** for MMA specimen and **Photo 4.7(a)** and **Photo 4.7(b)** for PCM specimen. It can be seen that the typical failures of the specimen were the interfacial debonding failure which occurred only one side of the prism. The failure occurred only one side because of the eccentricity of the load in the loading machine. Failure surface is about 2-5mm on the concrete with some of the concrete pieces were remained on all bonded interface of the CFRP strand sheet. These facts were related to the interface bonding performance between CFRP strand sheet and concrete.



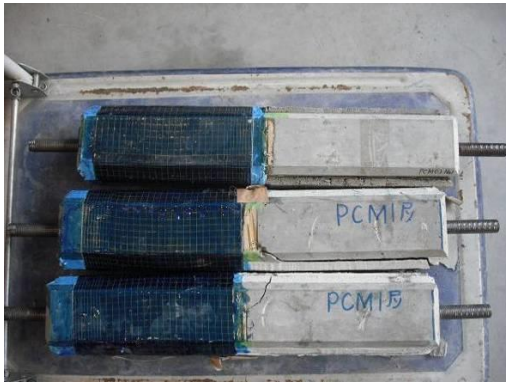
(a) The specimen tested



(b) The feature of failure

**Photo 4.6** Typical failure model of MMA specimens





(a) The specimen tested



(b) The feature of failure

**Photo 4.7** Typical failure model of PCM specimens

#### 4.5.2 Maximum load, average bond stress and interfacial fracture energy

Table 4.3 describes the specimen identification, the maximum load, the bond strength and the interfacial fracture energy results. For more details, the value of bond test results will be shown in the figure.

Table 4.3 Results of bond test

Adhesive type	Numb. of layers	No. of spec.	Max. load, $P_{max}$ (kN)		Ave. bond Stress, $\tau_u$ (MPa)		Interfacial fracture energy, $G_f$ (N/mm)	
			Result	Ave.	Result	Ave.	Result	Ave.
MMA	1	1MB1	40.6	36.0	1.45	1.29	1.01	0.80
		1MB2	32.2		1.15		0.64	
		1MB3	35.2		1.26		0.76	
	2	2MB1	42.2	42.3	1.51	1.51	0.55	0.55
		2MB2	41.4		1.48		0.53	
		2MB3	43.3		1.55		0.57	
	3	3MB1	43.7	47.1	1.56	1.68	0.39	0.46
		3MB2	50.7		1.81		0.53	
		3MB3	47.0		1.68		0.45	
PCM	1	1PB1	35.8	34.5	1.28	1.23	0.79	0.73
		1PB2	32.6		1.17		0.65	
		1PB3	35.0		1.25		0.75	
	2	2PB1	44.1	45.1	1.58	1.61	0.60	0.63
		2PB2	42.3		1.51		0.55	
		2PB3	49.0		1.75		0.74	

Average bond stress,  $\tau_u$ , is the value of maximum load divided by bond length and width of CFRP strand sheet. In addition, the interfacial fracture energy,  $G_f$ , is the area enclosed the local bond stress ( $\tau$ ) and slip ( $s$ ) curve relationship.  $\tau_u$  and  $G_f$  are important parameters for the bonding properties. In the analysis,  $\tau_u$  and  $G_f$  were calculated by **Eq. (3.1)** and **Eq. (3.2)**, respectively, based on JSCE–E543–2007.

$$\tau_u = \frac{P_{max}}{2bl} \quad (3.1)$$

$$G_f = \frac{P_{max}^2}{8nb^2E_f t} \quad (3.2)$$

Where,

- $G_f$  = interfacial fracture energy (N/mm)
- $\tau_u$  = average bond stress (MPa)
- $P_{max}$  = maximum load (N)
- $b$  = average width of the CFRP strand sheet (mm)
- $E_f$  = tensile modulus of the CFRP strand sheet (MPa)
- $t$  = thickness of the CFRP strand sheet (mm)
- $l$  = length of the bond (mm)
- $n$  = number of layers of the CFRP strand sheet

**Fig. 4.4** and **Fig. 4.5** depict the maximum load results of MMA specimen and PCM specimen respectively. Results of maximum load for each specimen are pictured on the value of each column while the dash-line represent the average value of the specimen on the same layers number. From the results of the average values, it can be seen that the number of layers affects the maximum load. There was an increase in the maximum load coincide with increasing the number of layers.

The maximum load was not twice or thrice even if the CFRP strand sheet were two or three layers. Nevertheless, for MMA specimen, the average maximum load of the two and three layers specimens increased by 17.5% and 30.8%, respectively, compared with the average one layer specimen. For PCM specimen, there is an increase in maximum load on average by 30.7% for two layers specimen compared the average maximum load of the specimen with the one layer.

**Fig. 4.6** shows the mean of average bond stress results and the layers number relationship of each specimen. The results indicate similar results with maximum load, that is, it can be seen that average bond stress have the significant correlation with number of layers. **Fig. 4.7** shows the average of interfacial fracture energy and the layers number relationship of each specimen. Among the results, the value shows a decrease as the number of layers increase and only MMA three layers has a value lower than 0.50N/mm. it can be concluded that MMA and PCM are a fairly good adhesive for CFRP strand sheet strengthening method.

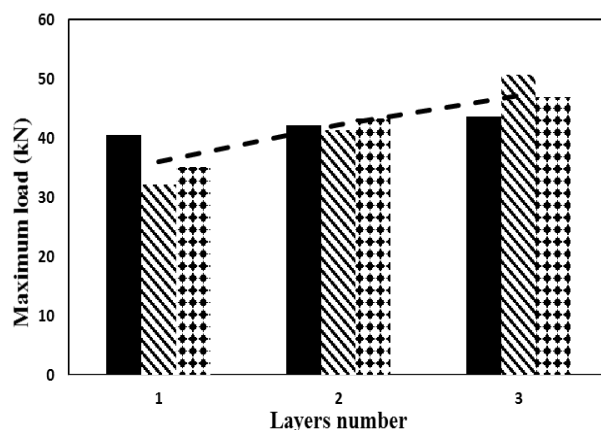


**Fig. 4.4** Maximum load results of MMA specimen

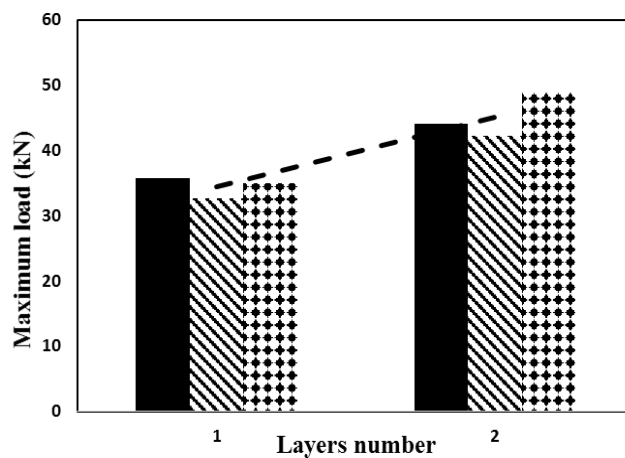


**Fig. 4.5** Maximum load results of PCM specimen

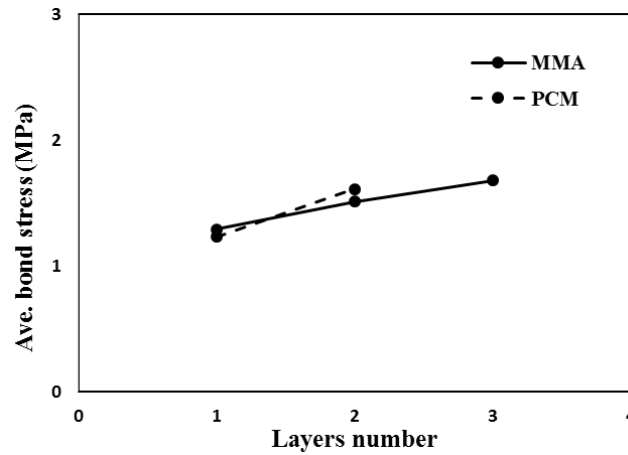


**Fig. 4.6** Average results of average bond stress

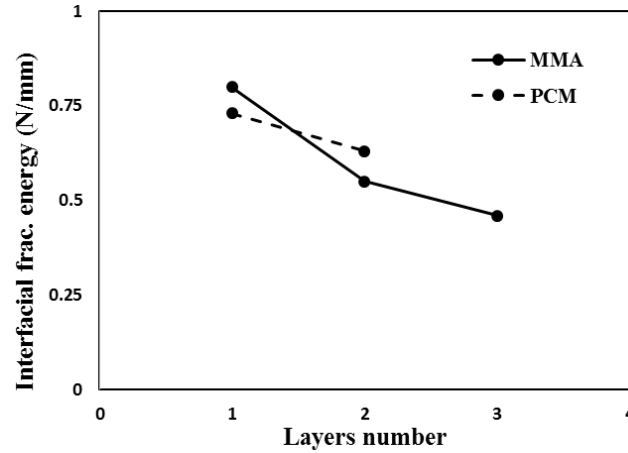


**Fig. 4.7** Average results of interfacial fracture energy

#### 4.5.3 Strain distribution of CFRP strand sheet

The data collected from the average strain gauges was used to develop the strain distribution. Each curve is plotted for a given a load level. **Fig. 4.8**, **Fig. 4.9** and **Fig. 4.10** show the strain distribution generated from one layer, two layer and three layers of specimen with MMA as adhesive. While the strain distribution of one layer and two layers of the specimen with PCM as adhesive are shown in **Fig. 4.11** and **Fig. 4.12**, respectively. The figures also include the FEM analysis results.

It can be seen that at early stages of loading, the curve has a non-linear shape. The strains decrease along with the distance from the center increase. As the load increase, the trend line attains to linear shape. At the certain load level, the strain distribution curve

becomes linear or a smaller strain in the area near the center which means the failure has started in this area. This corresponds to the attainment of a uniform bond stress (bond load) along the portion of bonding system which is taking the load. The linear decrease of strain gauges is more far from the mid-span which means the load transfer zone was shifted (active zone have changed).

At the maximum load, the strain distribution shows that there is a relationship between the number of layers and ultimate strain. The correlation indicates that the more the number of layers result in the smaller ultimate strain. This means that thickness affects the occurrence of strain. The strains is almost similar to the same layers specimen, it confirms that the types of adhesive do not provide a significant influence on the produced strain.

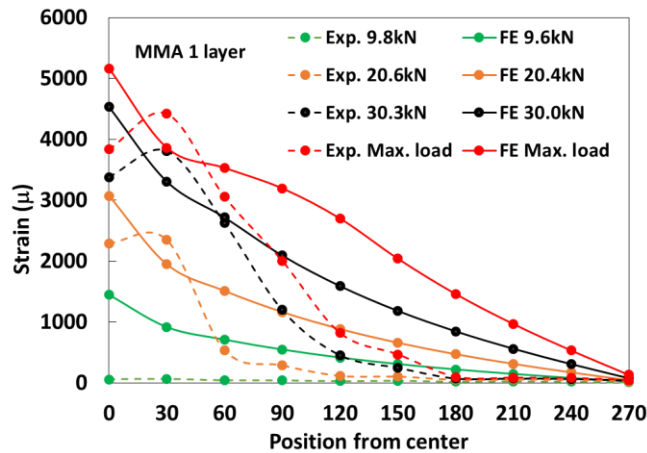


Fig. 4.8 MMA 1 layer strain distribution of FE analysis and experimental results

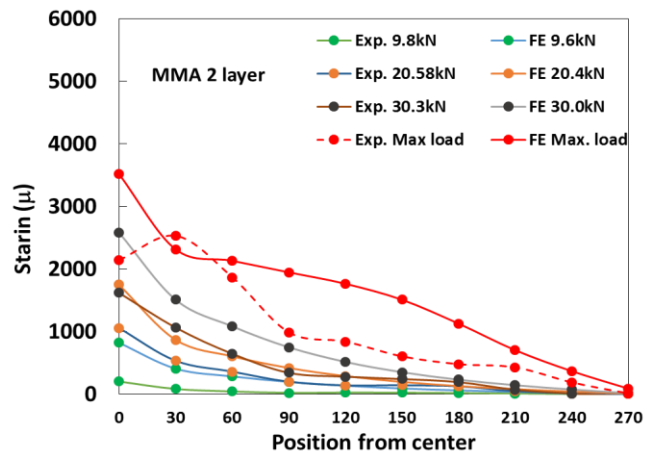


Fig. 4.9 MMA 2 layers strain distribution of FE analysis and experimental results

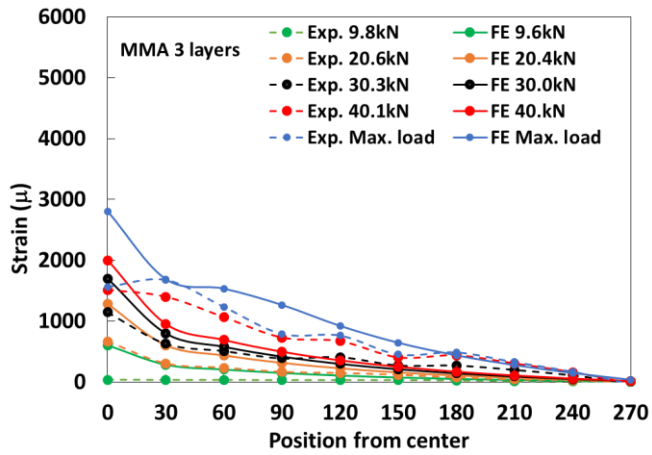


Fig. 4.10 MMA 3 layers strain distribution of FE analysis and experimental results

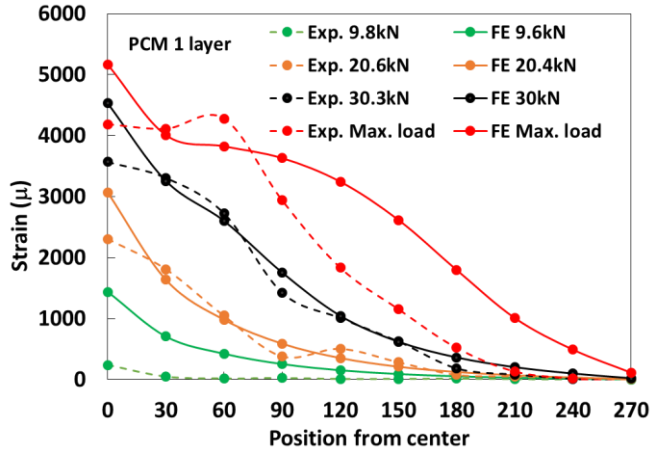


Fig. 4.11 PCM 1 layer strain distribution of FE analysis and experimental results

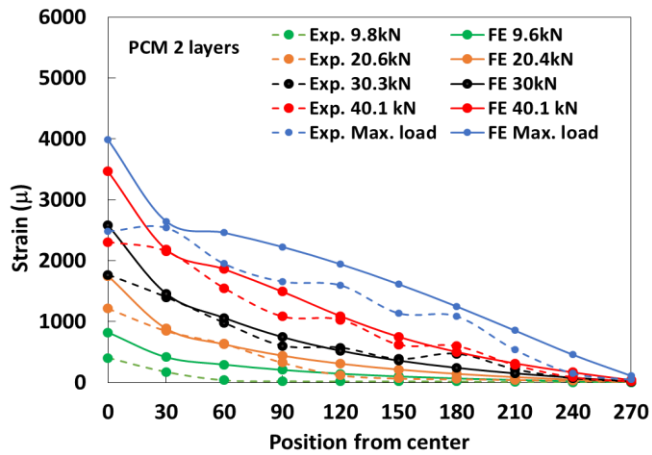


Fig. 4.12 PCM 2 layer strain distribution of FE analysis and experimental results

#### 4.5.4 Effective bond length

A very important aspect of the behavior of the bonding system is that there exists an effective bond length beyond which an extension of the bond length cannot increase the ultimate load. This is the fundamental difference between an externally bonded and an internal reinforcing bar for which a sufficiently long anchorage can always be found that the full tensile strength of the reinforcement can be achieved <sup>(4.11)</sup>.

Currently, many methods are used to evaluate the effective bond length. Effective bond length can be defined as a length over which majority of bond stress maintained. The effective bond length takes the entire load to a certain level at which localized debonding occurs, causing the effective bond length to shift to another active bonding zone. This phenomenon continued until the CFRP strand sheet was completely debonding from the concrete <sup>(4.11)</sup>.

In this chapter, effective bond length was obtained by determining the maximum stress that occurred in the CFRP strand sheet. A calculation was done on the strain distribution diagram of the maximum load by assuming that a constant maximum stress occurred to the longitudinal direction of the specimen that be computed by using **Eq. (4.3)** and the effective bond length could be determined by using **Eq. (4.4)**. **Fig. 4.13** shows how to specify the used points to determine the effective bond length in this study.

$$\tau_{max} = \frac{\Delta\varepsilon_f E_f A_f}{s_g b} \quad (4.3)$$

$$l_e = \frac{P_{max}}{2\tau_{max} b} \quad (4.4)$$

Where,

- $\tau_{max}$  = the maximum bond strength (N/mm<sup>2</sup>)
- $l_e$  = the effective bond length (mm)
- $\Delta\varepsilon_f$  = difference strain at a steepest area
- $E_f$  = tensile modulus of CFRP strand sheet (MPa)
- $A_f$  = area of CFRP strand sheet (mm<sup>2</sup>)
- $s_g$  = interval of strain at steepest area (mm)
- $b$  = average width of CFRP strand sheet (mm)

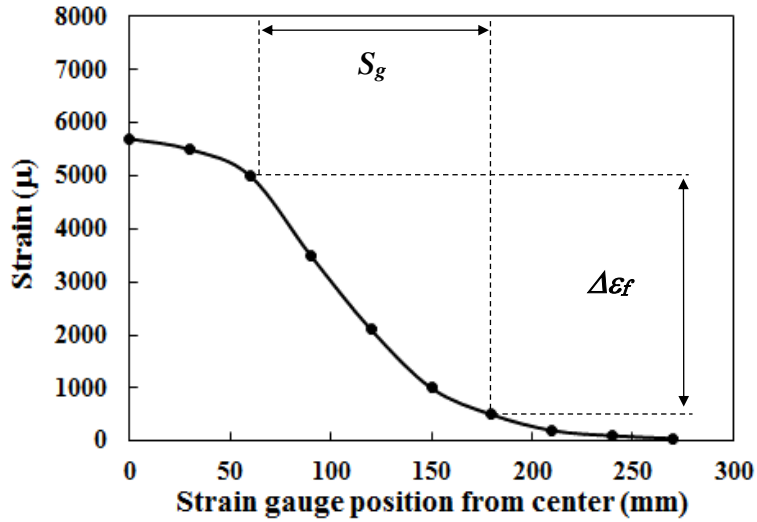


**Fig. 4.13** The used points to determine the effective bond length

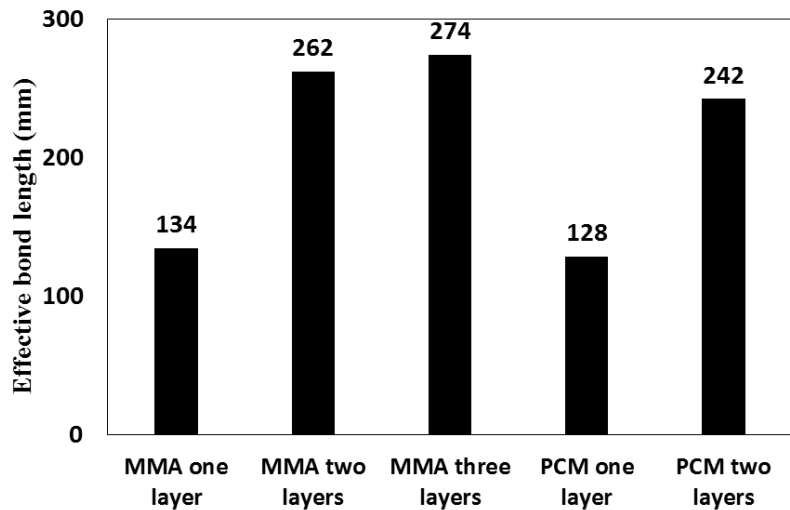


**Fig. 4.14** Effective bond length (mm)

The average results of the effective bond length are shown in **Fig. 4.14**. It can be seen that one layer specimens have effective bond length about 130mm and about 250mm for two layers specimens. Meanwhile, MMA three layers specimen has 274mm effective bond length. The effective bond length increases significantly on the two layers specimen, around twice, compared with one layer specimen. Whereas, the effective bond length for three layers specimen do not show a significant value increase compared with two layers specimen.



#### 4.5.5 Local bond stress-slip relationship

Based on the failure model of bonding test defined previously, it confirms that the role of the local bond stress-slip relationship is very important to observe. The previous study<sup>(4.8)</sup> stated that during bonding process adhesive infiltrated into the rough surface of the concrete. The interlocking between the adhesive and the concrete surface irregularities mainly provided the interface shear strength. As a result, the local bond stress and local slip occur at the interface area. The increase of the local bond stress with the slip is keeping until it reaches the peak stress,  $\tau_{max}$ , which the value of the slip,  $s_{max}$ . Then, the debonding failure starts with reducing the shear stress and increasing interfacial slip. Moreover, the bond stress reduces to zero when the slip exceeds and signifying the failure of a local element.

In order to plot the local bond-slip curve, the average bond stress and the average slip must be computed. The average bond stress,  $\tau$ , of the section between two strain gauges was calculated by dividing the difference of tensile by the surface of the bond area as shown in **Eq. (4.5)**. In addition, the average slip,  $s_i$ , was calculated as the incremental sum of the CFRP extension in **Eq. (4.6)**. In **Eq. (4.6)**, the concrete elongation was ignored since the concrete block was much stiffer than the CFRP strand sheet. Next, to simplify the analysis, the free end slip can be approximately as zero.

$$\tau = \frac{E_f(\varepsilon_{f,i+1} - \varepsilon_{f,i})t_f}{\Delta L} \quad (4.5)$$

$$s_i = \frac{(\varepsilon_{f,i+1} + \varepsilon_{f,i})}{2} \Delta L + s_{i-1} \quad (4.6)$$

Where,

- $\tau$  = average local bond strength (MPa)
- $s_i$  = slip of section i
- $\varepsilon_{f,i}$  = average of CFRP strand sheet strains in section i
- $E_f$  = tensile modulus of CFRP strand sheet (MPa)
- $t_f$  = thickness of CFRP strand sheet
- $\Delta L$  = distance between strain gauges (30mm)

**Fig. 4.15** shows an example of local bond-slip relationship result of one layer MMA specimen for 0-30mm, 30-60mm and 60-90mm interval of the strain gauge. The initial slope of the curve is same for each location, however, the maximum bond stress differs between locations. It is caused by the start of delamination. So, this curve ignores other results of strain gauge interval because of data consistency. As can be seen from the figure that the local bond stress-slip relationship has a tendency to become parabolic in form. A first step ascending area is followed by descending area or softening until an ultimate slip is reached. After the peak stress,  $\tau_{max}$ , the local bond slip decreases with increasing the slip.

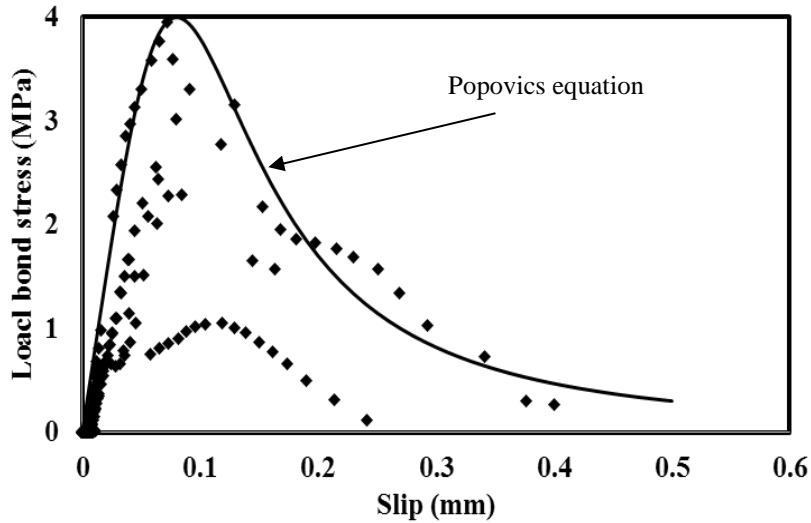


**Fig. 4.15** Local bond stress-slip relationship by Popovics equation for one layer MMA

After calculating all data, local bond stress versus slip was plotted in a graph for each interval of the strain gauge on each specimen. Popovich's equation <sup>(4.2), (4.6), (4.8), (4.12)</sup> was utilized to represent the local bond stress and slip relationship, shown as follows.

$$\frac{\tau}{\tau_{max}} = \frac{s}{s_{max}} \frac{n}{(n-1) + (s/s_{max})^n} \quad (4.7)$$

Where,

$\tau_{max}$  = maximum local bond stress (MPa)

$s_{max}$  = slip at  $\tau_{max}$

$n$  = constant

$\tau_{max}$  and  $s_{max}$  are value that is generated from experiment after local bond-slip relationship plotted. The value of  $n$  is obtained by using the trial and error method using deduced local bond stress-slip relationship. **Table 4.4** captures fitting results from each type of adhesive and layer. For the specimen with MMA as adhesive, the maximum local bond stress  $\tau_{max}$  is 4.0 MPa with the average value of  $\tau_{max}$  is 3.75 MPa with the value decrease with the number of layers but the value of  $s_{max}$  tends to same that is 0.100mm. Different from results of the  $n$ , the value of  $n$  increased with increasing of the layers number of CFRP strand sheet. The greater of the  $n$  value means the more brittle behavior of the composite system.

While the specimen with PCM as an adhesive shows that the maximum local bond stress  $\tau_{max}$  is 4.0 MPa with the average of  $\tau_{max}$  is 3.83MPa with the value of  $s_{max}$  decrease and the similar value of  $n$  with the increasing of the number of layer of CFRP strand sheet.

**Table 4.4** The Popovics's equation parameter

Numb. of layers	Adhesive	Max. bond stress approx. $\tau_{max}$ (MPa)	Slip at max bond stress approx. $s_{max}$ (mm)	Value of $n$
1	MMA	4.00	0.100	3.0
2		3.75	0.100	5.0
3		3.50	0.100	6.0
1	PCM	4.00	0.150	5.0
2		3.75	0.120	5.0

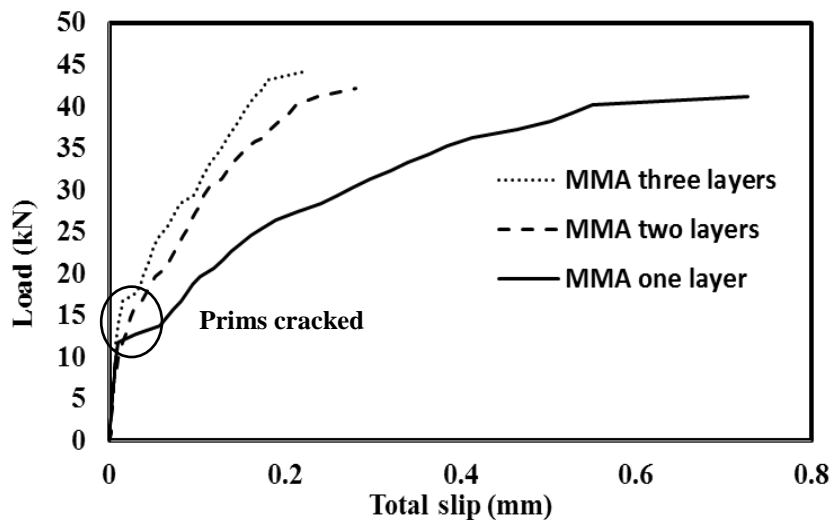


**Fig. 4.16** Load-total slip relationship for MMA specimen

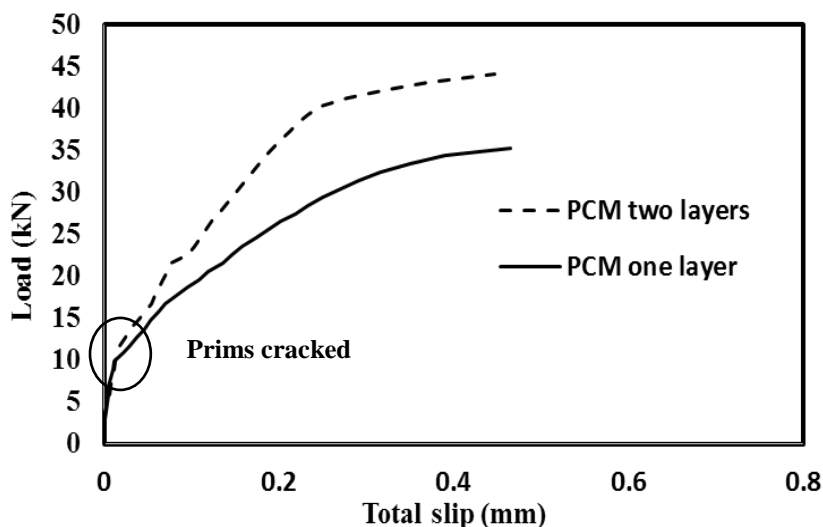


Fig. 4.17 Load-total slip relationship for PCM specimen

#### 4.5.6 Load-total slip relationship

Total slip is the integration results of the CFRP strand sheet strains along the bond length at the loaded end position. In this case, the total slip use **Eq. (4.6)** for calculating. All observed load and total slip at the loaded end can be made into a relationship. **Fig. 4.16** and **Fig. 4.17** show the load versus total slip at loaded end position for experimental results. **Fig. 4.16** shows for MMA specimen with one layer, two layers and three layers of CFRP strand sheet. While **Fig. 4.17** shows for PCM specimen with one layer and two layers. The circle points are considered to correspond crack occurrence of concrete prisms. Before cracks, the CFRP strand sheet did not bear the entire load. So, the initial peeling cannot be observed well. After prism cracked, the curve stiffness changes and decreases significantly.

The crack occurrence of the concrete prism and maximum load increase with the number of layers, but the total slip at the crack load do not change. The crack load is higher when more the layers number with the crack slip is almost same. For MMA specimen, the ultimate slip becomes shorter when the number of layers increases. This can be understood as follows: the lower CFRP strand sheet number of layers leads to higher local strain level but shorter load transfer length. The overall stiffness decreases more slowly when the stiffness of CFRP strand sheet layers is lower. Overall, the MMA specimen show that the lower layers make the composite system more ductile, meanwhile, the PCM specimen show an equivalent level of ductility.

#### **4.6 Finite element analysis of bonding behavior between CFRP strand sheet and concrete**

##### *Finite element idealization*

A typical finite mesh and boundary were successfully used to model of the bonding between CFRP and concrete in previous research. For numerical analysis, this study will adopt a typical finite element used in previous research <sup>(4,8)</sup>. This simulation was doing by using two-dimensional of FE analysis DIANA (version 9.4.3). The process of idealization of specimen, load, boundary conditions and typical of the finite element mesh are shown in **Fig. 4.18**.

The concrete prism had an assumption that a load of FE analysis was half of the actual load in the laboratory. The concrete block was modeled using two models of mesh. A fine layer and a coarse layer with element size were approximately 4mm and 46mm, respectively. The element sizes of CFRP strand sheet layer were 0.333mm for one layer, 0.666mm for two layers and 0.999mm for three layers. The concrete and the CFRP strand sheet were assumed to be isotropic with thicknesses of two-dimensional material were 100mm and 50mm, respectively.

The CFRP strand sheet was connected to the top of the concrete through an interface element replaced adhesive behavior. The interface was assumed with 0.05mm element size and thickness of the two-dimensional material was 50mm. For overall interface of the specimen, including PCM as a surface at the specimen with PCM as adhesive, used bond–slip relationship that obtained from the experiment after fitted by Popovics’s equation. This treatment differs from previous research <sup>(4,8)</sup> that considers the connection between CFRP-concrete is linear elastic.

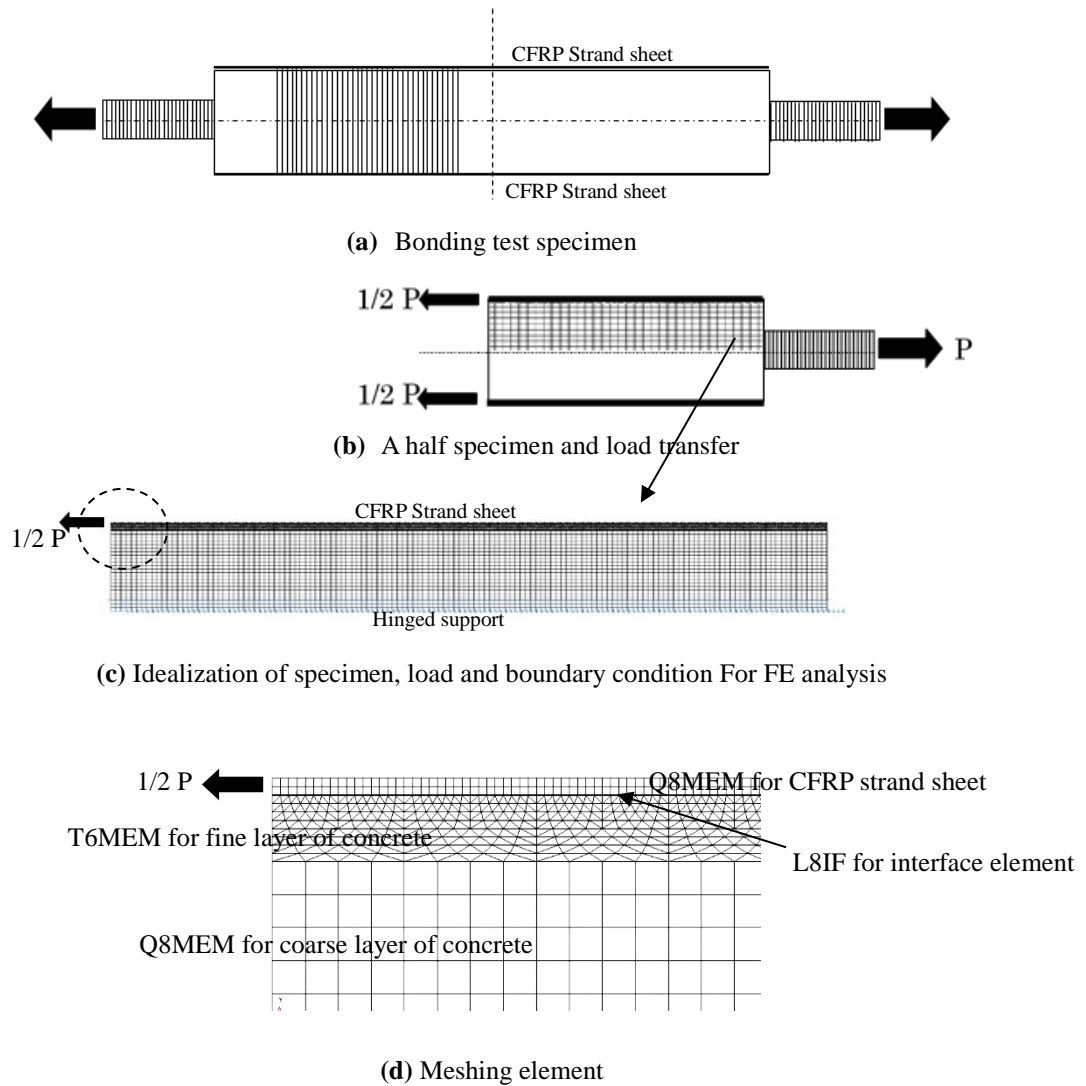


**Fig. 4.18** Idealization and typical finite element mesh

The CFRP strand sheet and the concrete in the coarse layer were modeled using Q8MEM four-nodes quadrilateral linear plane stress element with each element had eight degrees of freedom with two displacement  $u_x$  and  $u_y$  at each node <sup>(4.13)</sup>. The concrete in the fine layer was modeled using T6MEM three-nodes quadrilateral linear plane stress element, each element had six degrees of freedom with two-displacement  $u_x$  and  $u_y$  at each node <sup>(4.13)</sup>. Interface element was using L8IF. The L8IF was a four nodes line interface element between two lines in a two-dimensional configuration, the local  $xy$  axes for the displacements were evaluated in the first node with  $x$  from node 1 to node 2 <sup>(4.13)</sup>.

Concrete was idealized using total strain rotating crack model. In tension, this model used a non-linear tension softening stress-strain relationship proposed by Hordijk (4.14) as shown in **Fig. 4.19(a)**. This relationship was using expression provided by CEB-FIP Model Code (4.15), where  $G_{fc}$  was the fracture energy or energy required to spread a tensile crack of unit area and  $h$  was the crack bandwidth that related to the area of element. The  $G_{fc}$  was computed to be 0.0833N/m. The tensile strength of concrete was determined to be 4.23MPa. In compression, the concrete model applied the model which was described by the function proposed by Thorenfeldt, et.al (4.16) as shown in **Fig. 4.19(b)**. Moreover, CFRP strand sheet was modeled with linear elastic properties.

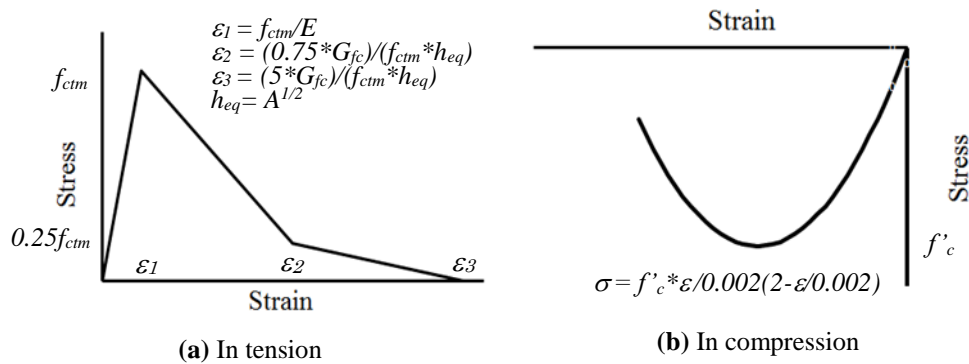


**Fig. 4.19** Constitutive law of concrete

## 4.7 Verification of finite element model with experimental results

### 4.7.1 Strain distribution

**Fig. 4.8 ~ Fig. 4.12** compare the strain distribution of the FEM analysis and the experiment results for one layer MMA, two layers MMA, three layers MMA, one layer PCM and two layers PCM specimen, respectively. The data of strain distribution were taken for several load condition of about 10kN, 20kN, 30kN, 40kN, and 50kN or any maximum load. It can be seen that at the same load level the strain of FE is generally larger than experiment result, although there are some parts that show the experiment are greater. There are some specimens have a good agreement between FE and experiment results. However, some of them do not show a good correspondent such as MMA 1 layer specimen. In addition, at the early stage of loading especially at 10kN loading stage, the

strain distribution of experiment does not appear so sensitive, this is because at that loading stage the concrete prism has not yet cracked so the CFRP strand sheet is not received the entire load.

#### 4.7.2 Maximum load

The maximum load calculated by the finite element analysis and experimental results for all specimens are compared in **Fig. 4.20**. Load results were obtained from the FE analysis multiplied by two and compared with experimental results. It can be seen that the maximum load trends can be simulated well by the FE models. The differences from the experimental results range from 0,4% to 16,2%. **Fig. 4.20** also shows that the maximum load results related with the area of the CFRP strand sheet.

#### 4.7.3 Effective bond length

With using strain distribution data, the determination of the effective bond length by FE model were done in the same method with the experimental test. **Fig. 4.21** illustrates the comparison of FE analysis and experimental results. In general, they have a good correspondence and have a value of comparison below 10% from experimental results. Although, on the specimen MMA1 and PCM1 have differences of 52% and 32%, respectively.



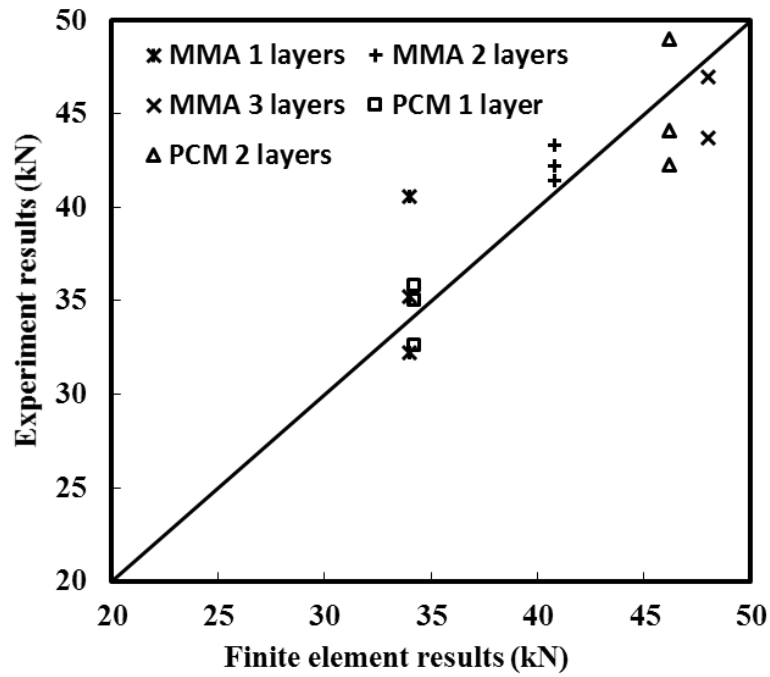


Fig. 4.20 Comparison of the maximum load by FE model and experimental results

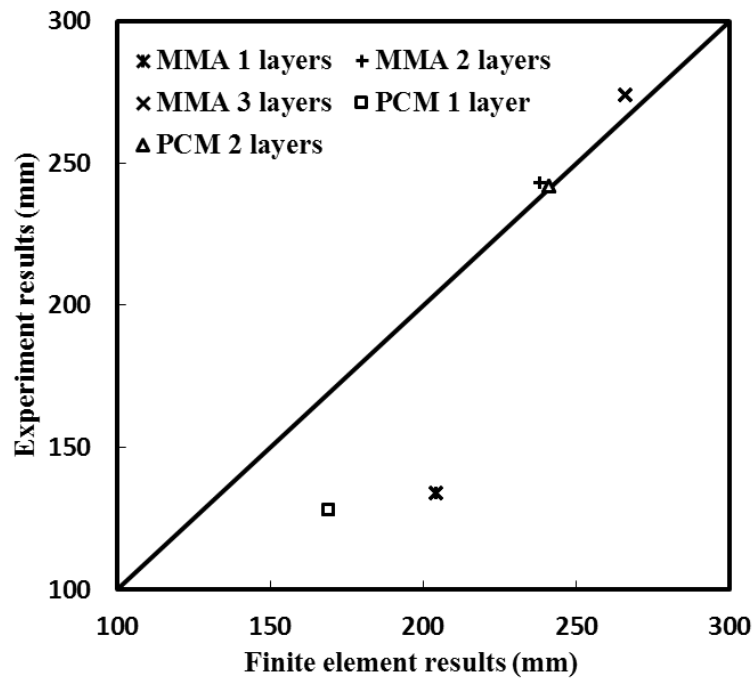


Fig. 4.21 Comparison of the effective bond length by FE model and experimental results

#### 4.8 Verification of CFRP strand sheet strengthened RC beams with the local bond stress-slip relationship

Based on the summary of the **Chapter 3**, it have known that the interface model need to be corrected. In this section, the application of local bond stress-slip behavior after fitted by popovics's equation will be applied to improve the interface model of strengthened beam. Concrete and reinforcement modelling are same with modelling in the previous section. The difference is only in the interface modelling.

The maximum load results of new FEM analysis and comparison with the experimental one for new and old model specimen (from **Chapter 3**) results are shown in **Table 4.5**. It can be seen that generally the maximum load shows a good agreement with the experimental results. Even when compared to the old specimen comparison. By ignoring PCM2 result, the differences of experimental results and FEM analysis is lower than 6%.

**Table 4.5** Experimental and FEM load results

Spec.	Layers numbers	P <sub>Max.</sub> Experiments (kN)	P <sub>Max.</sub> FEM (new) (kN)	P <sub>exp./P<sub>FEM</sub></sub> (new)	P <sub>exp./P<sub>FEM</sub></sub> (old)
N	-	165	155	1.06	1.06
MMA1	1	255	250	1.02	1.04
MMA2	2	272	265	1.02	1.04
PCM1	1	223	215	1.04	1.14
PCM2	2	201	225	0.90	0.91

The experimental and the FEM analysis load and midspan displacement curve of specimen MMA1 as representative are plotted in **Fig. 4.22**. it can be seen that the figure shows not only specimen MMA1 new analytical model but also the old FEM model. It can be seen that the new FEM model shows almost identic behavior compared with the old FEM model. Small discrepancies between the new model of FEM and experimental result mode when approaching the maximum load is observed.

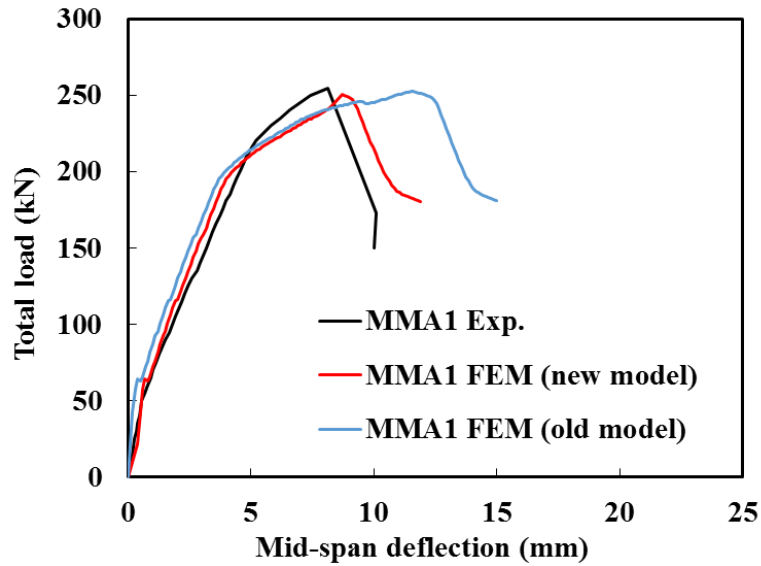


**Fig. 4.22** Load and midspan deflection of specimen MMA1

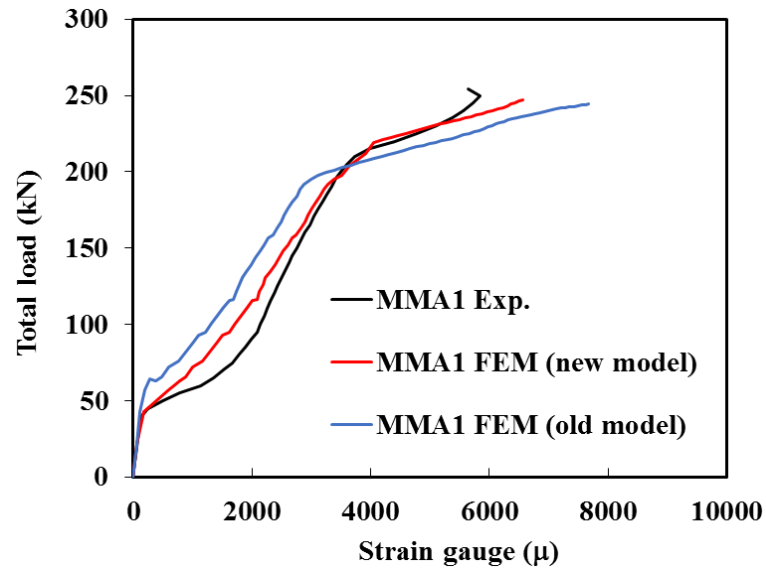


**Fig. 4.23** Total load and CFRP strand sheet strain at midspan of specimen MMA1

**Fig. 4.22** captures the curve of total load and CFRP strand sheet strain at the RC beam midspan. The MMA1 FEM with bond stress-slip interface model (new FEM model) provide a more acceptable result than the old FEM model (linier behavior interface model). It can be said that interface bond slip behavior for FEM model can provide a powerful predictive for analysis of externally strengthened RC beams.

#### 4.9 Conclusive remarks

This chapter provided results from the CFRP strand sheet and concrete bonding properties. Based on the experimental and FE analysis results and discussion, the following conclusions can be drawn up;

1. The typical failure of bonding test was the interfacial failure occurred on only one side of the prism. Failure surface was about 2-5mm on the concrete with some of the concrete pieces were remained on all bonded interface of the CFRP strand sheet.
2. For MMA specimen, compared with the average one layer specimen, the average maximum load of the two and three layers specimens increased by 17.5% and 30.8%, respectively. In addition, two layers specimen using PCM adhesive increase in average maximum load by 30.7% compared the average maximum load of one layer specimen.
3. The results show that only MMA three layer has the interfacial fracture energy lower than 0.50N/mm. Based on these results showed that MMA and PCM are a fairly good adhesive for CFRP strand sheet strengthening method.
4. The number of layers affected the maximum load. There was an increase in the maximum load coincide with increasing the number of layers.
5. The effective bond length increased almost twice on the two layers specimen compared with one layer specimen. Whereas, for three-layers specimen had similar results with two layers specimen.
6. The local bond slip of MMA specimen showed that the lower layers made the composite system more ductile, meanwhile, the PCM specimen showed an equivalent level of ductility.
7. The strains are almost similar on the same layers specimen, it confirms that the adhesive type did not have a significant effect the value of CFRP strand sheet strain that occurred.
8. When the maximum load was achieved, the strain distribution showed that there is a relationship between the number of layers and ultimate strain. The correlation indicated that the more the number of layers results the smaller ultimate strain. This mean that thickness affects the occurrence of strain.
9. Comparison between the FEM of this model and selected experimental results have shown that the ultimate load, effective bond length and strain distribution in the CFRP strand sheet at different load levels can nearly be closely predicted.
10. By verification of strengthened RC beams, it can be concluded that interface bond slip behavior is one of important parameter for FEM model.

## REFERENCES

- 4.1 Bahsuan R., Hino S. and Yamaguchi K., “Bonding Behavior of Interface between CFRP Strand Sheet and Concrete with Various Types of Adhesive” *Memoirs of the Faculty of Engineering, Kyushu University*, Vol. 75, No. 1, pp 1-15, July 2015.
- 4.2 Nakaba K., Kanakubo T., Furuta T. and Yoshizawa H., “Bond Behavior between Fiber-Reinforced Polymer Laminates and Concrete” *ACI Structural Journal*, Vol. 98, No. 3, pp.1-9, 2001.
- 4.3 Yuan H., Teng J. G. , Seracino R., Wu Z. S. , Yao J., "Full-Range Behavior of FRP-to-Concrete Bonded Joints" *Engineering Structures*, V. 26, No. 5 , pp. 553-65, 2004.
- 4.4 X. Z. Lu, L. P. Ye, et al “Meso-Scale Finite Element Model for FRP Sheets/Plates Bonded to Concrete” *Engineering Structures*, 27, pp. 564-75, 2005.
- 4.5 X. A. Lu, J. G. Teng, et al “Bond-Slip Models for FRP Sheets/Plates Bonded to concrete” *Engineering Structures*, 27, pp 920-37, 2005.
- 4.6 Z. G. Guo, S. Y. Cao, et al “Experimental Study on Bond Stress-Slip Behavior Between FRP Sheets and Concrete” *Proc. International Symposium on Bond Behavior of FRP in Structures*, Hongkong, December 2005.
- 4.7 Pelegrino C. and Modena C. “Bond-Slip Relationships between FRP Sheets and Concrete” *Proc. Fourth International Conference on FRP Composites in Civil Engineering (CICE 2008)*, Zurich, Switzerland, July 2008.
- 4.8 Pham H. B. and Mahaidi R. “Modelling of CFRP-Concrete Shear-lap Tests” *Journal of Construction and Building Material*, V. 21, pp. 727-35, 2007.
- 4.9 Bahsuan R., Yamaguchi K. and Hino S. “Bonding Properties of CFRP Strand Sheet and Concrete with Various Types of Adhesive” *Proc. The 6<sup>th</sup> International Conference of Asian Concrete Federation*, Seoul, September 2014.
- 4.10 Japan Society of Civil Engineering (JSCE) “Standard specification for concrete and structure, test method and specification” May 2007.
- 4.11 Mongi B.O., et all “Effective Bond Length of FRP sheet externally bonded to concrete” *International Journal of Concrete Structure and Material* Vol. 3 No. 2, pp 127 –31, Dec. 2009.
- 4.12 Kanakubo T., Furuta T., Fukuyama H. “Bond Strength between Fiber Reinforced

- Polymer and Concrete” In: FRPRCS-6, Fiber Reinforced Polymer Reinforcement for Concrete Structures, Singapore, 2003.
- 4.13 TNO DIANA “DIANA User’s Manual Version 9.4.3” 1<sup>st</sup> edition, Delft, The Netherlands, November 2010.
- 4.14 Hordijk D. A. “Local Approach to Fatigue Concrete, Delft University of Technology, 1991.
- 4.15 Comite Euro-International du Beton; CEB-FIB Model Code 1990, London, Great Britain, Thomas Telford, 1991.
- 4.16 Thorenfeldt E., Tomaszewics A., and Jensen J. J. “Mechanical Properties of High-Strength Concrete and Application in Design” Proc. Symposium Utilization of High-Strength Concrete , Stavanger, Norway, 1987.

## CHAPTER 5

### **BONDING BEHAVIOR OF CFRP PLATE AND CONCRETE WITH AND WITHOUT POLYUREA SOFT LAYER**

---

#### **5.1 Introduction**

External bonding of carbon fiber reinforced polymer (CFRP) plate is commonly used for strengthening and retrofitting of both concrete and steel structure. Despite having a relatively high price, CFRP plate has many advantages such as corrosion resistance, high tensile strength, durability, excellent fatigue resistance, lighter specific gravity, easy and fast work in the application. Bonding behavior of plate-concrete interface in producing an effective stress transfer is an important issue in the application of this method. Therefore, a good understanding of the bonding behavior of the CFRP plate and concrete interface has to be developed for the efficient use of this method. It can be noted that the term interface that utilized in this paper is used to refer to the interfacial part of bonded joint that experienced relative slip between CFRP plate and concrete, during loading, including the adhesive and the concrete surface <sup>(5.2)</sup>.

An important task facing the CFRP strengthening technology is to improve the bonding behavior. Recently, many researchers have been undertaken to understand the bonding behavior of interface between concrete and FRP. Nakaba et al <sup>(5.3)</sup> have researched about the bond behavior of interface between FRP and concrete and used the Popovic's equation fitting and applied it to their experiments. Pelegrino and Modena <sup>(5.4)</sup> have reported their study about bonding behavior between FRP sheets and concrete and produced a simple relationship for their research by attempting to find a correlation between the maximum bond stress, the slip at maximum bond stress and ultimate slip using the bending test and double shear test.

Dai et al <sup>(5.5)</sup> and Zhou et al <sup>(5.6)</sup> developed a simple method to derive the local bond-slip relationship at the FRP-concrete interface based on the relationship between load and slips at the loaded end from a pull-off test. Research from Ko and Sato <sup>(5.7)</sup> proposed a bond stress-slip relationship between FRP sheet and concrete interface under cyclic load with three types of FRP sheets (aramid, carbon, and polyacetal). Pham and Al-

Mahaidi <sup>(5.8)</sup> reported about modeling of CFRP bonded on concrete using a wet lay-up method and compared with bond slip curve from experimental and theoretical result.

A set of three bond-slip model for FRP sheet/plate bonded to concrete was developed by Lu et al <sup>(5.2)</sup>. It should be noted that the scope of this research has been limited to adhesive layer that has shear stiffness,  $K_a (= G_a/t_a$ , where  $G_a =$  elastic shear modulus of the adhesive and  $t_a =$  the adhesive layer thickness), is no less than 2.5 GPa/mm. Dai and Ueda <sup>(5.9)</sup> reported that the use of very soft adhesive layer could increase the bond strength of FRP-concrete. This research was limited with shear stiffness between 0.14 and 1.00 GPa/mm.

However, the research regarding bonding behavior of the CFRP plate and concrete with a soft layer system almost has never been done. Therefore, in this chapter, the application method of polyurea soft layer as an additional adhesive beside epoxy will be discussed. It can be noted in CFRP plate strengthening method that by adding a soft layer adhesive between usual adhesive, such as epoxy, and concrete, the active bond zone will be longer. It means that the effective bonding length will be increased so it is expected that the use of soft layer can enhance bond strength and bonding behavior. Arazoe et al <sup>(5.10)</sup> have conducted a similar study using CFRP strand sheet and polyurea soft layer system to find out the bonding and flexural behavior. It was reported that specimen with polyurea soft layer system could increase the maximum load more than three times than specimens without polyurea soft layer system.

## 5.2 Research objective

The objective of this study is to clarify the effect of putting a polyurea soft layer between usual adhesive (epoxy) and concrete. To reach the general aim, the following specific objectives have been defined:

- To investigate the differences of failure mode or fracture mode from specimen with polyurea soft layer and without polyurea soft layer system.
- To compare the bonding behavior of specimen with polyurea soft layer and without polyurea soft layer system for both high tension and high modulus type of CFRP plate.
- To determine effective bonding length on the specimen with and without polyurea soft layer system. FEM analysis will be used to solve this analysis problem for



specimen which have a fairly long bonding length and that could not be carried out by experiment.

- To propose a new simple equation that can be applied to the application of CFRP plate strengthening method with application of both soft layer and no soft layer.

### 5.3 Material properties

Two types of CFRP plate used in this experiment that is high tension type and high modulus type. **Photo 5.1(a)** and **Photo 5.1(b)** show the appearance for high tension type and high modulus type of CFRP plate, respectively. **Table 5.1** shows the mechanical properties of the CFRP plate. The ultimate strain of both CFRP plate high tension and high modulus type are around  $14,300\mu$  (microstrain) and  $3,900\mu$  (microstrain). **Table 5.2** shows properties of concrete used in this research.

This study used polyurea putty as soft adhesive material with the polyurethane primer and epoxy putty as common adhesive material with the epoxy resin primer. Resin/hardener mixing ratio for both polyurethane primer and polyurea putty are 1:1 and 1:3, respectively. Meanwhile, resin/hardener mixing ratio by weight for both epoxy resin primer and epoxy putty are 2:1.

**Photo 5.2(a)** and **Photo 5.2(b)** show the material of primer for both polyurea and polyurea putty, respectively and **Photo 5.3(a)** and **Photo 5.3(b)** show the material of primer for both epoxy and epoxy putty, respectively. **Table 5.3** shows the properties of epoxy putty adhesives and polyurea soft layer putty.



(a) High tension type



(b) High modulus type

**Photo 5.1** CFRP plate

**Table 5.1** CFRP Plate material properties

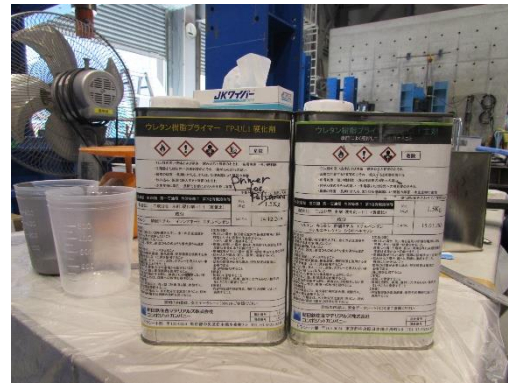
Material Properties	High modulus type	High tension type
Tensile modulus (MPa)	410,000	167,000
Tensile strength (MPa)	1,625	2,400
Unit weight (kg/mm)	1,700	1,600

**Table 5.2** Concrete material properties (MPa)

Material Properties	Concrete
Compressive strength	49.8
Tensile strength	4.3



(a) Polyurethane primer



(b) Polyurea putty

**Photo 5.2** Primer and polyurea putty



(a) Epoxy resin primer



(b) Epoxy putty

**Photo 5.3** Primer and epoxy putty

**Table 5.3** Material property of adhesive and soft layer (MPa)

Material Properties	Epoxy putty	Polyurea putty
Compressive modulus	7,233	34
Tensile modulus	5,300	20
Compressive strength	96.0	6.8
Tensile strength	37.0	12.0
Flexural strength	63.0	-
Tensile shear strength	16.6	5.6
Density	1.60	1.16

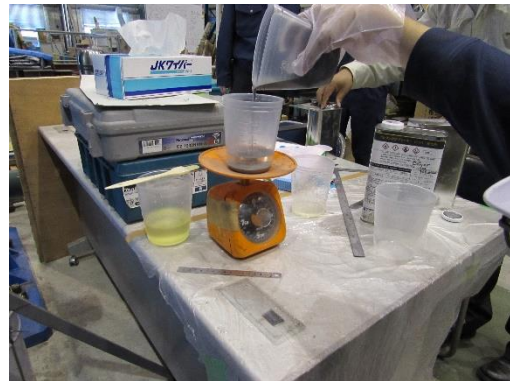
## 5.4 Specimen preparation

### 5.4.1 With soft layer specimen

**Photo 5.4(a) ~ Photo 5.4(h)** describe steps the making of soft layer specimen in this research.



(a) Concrete prisms



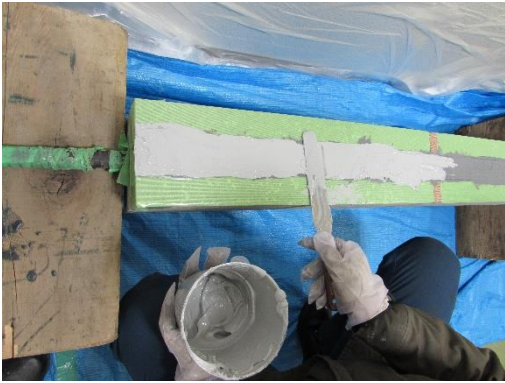
(b) Polyurethane primer measurement (200gr/m<sup>2</sup>)



(c) Polyurethane primer application (treatment  $\pm$  2 hours)



(d) Polyurea putty measurement (928gr/m<sup>2</sup>)



(e) Polyurea putty application (treatment  $\pm$  8 hours)



(f) Epoxy putty measurement (1600gr/m<sup>2</sup>)



(g) Epoxy putty application (treatment  $\pm$  2days)



(h) Completed

**Photo 5.4** The making process of specimen with soft layer

#### 5.4.2 Without soft layer specimen

**Photo 5.5(a) ~ Photo 5.5(f)** describe steps the making of without soft layer specimen in this research.



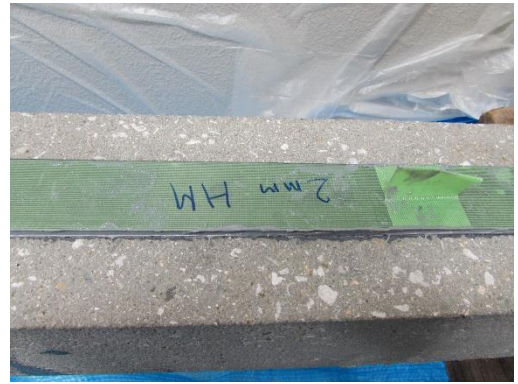
(a) Concrete prism



(b) Epoxy resin primer measurement (200gr/m<sup>2</sup>)



(c) Epoxy resin primer application (treatment  $\pm 4$  hours) (d) Epoxy putty measurement (1600gr/m<sup>2</sup>)



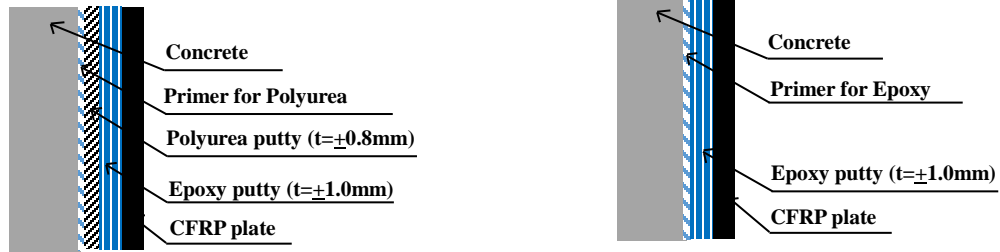
(e) Epoxy putty application (treatment  $\pm 2$  days)

(f) completed

**Photo 5.5** The making process of specimen without soft layer

### 5.5 Test program

Because of the primary objective of this research is to find out the effect of polyurea soft layer, twenty-four specimens comprising 1mm and 2mm in thickness for high tension type of CFRP plate and 2mm and 4mm in thickness for high modulus type of CFRP plate with soft layer and without soft layer for three specimens each case were tested in this study. For more detail, **Fig. 5.1(a)** and **Fig. 5.1(b)** show the application methods of with and without polyurea soft layer. The detail of specimen can be seen in **Fig. 5.2** and **Fig. 5.3**. The identity of each specimen can be seen at the **Table 5.4**.



(a) With polyurea soft layer

(b) Without polyurea soft layer

**Fig. 5.1** Detail of specimen bonding method

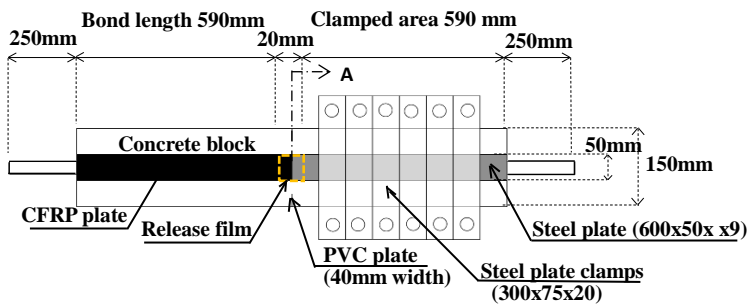


**Fig. 5.2** Specimen detail

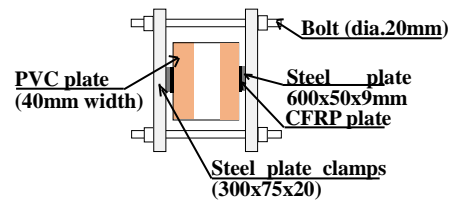


**Fig. 5.3** Cross section A-A

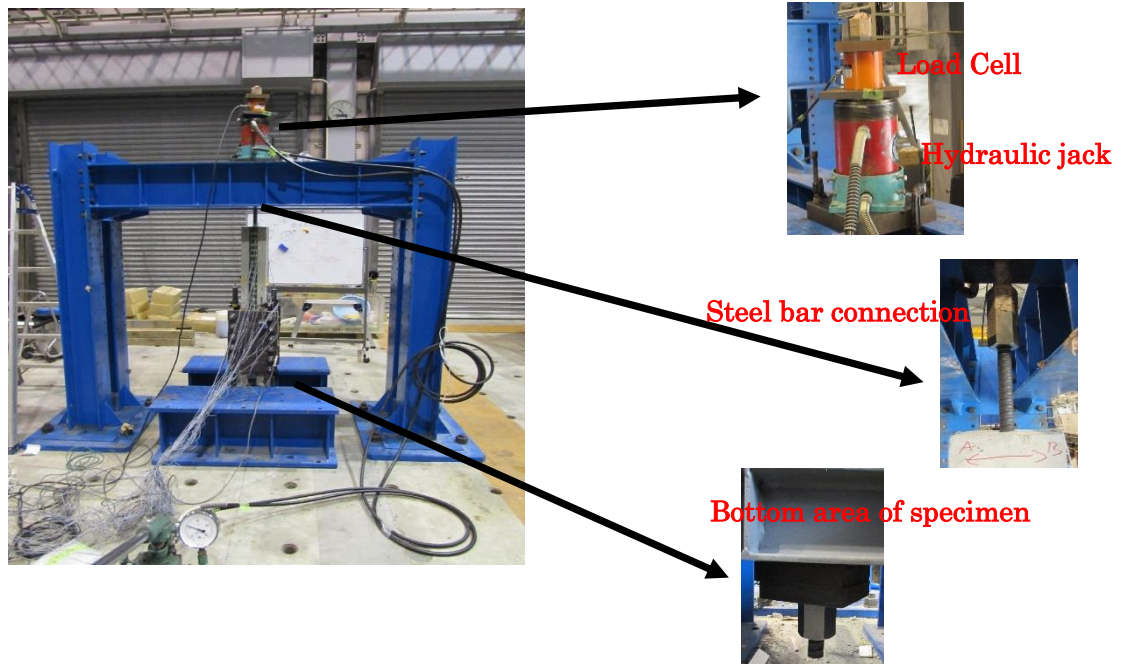


**Photo 5.6** Experiment setting up

**Table 5.4** Specimen identity and experimental results

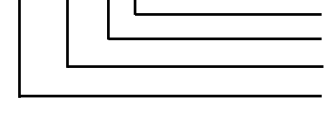
Specimen code	Soft layer	$E_p t_p$ (kN/mm)	$P_{max}$ (kN)	$\tau$ (MPa)	$G_f$ (N/mm)	$\tau_{b,max}$ (MPa)		$s_{max}$ (mm)		$n$	Failure Mode
						$\tau_{b,max}$	Ave.	$s_{max}$	Ave.		
1HTS1	Yes	167	167	2.83	8.35	3.68		1.14		3.0	AF+CF
1HTS2			163	2.76	7.95	3.55	3.54	1.20	1.28		AF+CF
1HTS3			149	2.53	6.65	3.39		1.50			AF
1HTN1	No	167	59	1.00	1.04	4.68		0.26		4.0	AF
1HTN2			76	1.30	1.77	5.56	5.08	0.11	0.18		AF
1HTN3			57	0.97	0.99	5.01		0.15			AF
2HTS1	Yes	334	177	3.00	4.69	5.45		0.65		5.0	CF
2HTS2			166	2.81	4.12	4.55	4.27	0.76	0.75		CF
2HTS3			167	2.83	4.18	3.81		0.84			CF
2HTN1	No	334	87	1.47	1.13	5.54		0.14		5.0	IF
2HTN2			98	1.66	1.44	6.16	5.79	0.22	0.18		IF
2HTN3			88	1.49	1.16	5.66		0.21			IF
2HMS1	Yes	820	161	2.73	1.58	3.34		0.39		4.5	IF
2HMS2			183	3.10	2.04	3.38	3.58	0.31	0.35		CF
2HMS3			164	2.79	1.65	4.03		0.34			CF
2HMN1	No	820	170	2.88	1.76	6.13		0.31		5.5	AF
2HMN2			154	2.60	1.43	5.19	5.57	0.19	0.23		AF+IF
2HMN3			155	2.63	1.46	5.40		0.20			AF+IF
4HMS1	Yes	1640	180	3.05	0.99	4.84		0.22		10.0	CF
4HMS2			206	3.49	1.29	6.89	6.06	0.26	0.25		CF
4HMS3			188	3.19	1.08	6.44		0.26			CF
4HMN1	No	1640	215	3.64	1.41	6.18		0.24		10.0	IF
4HMN2			215	3.64	1.41	7.56	7.24	0.24	0.24		IF
4HMN3			229	3.88	1.60	7.99		0.23			IF

Note:  $\tau$  = average shear stress,  $\tau = P_{max} / (b_f l_b)$ ,

CF= concrete failure, IF= interfacial failure, AF= adhesive failure

Specimen identification;

1 HT S 1



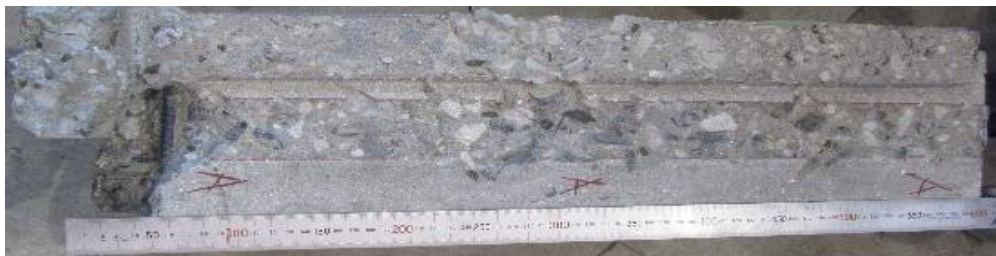
The bonding test was done by adopting the JSCE-E543–2007<sup>(5.11)</sup>, about the test method for bonding properties of continuous fiber sheet to concrete. A typical double lap shear pull out test setup was applied in this study. CFRP plate used in this research had a width of 50mm. The specimen consists of a concrete block with the size of 150x150x1200mm. In the block center was installed PVC plate has the width of 4mm. The two steel bars embedded in concrete and also had no connection. It means that the concrete block was divided into two sections and connected only through by CFRP plate.

The one side of the concrete block was clamped by steel plate to ensure the occurrence the failure only on the other side where strain gauges were set. On the two surfaces of the prism, the strain gauge interval was set at 40mm and distributed in range from 10mm to 570mm from the center of the prism. To avoid stress concentration, a release film was placed on the concrete surface at the block center. The loading rate and recording data on the data logger were 5kN/min. The detail of the test setup can be seen in **Fig. 5.2**, **Fig. 5.3** and **Photo 5.6**.

## 5.6 Result and discussion

### 5.6.1 Failure mode

The experimental results are shown in **Table 5.4**. The failure mode of each specimen is demonstrated by CF, IF, and AF representing concrete, interfacial, epoxy and/or polyurea adhesive failure, respectively. Generally, specimen with polyurea soft layer show concrete failure mode. As a representative, the failure condition in specimen 4HMS1, 2HTN1 and 1HTN3 are presented in **Photo 5.7(a)**, **Photo 5.7(b)** and **Photo 5.7(c)** for CF, IF and AF, respectively. Concrete failure was identified by destruction of the concrete prisms as deep as 5mm to 10mm or more. The surface of concrete prism failure zone was uneven, with the aggregate being clearly seen. Interfacial failure was mostly along the concrete-adhesive interface. The failure surface of interfacial failure was a few millimeter on the concrete-adhesive interface. Much less or little concrete was attached to the CFRP plate elsewhere. Then, the adhesive failure was identified as a separation on the epoxy or the polyurea or between epoxy and polyurea.



(a) 4HMS1





(b) 2HTN1



(c) 1HTN3

**Photo 5.7** Failure types of specimen

## 5.6.2 Strain distribution

### 5.6.2.1 CFRP plate high tension type

**Fig. 5.4** shows the example of strain distribution along the plate at typical loading levels as obtained in the experiment for CFRP plate high tension type. **Fig. 5.4(a)**, **Fig. 5.4(b)**, **Fig. 5.4(c)** and **Fig. 5.4(d)** show strain distribution for 1HTS2, 1HTN3, 2HTS3 and 2HTN2, respectively, as a representative for CFRP plate high tension type 1mm and 2mm in thickness with and without polyurea soft layer.

Specimen with soft layer showed linear strain reduction from the beginning of the loading level after the prism concrete was crack and there was a possibility of slip happening at the free end because some strain could be seen near from free end. This indicated that all the surface of the concrete was the actual bond-resisting area from plate to concrete, and naturally, delamination could start from anywhere on bonding area.

This behavior was different for specimen without soft layer. At the low level of load, the strain distribution tend to be linear fall from center up to around 100mm from the center with strain at the others bonding area was close to zero. However, at the maximum load, the active area shifts to the other region towards free end area, which

could be interpreted that the actual bond-resisting area was a part of the plate to the concrete surface.

Specimen with soft layer showed an increase of both load capacity and ultimate strain. Specimens that had a thick of 1mm have an increase in capacity almost three times than without soft layer specimen. This result was parallel with the ultimate strain growth. In the case of 2mm in thickness, the maximum load capacity and ultimate strain rose nearly double. If compared with the each of case, on the soft layer specimen, a decrease in the value of ultimate strain was observed until a half when compared between specimen had a thick of 2mm and 1mm. Whereas, on the specimen without soft layer the resulting strain at the specimen with thick of 2mm was only slightly smaller than thick of 1mm one.

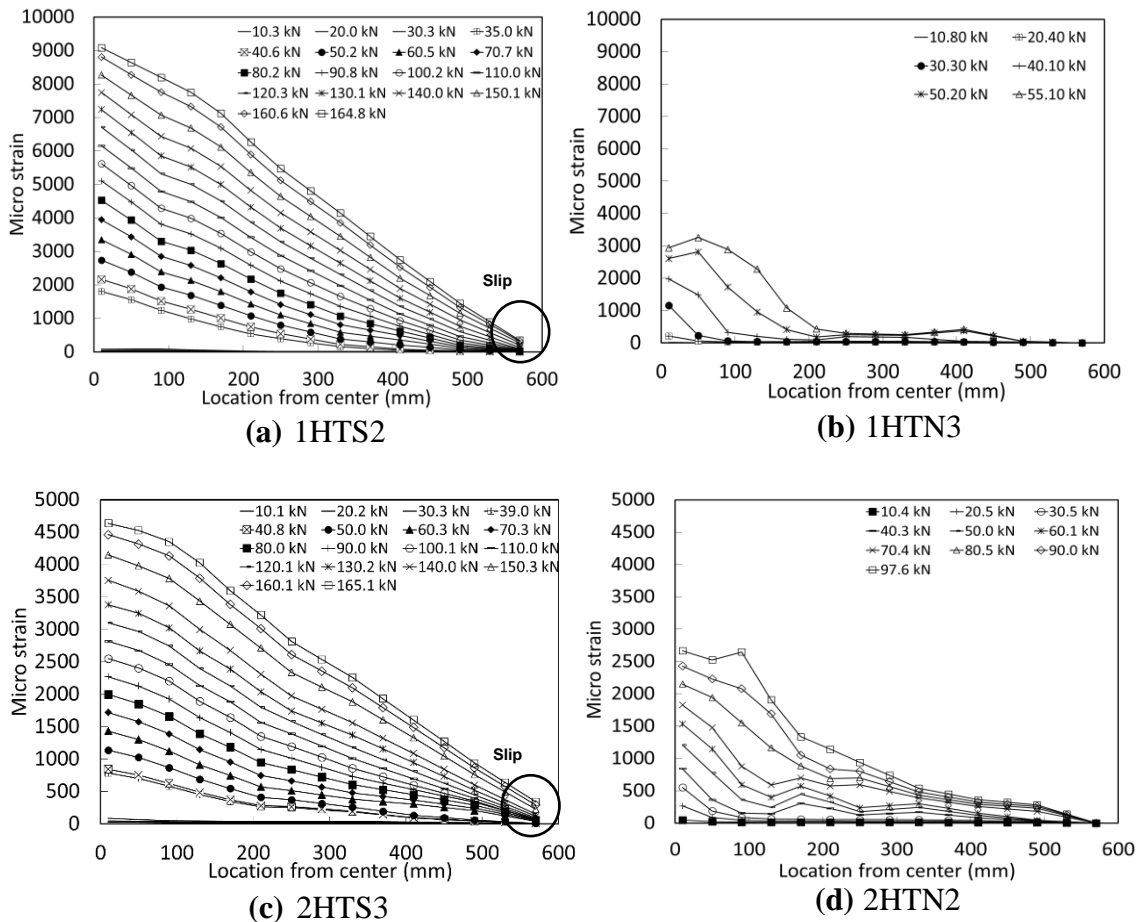


**Fig. 5.4** Strain distribution of CFRP plate high tension type

### 5.6.2.2 CFRP plate high modulus type

**Fig. 5.5** shows the example of strain distribution along the plate at typical loading levels as obtained in the experiment for CFRP plate high modulus type. As a representative for CFRP plate high modulus has a thickness of 2mm and 4mm with polyurea soft layer and without polyurea soft layer, **Fig. 5.5(a)**, **Fig. 5.5(b)**, **Fig. 5.5(c)** and **Fig. 5.6(d)** show strain distribution for 2HMS2, 2HMN1, 4HMS1 and 4HMN2, respectively.

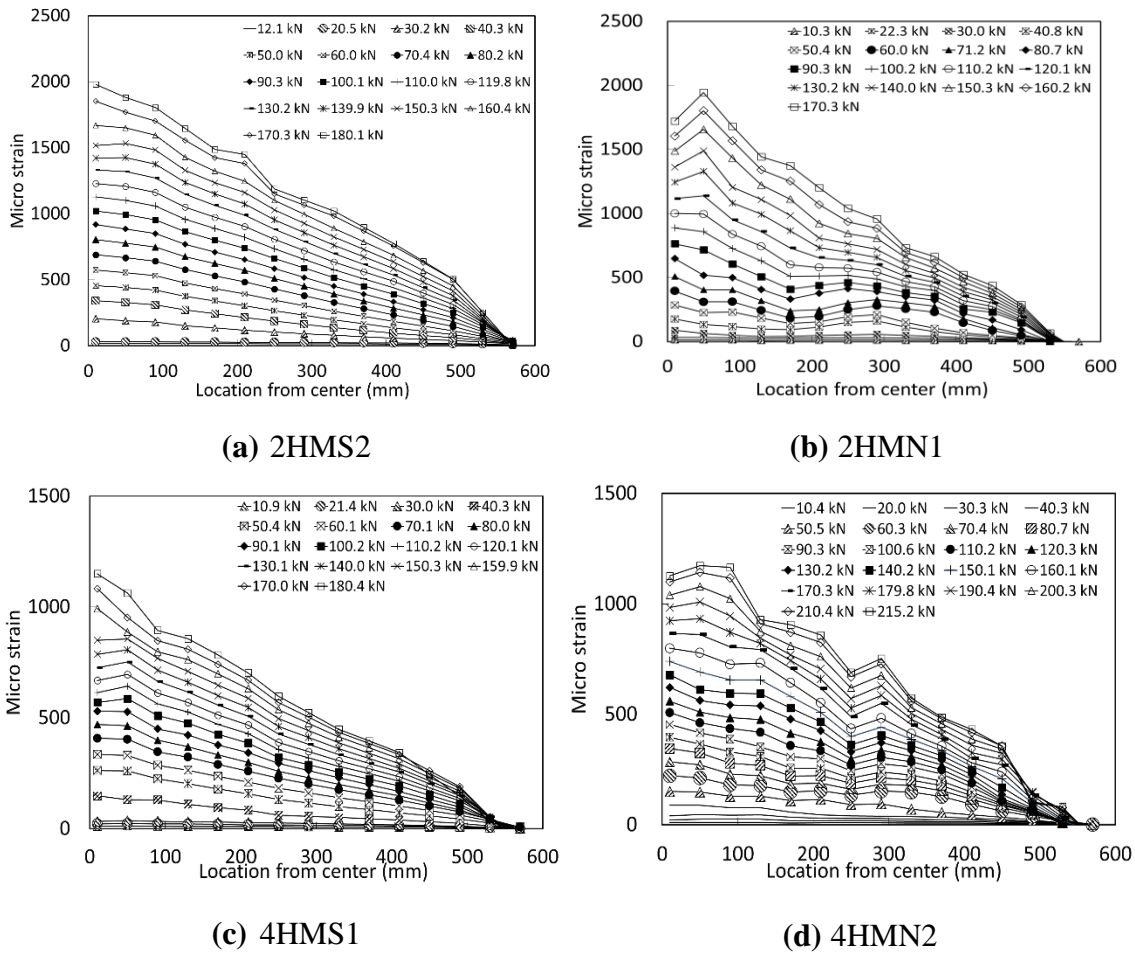


**Fig. 5.5** Strain distribution of CFRP plate high modulus type

The specimen both with soft layer and the without soft layer exhibited similar behavior. This showed that the polyurea soft layer specimen did not give significant effect on the CFRP plate high modulus type specimen. For 2mm in thickness of CFRP plate

specimen, the maximum load capacity for both with soft layer and without soft later system produced almost the similar maximum load. In the other hand, for CFRP plate 4mm in thickness specimen, the maximum load capacity resulted different load where specimen without polyurea soft layer having a bigger load compared than with polyurea soft layer specimen.

For all specimen, the strain distributions decrease linearly. It can be seen that all the surface of the concrete was the active area which resists bonding plate to concrete. The maximum strain of both with soft layer and without soft layer specimen are almost similar that is around 2,000 microstrain for 2mm in thickness and around 1,200 microstrain for 4mm in thickness specimen.

#### 5.6.2.3 Strain distribution at the maximum load

As a comparison for each of specimen, **Fig. 5.6(a) ~ (d)** show the strain distribution when the maximum load was achieved. It could be found that high tension type (1mm and 2mm in thickness of CFRP high tension type) specimen with polyurea soft layer shows a more uniform distribution of strain. This indicated that all the surface of the concrete was the actual bond-resisting area from plate to concrete. This phenomenon given fact that the effective bonding length of polyurea soft layer specimen was longer than the bonding length. Meanwhile, for specimen without polyurea soft layer show the actual bond-resisting area only a part of the bonding length which is about 200-240mm effective bonding length ( $l_e$ ) for 1mm in thickness and 270-330 for 2mm, ( $l_e$ ), for 2mm in thickness of CFRP plate high tension type.

This behavior is different for high modulus type (2mm and 4mm in thickness of CFRP high modulus type) specimen. It can be seen that the strain distribution exhibit more evenly for both with soft layer and without soft layer specimen with a similar ultimate strain value. This phenomenon, obviously, produces the similar maximum load. Moreover, maximum load of the 4HMS specimen (4mm HM type with soft layer specimen) is smaller than the 4HMN specimen (4mm HM type without soft polyurea layer specimen) (see **Table 5.4**). This also is due to the bonding length of high modulus type specimen is shorter than effective bonding length. To give a clear explanation, it can be done by conducting research with a longer specimen, although in the fact that it is difficult to be conducted because of the limitation of existing equipment. Furthermore, in the next section of this

chapter will be conducted analysis and verification using FEM analysis to get a complete information on the longer specimen that using polyurea soft layer system.

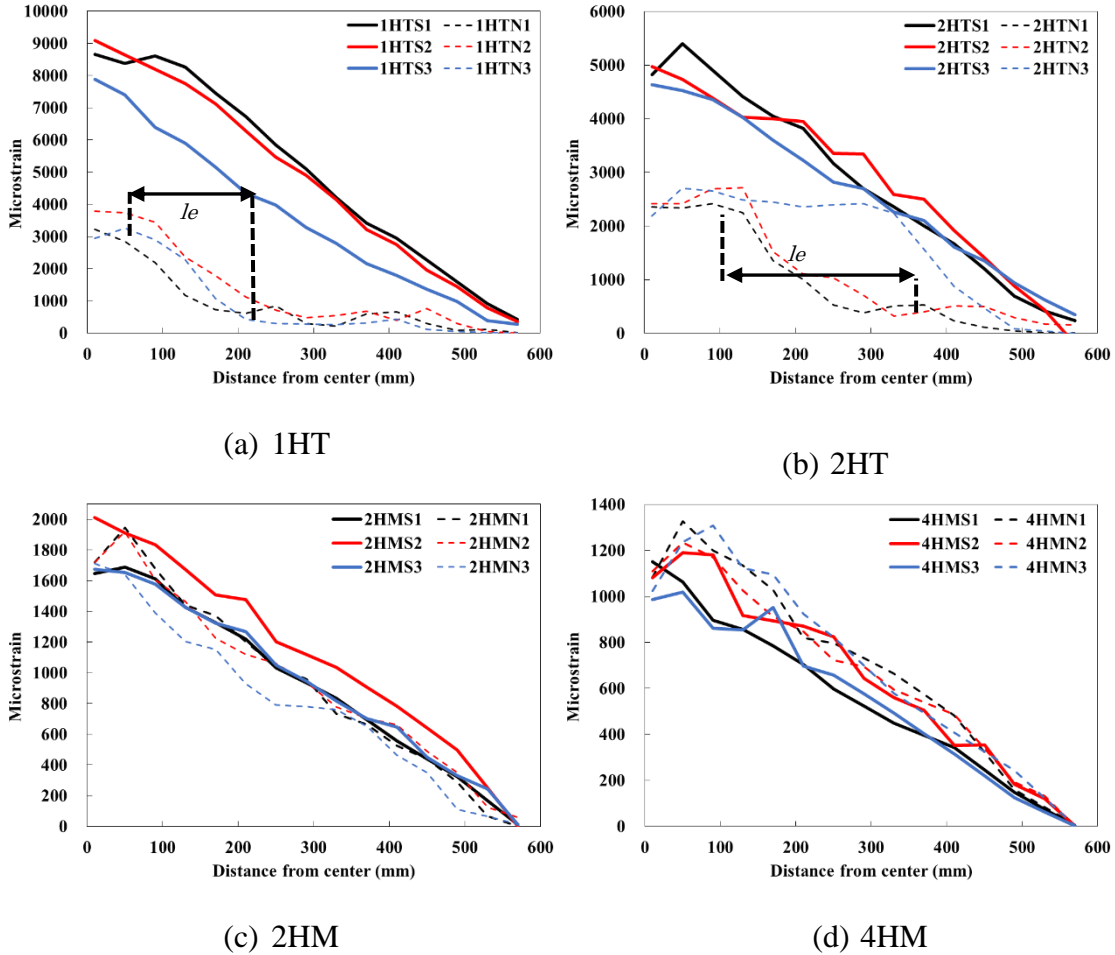


**Fig. 5.6** Strain distribution at maximum load

### 5.6.3 Maximum load and CFRP plate stiffness relationship

Due to the constant bonding width of 50mm used in this study for all specimen, the stiffness of the CFRP plate can be defined as the multiplication of the elasticity modulus of the plate and thickness of the plate ( $E_{ptp}$ ). **Fig. 5.7** shows the relationship between maximum load and stiffness of CFRP plate. This figure is divided into two lines that are the solid line and the broken line for soft layer specimen and no soft layer specimen, respectively. Clearly, it can be seen from the results of the regression line that soft layer specimens produce almost similar the maximum load for each of CFRP plate

stiffness. The mean maximum load of the soft layer specimen is 172.58kN. The broken line, for the without soft layer specimen, shows different behavior. The without soft layer specimen shows that the maximum load increases as the CFRP plate stiffness is increased and the results of regression analysis on maximum load is proportional almost equal to  $\sqrt{E_p t_p}$ . This result is consistent with the previous study <sup>(5.5), (5.9)</sup>. In addition, it can be seen that the comparison of soft layer specimen and without soft layer specimen in average are 2.49, 1.87, 1.06 and 0.87 for 1mm HT, 2HT, 2HM and 4HM type, respectively.

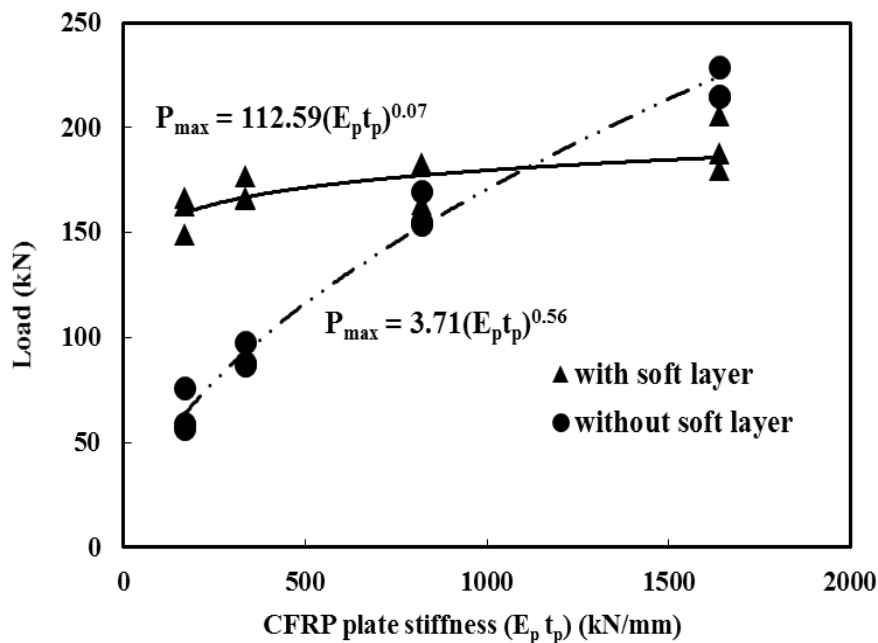


**Fig. 5.7** Maximum load – CFRP plate stiffness relationship

#### 5.6.4 Bond stress-slip relationship

##### *Local Bond Stress*

The bond stress-slip relationship is one of the important parameter to understand at the interface between two bonding material. The bond stress-slip curve is made up of an ascending and a descending branch. Some of bond stress-slip relationship have been recommended by many researchers. For example, the configuration of bond stress-slip relationship, including bilinear, cut off, tensile softening type and popovic's type have been proposed <sup>(5.3), (5.12), (5.13), (5.14)</sup>. In order to obtain the local bond stress-slip relationship,

the average bond stress of section  $i$  is calculated the following equation:

$$\tau_{b,i} = \frac{(\varepsilon_{f,i} - \varepsilon_{f,i-1})t_f E_f}{\Delta x} \quad (5.1)$$

Where;

$\tau_{b,i}$  = average bond stress between the section  $i$  and  $i-1$  from free end of the laminate (MPa)

$\varepsilon_{f,i}$  = strain of CFRP plate at the section  $i$

$t$  = thickness of CFRP plate (mm)

$E_f$  = elastic modulus of CFRP plate (kN/mm<sup>2</sup>)

$\Delta x$  = strain gages interval (mm)

#### *Local Slip*

Local slip or slip is caused by the strain differences between CFRP plate and concrete. However, due to the stiffness of the concrete is very large, the concrete strain can be neglected. Next, to simplify the analysis, the free end slip can be approximately as zero. The slip can be calculated by the following equation:

$$s_i = \frac{\Delta x}{2} (\varepsilon_0 + 2\sum_{j=1}^{i-1} \varepsilon_j + \varepsilon_i) \quad (5.2)$$

Where;

$s_i$  = slip between CFRP plate and concrete corresponding with average bond stress between sections  $i$  and  $i-1$  from the free end of the laminate (mm)

$\varepsilon_0$  = CFRP plate strain gauge at the free end

$\varepsilon_j$  =  $j$  strain gauge on CFRP plate

**Fig. 5.8(a)** and **Fig. 5.8(b)** show the bond stress-slip for the specimen of soft layer and no soft layer, respectively, which have a thick of 2mm for high tension type. Plotted points are from four points of strain gauge from the center of the concrete prism (loaded end,  $x=0$ ). From both **Fig. 5.8(a)** and **Fig. 5.8(b)** can be seen that soft layer makes a longer slip with a smaller bond stress than no soft layer one. Furthermore, a long slip can be observed after the peak in the bond stress-slip curves, which indicates a ductile bond

behavior of soft bond specimen. By considering the failure mode of soft layer specimen, the possibility the ultimate slip can be more than present results if the concrete strength is increased.

*Fitting for Popovics's equation*

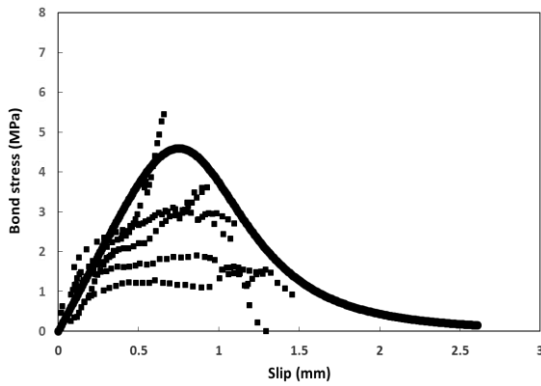
The Popovics's equation is one of the methods to define the bond stress-slip into a mathematical function. The Popovic's equation can be written as:

$$\frac{\tau_b}{\tau_{b,max}} = \frac{s}{s_{max}} \frac{n}{(n-1) + \left(\frac{s}{s_{max}}\right)^n} \quad (5.3)$$

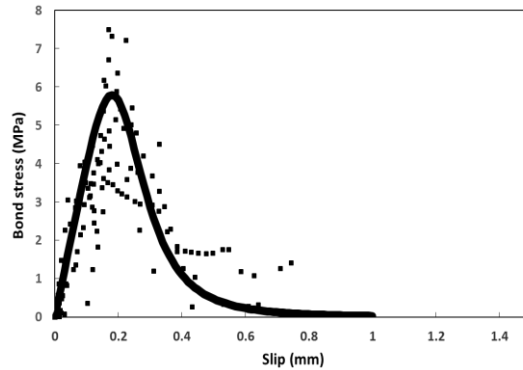
Where;

- $\tau_{b,max}$  = the maximum bond stress (MPa)
- $s_{max}$  = the slip corresponding to the maximum bond stress (mm)
- $n$  = the constant of the curve.

The use of this formula has been applied by previous researchers as Nakaba <sup>(5.3)</sup>. **Table 5.4** contains the parameter of fitting Popovics's equation, and the illustration of the fitting result of bond stress-slip can be seen in **Fig. 5.8(a)**, **Fig. 5.8(b)** and **Fig. 5.8(c)**.

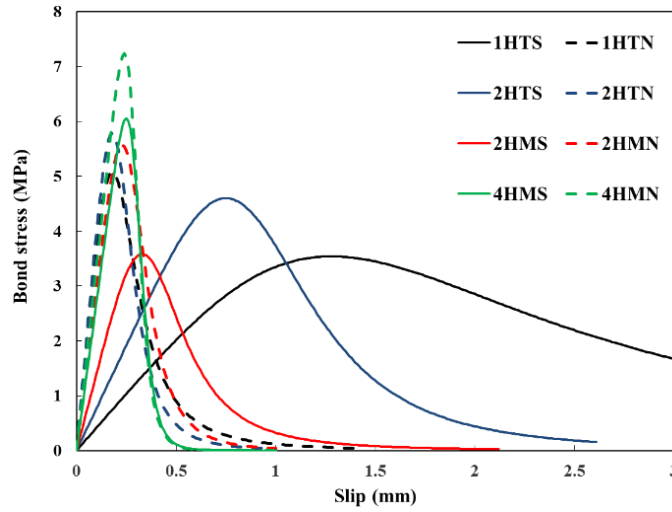


**(a)** Bond stress-slip relationship and fitting by Popovics equation for with soft layer spec. 2mm HT.



**(b)** Bond stress-slip relationship and fitting by Popovics equation for without soft layer spec. 2mm HT.





(c) Fitting results for all specimen

**Fig. 5.8** Local bond stress-slip relationship

**Fig. 5.8(c)** show the bond stress-slip after fitting by popovics's equation for all specimen. It can be seen that soft layer makes a longer slip with a smaller bond stress than no soft layer specimen for CFRP high tension type. Furthermore, a long slip can be observed after the peak in the bond stress-slip curves, which indicates a ductile bond behaviour. The local bond stress-slip is unique for specimen that have bond length longer than effective bonding ( $l_b > l_e$ ). Obviously, the local bond stress-slip of the specimen that have bonding length shorter than effective bonding length ( $l_b < l_e$ ) can produce different result.

#### 5.6.5 Interfacial fracture energy ( $G_f$ )

Theoretically, based on the nonlinear fracture mechanics, area under bond stress-slip curve is defined as interfacial fracture energy ( $G_f$ ). JSCE <sup>(5.11)</sup> given the theoretical value of  $G_f$  as follows;

$$G_f = \frac{P_{max}^2}{8b^2 E_p t_p} \quad (5.4)$$

Where;

$G_f$  = Interfacial fracture energy (N/mm)

- $P_{max}$  = Maximum load (N)  
 $b$  = width of CFRP plate (mm)  
 $l_b$  = bond length (mm)  
 $E_p$  = tensile modulus of CFRP plate (N/mm<sup>2</sup>)  
 $t_p$  = thickness of CFRP plate (mm)

With the assuming that the stiffness of concrete is very large, it is clearly shown that **Eq. 5.4** can be used for any unknown bond stress-slip relation. **Table 5.4** shows the results of each of specimen calculated by based on **Eq. 5.4**. The larger interfacial fracture energy, the harder debonding becomes. With the increase of interfacial fracture energy, the maximum load and structural ductility can be improved and the low interfacial fracture energy can result early debonding <sup>(4.15)</sup>.

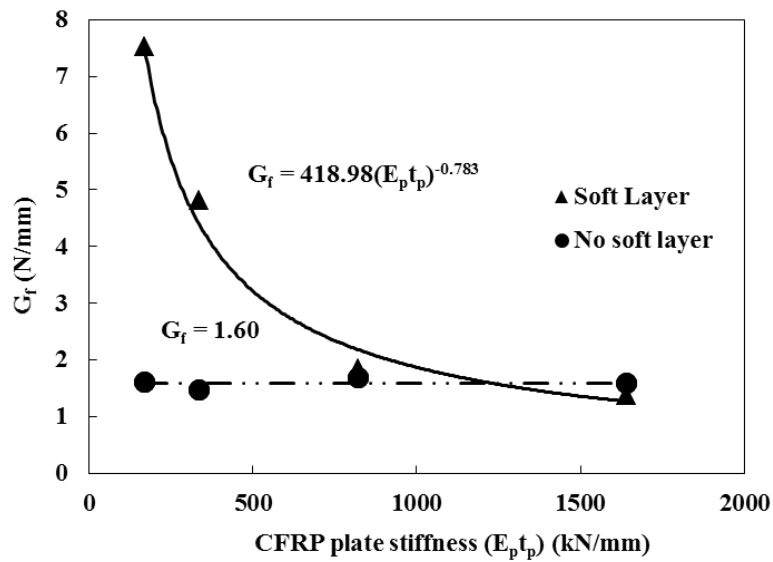


**Fig. 5.9** Interfacial fracture energy-CFRP plate relationship of experimental results

**Fig. 5.9** shows the experimental  $G_f$  is derived from the integration of bond stress-slip area after fitting by Popovics's equation and CFRP plate stiffness for both with soft layer specimen and without soft layer specimen. It is clearly seen that on the soft layer specimens show an increase of interfacial fracture energy with decreasing the plate stiffness. The smaller the CFRP plate stiffness, the more effective soft layer can increase the interfacial fracture energy. However, for the without soft layer specimen, it can be seen that the interfacial fracture energy is almost a constant value for all CFRP plate

stiffness. The specimen without soft layer results are similar to the previous study <sup>(5.9)</sup>.

### 5.6.6 Effect of polyurea soft layer for experiment result

Effect of polyurea soft layer for this experiment specimen can be expressed by comparing the maximum load capacity from specimen with soft layer and without soft layer or it can be written with;

$$n = \frac{P_{max\ softlayer}}{P_{max\ no\ softlayer}} \quad (5.5)$$

Where;

$P_{max\ softlayer}$  = average ultimate load capacity for specimen with soft layer (kN)

$P_{max\ no\ softlayer}$  = average ultimate load capacity for specimen without soft layer (kN)

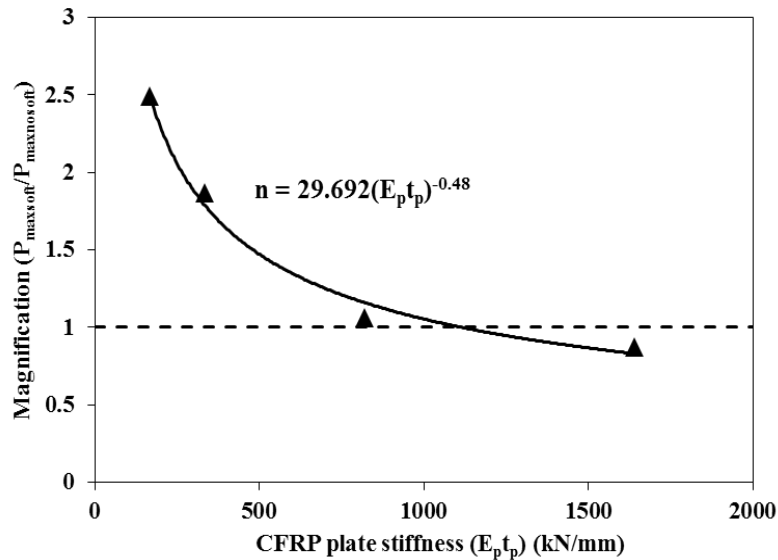


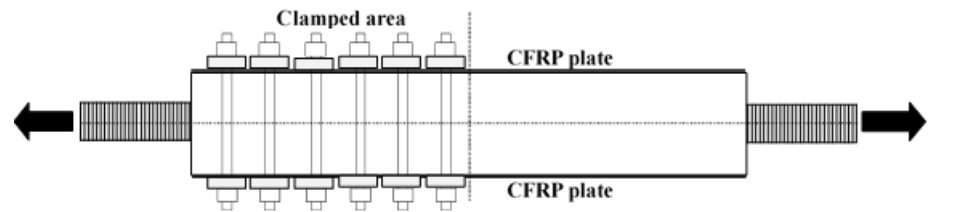
**Fig. 5.10** Effect of soft layer for each of CFRP plate stiffness

To find the magnification factor from this experiment, it is obtained by dividing average ultimate load capacity for each of CFRP plate stiffness. **Fig. 5.10** shows the effect of soft layer for each of CFRP plate stiffness. It can be seen that the smaller stiffness of CFRP plate, the greater the magnification factor that can be produced. It can be noted that this result is only valid in this experiment, this relationship will have different results when specimen have bonding length is longer than effective bonding length.

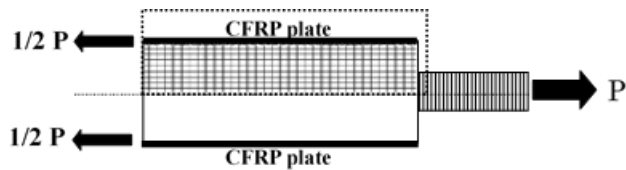
## 5.7 Finite element analysis of CFRP plate and concrete bonding behavior

### 5.7.1 Idealization

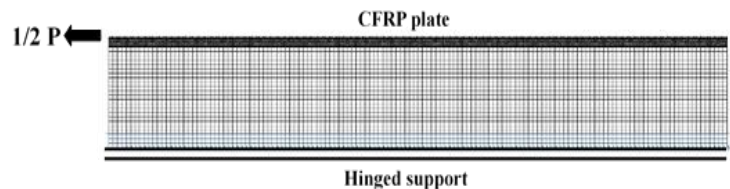
A typical finite mesh and boundary were successfully used to model the bond between CFRP and concrete in previous research. For numerical analysis, this study adopted a typical finite element used in previous research <sup>(5,8)</sup>. The simulation was done by using two-dimensional non linear FE analysis DIANA (version 9.5). The idealization process of the specimen, the load application and the boundary conditions are shown in **Fig. 5.11(a) ~ (c)**. For simplicity, a quarter of concrete prism was modelled in this study with the produced load was a half of actual load. Next, to simulate the real response of debonding process, it was necessary for modeling the behavior of concrete, CFRP plate and local bond-slip between CFRP plate-concrete including interfacial fracture energy of CFRP plate-concrete.



(a) Bonding test specimen



(b) A half of specimen and load transfer



(c) Idealization of specimen, load and boundary condition for FE analysis

**Fig. 5.11** Idealization of the finite element analysis

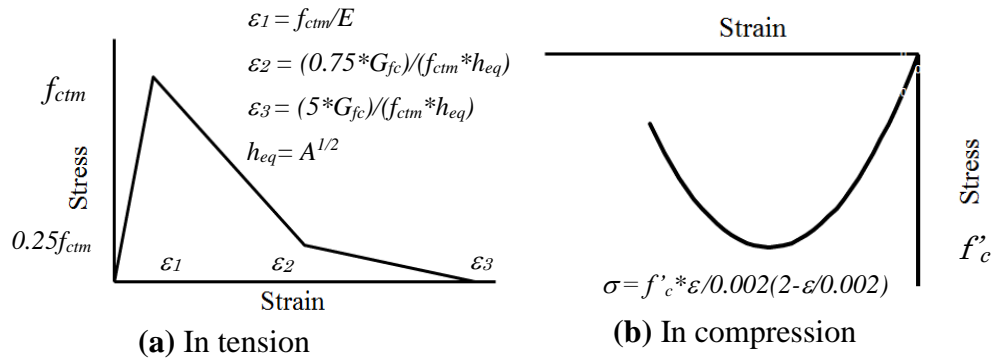


**Fig. 5.12** Constitutive law of concrete

### 5.7.2 Modelling of the material and interface

Concrete was idealized using total strain rotating crack model. In tension, this model used a non-linear tension softening stress-strain relationship proposed by Hordijk<sup>(5.16)</sup> as shown in **Fig. 5.12(a)**. This relationship is using expression provided by CEB-FIP Model Code<sup>(5.17)</sup>, where  $G_{fc}$  is the fracture energy or energy required to spread a tensile crack of unit area and  $h$  is the crack bandwidth that related to area of the element. The  $G_{fc}$  was computed to be 0.105N/m. In compression, the concrete model applied the model which was described by the function proposed by Thorenfeldt, et. al<sup>(5.18)</sup> as shown in **Fig. 5.12(b)**. Moreover, CFRP plate and epoxy adhesive were assumed to be isotropic and modeled with linear elastic properties, while, polyurea adhesive was considered as steel material with strain hardening after reach the yield point. Furthermore, the interface behavior between plate and concrete is a full composite model.

### 5.7.3 Verification of FEM results with experimental results

The FEM result were compared with the experimental results in order to find the curve and value of maximum load, strain distribution, total load and total slip of CFRP plate at the loaded end or  $x=0$ , and stress distribution that give the best fit.

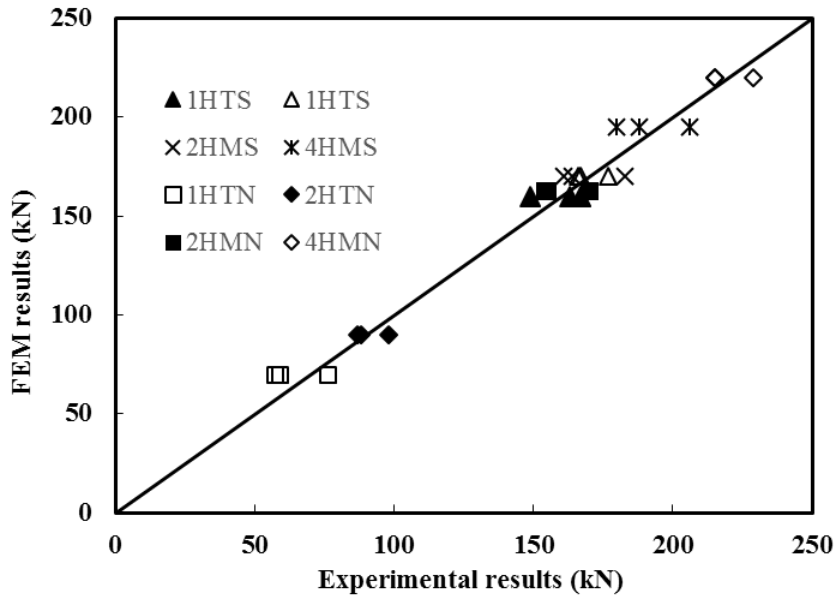


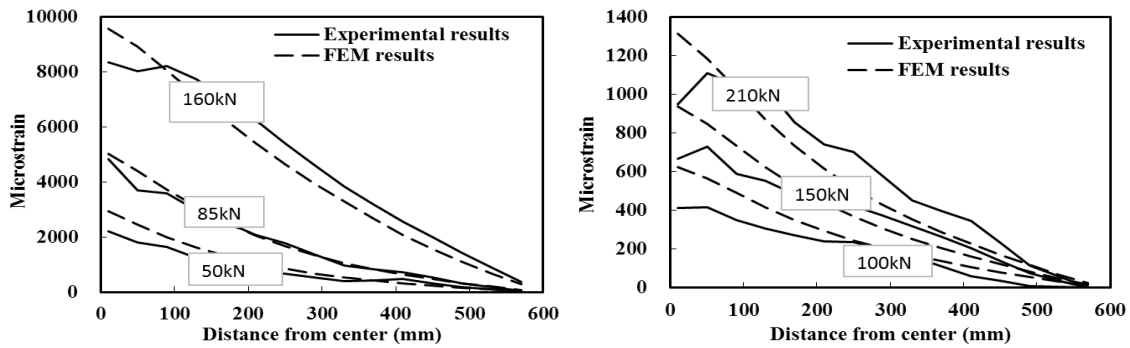
**Fig. 5.13** Comparison of the maximum load by FE model and experimental results

#### 5.7.3.1 Maximum load

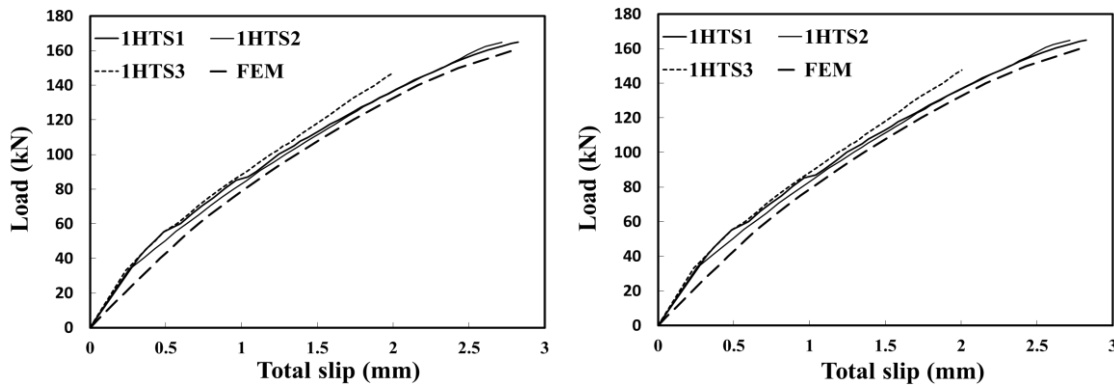
The maximum bond strength results as produced by finite element analysis and experimental results measured in the experiments for all specimen are compared in **Fig. 5.13**. The predictions are fairly accurate given the fact that the deviation of the load from FEM results and experimental results are from 0.61% to 18.57%. The ratio average of the experimental results to FEM results is 0.99 with the coefficient of determination of 0.96.

#### 5.7.3.2 Strain distribution

As a representative, From **Fig. 5.14(a)** and **Fig. 5.14(b)** depict the predicted strain distributions from FEM analysis compared with the experimental ones for specimen 1HTS1 and 4HMN3, respectively. The strain distribution data were taken for several load condition for the same applied load. It can be said that FE and experiments results have fairly a good agreement. However, there is a little difference between FEM and experiments results, particularly at the loaded end area. This is due to the stress concentration that occurs at the loaded end area from the experimental data.



(a) 1HTS1 (b) 4HMN3  
**Fig. 5.14** Comparison between experiment and FEM analysis strain distribution



(a) 1mm HT type with soft layer specimen (b) 4mm HM type without soft layer specimen

**Fig. 5.15** Comparison between experimental and FEM load-total slip

### 5.7.3.3 Total load and total slip at loaded-end relationship

**Fig. 5.15(a)** and **Fig. 5.15(b)** show total load-total slip at loaded-end curve from FEM result compared with the experimental result for all specimen 1HTS (1mm HT type with soft layer) and 4HMN (4mm HM type without soft layer), respectively. Total slip curve is generated from the result of the strain reading at the loaded end for each of loading step. In general, the FEM models capture the curve relatively well. The curves show similar trends to those found from experiments. However, there is a slope difference of the curve at the low load level due to cracked concrete prism has not yet happened at that time, and the tensile load was not entirely taken by CFRP plate-concrete composite system.

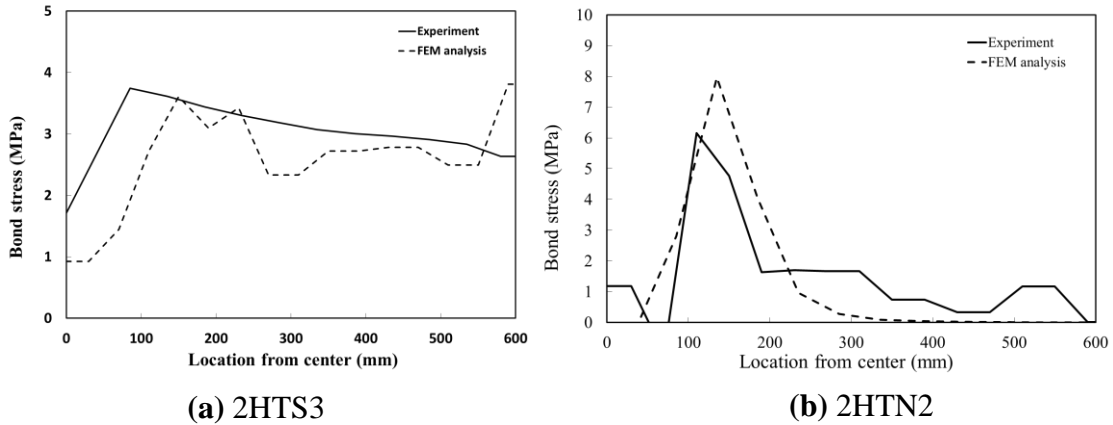


**Fig. 5.16** Comparison between experimental and FEM internal stress distribution at the maximum load

#### 5.7.3.4 Local bond stress distribution

A comparison of local bond stress distribution at the maximum load is shown in **Fig. 5.16(a)** and **Fig. 5.16(b)** for 2HTS3 specimen and 2HTN2 as a representative of specimen with soft layer and without soft layer, respectively. The thick solid line represent the experimental result distribution and the dashed line represent FEM analysis result distribution. The local bond stress is the average experimental stress between two strain gauges calculated using the same equation for bond slip relationship. The equation is;

$$\tau_{b,i} = \frac{(\varepsilon_{f,i} - \varepsilon_{f,i-1})t_f E_f}{\Delta x} \quad (5.1)$$

The local stress distribution from experiments vary significantly from one location to the other along the CFRP plate length. But, in general, the FEM analysis simulated the local bond stress distribution along bonding area relatively well and similar to what observed from experiment. The FEM analysis can capture well the existence of the stress degradation concentration near both the loaded ends of CFRP plate due to the debonding. The **Fig. 5.16(a)** shows that the specimen with polyurea soft layer the stress concentration not occur as well as can spread the stress more evenly and will produce a longer effective bonding length.



#### 5.7.4 The simulation of the FEM model

Theoretically, a clear information of bonding behavior of test specimen will look best when the effective bonding length ( $l_e$ ) is shorter than its bonding length. Based on the experiment result, it can be seen that only the 1HTN and 2HTN specimen that have effective bonding length ( $l_e$ ) is shorter than its bonding length. As a results, a complete explanation of bonding specimen behavior cannot be conveyed.

To get a more complete information of the bonding behavior of the specimen that has a longer bonding length than the effective bonding length the FEM model is used. Using the same material parameters as discussed before is expected to provide a thorough overview of the results obtained thus can represent the real situation and be used as a basis for the simple designs on CFRP strengthening method of applying either soft layer or no soft layer.

##### 5.7.4.1 Specimen with polyurea soft layer

Regarding the objective above, there were 19 (nineteen) new specimens of varying sized were analyzed by FEM analysis comprises 11 (eleven) for CFRP plate high tension type and 8 (eight) for CFRP high modulus type with variation of CFRP plate stiffness ( $E_{ptp}$ ), bonding length ( $l_b$ ) and polyurea thickness ( $t$ ) for soft layer specimen. Next, these new specimen results were combined with results from experiment. **Table 5.5(a)** and **Table 5.5(b)** show not only the parameter and the results of experimental specimens (old specimen) but also the parameter of new specimens for FEM analysis with their results. Among the FEM specimen, only one specimen rupture that is 1mm HM type specimen has a length of 2000mm.

$l_e$  column in the **Table 5.5(a)** and **Table 5.5(b)** show the effective bonding length of each specimens. Based on theory in **Fig. 5.17**, as mentioned in the previous section,  $l_e$  is determined. As mentioned before that all the experiment specimens have bonding length ( $l_b$ ) shorter than effective bonding length ( $l_e$ ) and combined with some FEM specimens. Then,  $l_e$  plate is maximum  $l_e$  of each plate stiffness ( $E_{ptp}$ ).

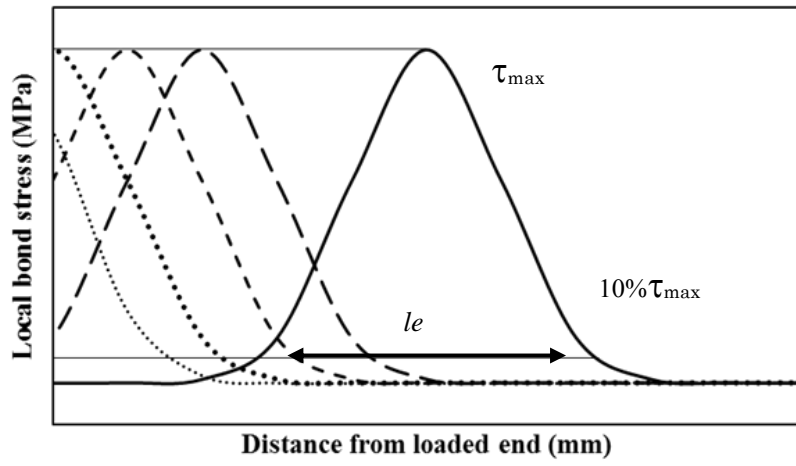


**Fig. 5.17** Effective bonding length ( $l_e$ )

**Table 5.5(a)** The parameter and results of laboratory specimen (experimental and FEM analysis) for with soft layer specimen

Series Spec.	Type of spec.	Test	CFRP plate			Bond. Length, $l_b$ (mm)	Poly. $t$ (mm)	$P_{max}$ (kN)	$l_e$ (mm)	$l_e$ plate (mm)	$l_b / l_e$ plate	$\alpha$	Note		
			type	$t$ (mm)	$E_{ptp}$ (kN/mm)										
1HTS1	Old spec.	Experimental	HT	1	167	590	0.80	167	$> l_b$	725	0.81	0.98			
1HTS2								163	$> l_b$	725	0.81	0.95			
1HTS3								149	$> l_b$	725	0.81	0.87			
2HTS1				2	334			177	$> l_b$	850	0.69	0.89			
2HTS2								166	$> l_b$	850	0.69	0.84			
2HTS3								167	$> l_b$	850	0.69	0.84			
2HMS1			HM	2	820			161	$> l_b$	1315	0.45	0.58			
2HMS2								183	$> l_b$	1315	0.45	0.65			
2HMS3								164	$> l_b$	1315	0.45	0.59			
4HMS1								4	1640	180	$> l_b$	1970	0.30	0.41	
4HMS2										206	$> l_b$	1970	0.30	0.47	
4HMS3										188	$> l_b$	1970	0.30	0.43	
1HTSF			FEM	HT	1			167	164	$> l_b$	725	0.81	0.96		
2HTSF									180	$> l_b$	850	0.69	0.91		
2HMSF	HM	2		820	180	$> l_b$	1315	0.45	0.64						
4HMSF					182	$> l_b$	1970	0.30	0.41						

**Table 5.5(b)** The parameter and results of simulation specimens (FEM analysis) for with soft layer specimen

Series Spec.	Type of spec.	Test	CFRP plate			Bond. Length, $l_b$ (mm)	Poly. $t$ (mm)	$P_{max}$ (kN)	$l_e$ (mm)	$l_e$ plate (mm)	$l_b / l_e$ plate	$\alpha$	Note	
			type	$t$ (mm)	$E_p t_p$ (kN/mm)									
FEMS1	New spec.	FEM	HT	1	167	750	0.80	167	715	725	1.03	-		
FEMS2				2	334			190	$> l_b$	850	0.88	0.96		
FEMS3				3	501			240	$> l_b$	1050	0.71	1.00		
FEMS4				4	668			250	$> l_b$	1360	0.55	0.86		
FEMS5				1	167	2000		170	725	725	2.76	-		
FEMS6				2	334	2000		198	850	850	2.35	-		
FEMS7				3	501	2000		240	1050	1050	1.90	-		
FEMS8				4	668	2000		292	1360	1360	1.47	-		
FEMS9			1	167	1000	1.0	180	750	750	1.33	-			
FEMS10						0.8	171	725	725	1.38	-			
FEMS11						0.6	150	595	595	1.68	-			
FEMS12			HM	1640	2000	1	410	0.8	160	-	-	-	-	rupture
FEMS13						2	820		280	1315	1315	1.52	-	
FEMS14						3	1230		360	1650	1650	1.02	-	
FEMS15						4	1640		440	1970	1970	1.02	-	
FEMS16					4	1640	750	0.8	230	$> l_b$	1970	0.38	0.52	
FEMS17							1000		310	$> l_b$	1970	0.51	0.71	
FEMS18					2000	1640	1.0	490	$> l_b$	-	-	-		
FEMS19								0.6	390	1750	1750	1.14		

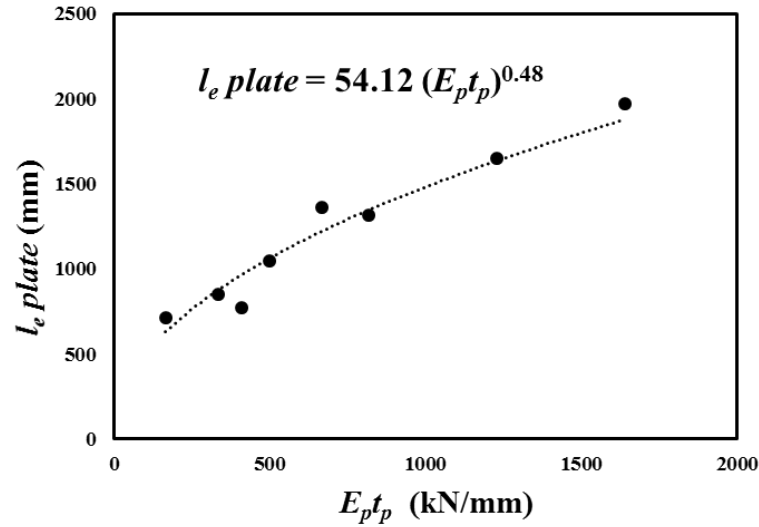


**Fig. 5.18**  $l_e \text{ plate}$  vs  $E_p t_p$

Next, the relationship between effective bonding length ( $l_e \text{ plate}$ ) and plate stiffness ( $E_p t_p$ ) for each specimen can be seen in **Fig. 5.18**. This relationship is for  $l/l_e \text{ plate} \geq 1$ . This figure shows that the  $l_e \text{ plate}$  increase with the  $E_p t_p$  increase. Based on this observation, the following relationship is proposed as,

$$l_e \text{ plate} = 54.12 (E_p t_p)^{0.48} \quad (5.6)$$

Where,

$l_e \text{ plate}$  = Effective bonding length of each plate stiffness (mm)

$E_p t_p$  = Plate stiffness (kN/mm)

A correlation coefficient,  $R^2$ , of 0.912 was obtained for this equation.

Furthermore, relationship between maximum load ( $P_{max}$ ) from specimens that have bonding length ( $l$ ) longer than  $l_e$  ( $l/l_e \text{ plate} \geq 1$ ) and plate stiffness ( $E_p t_p$ ) is shown in **Fig. 5.19**. The  $P_{max}$  increase as the  $E_p t_p$  increase and it can be seen that this relationship is similar to  $l_e \text{ plate}$  vs  $E_p t_p$  relationship. The relationship is proposed as,

$$\bar{P}_{max} = 21.93 (E_p t_p)^{0.39} \quad (5.7)$$

Where,

$\bar{P}_{max}$  = Maximum load of each effective bonding length related the plate stiffness (kN)

A correlation coefficient,  $R^2$ , of 0.969 was obtained for this equation.

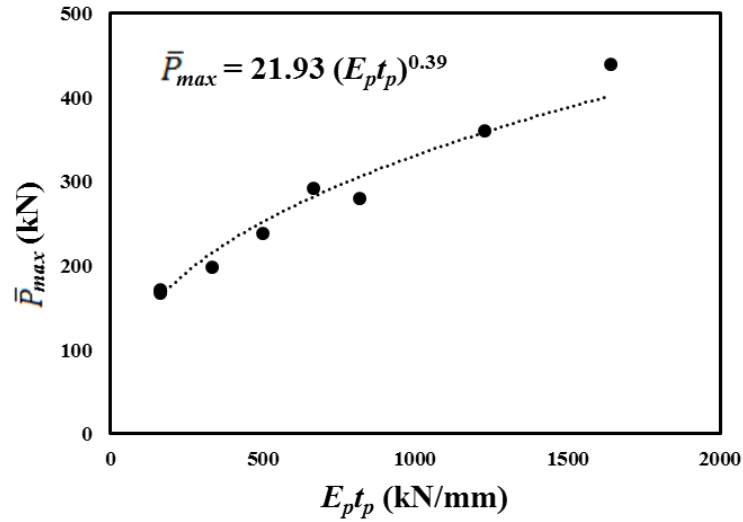


**Fig. 5.19**  $\bar{P}_{max}$  vs  $E_p t_p$

**Eq. (5.7)** can be used only for specimen that have bonding length longer than effective bonding length ( $l_b/l_{eplate} \geq 1$ ). Meanwhile, in order to be used for the specimens that have bonding length shorter than effective bonding length each of plate stiffness ( $l_b/l_{eplate} < 1$ ), a length factor is required. The length factor is namely as  $\alpha$ , is expressed as:

$$\alpha = \frac{P_{max} \text{ from specimens have } l/l_{eplate} < 1}{P_{max} \text{ from specimens have } l/l_{eplate} \geq 1}$$

**Fig. 5.20** shows a relationship between length factor and ratio of bonding length ( $l$ ) and effective bonding length ( $l_{eplate}$ ) on related plate stiffness. A correlation coefficient,  $R^2$ , of 0.952 was obtained for this equation. Then, **Eq. (5.7)** can be corrected to

$$P_{max} = \alpha 21.93 (E_p t_p)^{0.39} \quad (5.8)$$

Where,

$P_{max}$  = Maximum load (kN)

$\alpha$  =  $1.14 (l_b/l_{eplate})^{0.79} \leq 1$

$l_{eplate}$  =  $54.12 (E_p t_p)^{0.48}$  (mm)

$l_b$  = bonding length (mm)

$E_p t_p$  = plate stiffness (kN/mm)

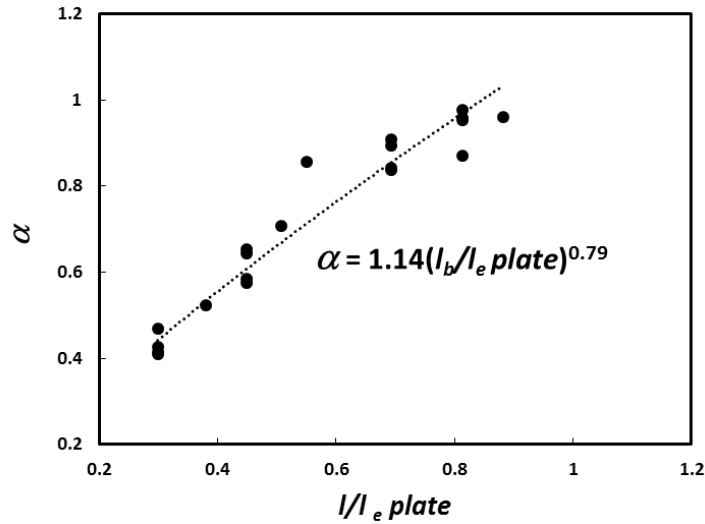


**Fig. 5.20**  $\alpha$  vs  $l_b/l_e \text{ plate}$

This proposed relationship (**Eq. (5.8)**) is to predict the maximum load for soft layer specimen ( $P_{max}$ ) with the compressive strength of the concrete is around 50MPa. The differences of concrete quality need to be considered because can produce different result (equation). The maximum load ( $P_{max}$ ) values as calculated by **Eq. (5.8)** and those measured in the experiments and FEM analysis for all specimen are compared in **Fig. 5.21**. It can be seen that a good agreement is shown graphically. The deviation of calculated results value from experimental and FEM analysis value vary from 0.11% to 13.32%. The average of the ratio is 1.01 with the coefficient of variation of 9.3%

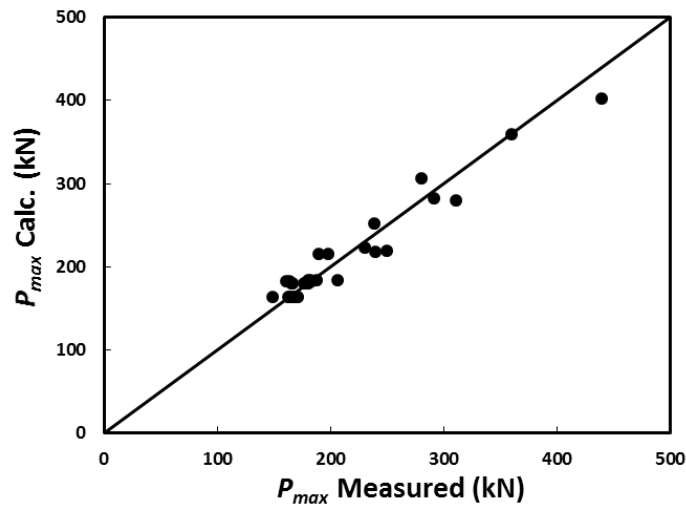


**Fig. 5.21** Calculated prediction vs Experimental and FEM analysis results for specimen with soft layer

**Table 5.6(a)** The parameter and results of laboratory specimen (experimental and FEM analysis) for without soft layer specimen

Series Spec.	Type of spec.	Test	CFRP plate			Bond. Length, $l_b$ (mm)	$P_{max}$ (kN)	$l_e$ (mm)	$l_e$ plate (mm)	$l_b / l_e$ plate	$\alpha$	Note		
			type	$t$ (mm)	$E_p t_p$ (kN/mm)									
1HTN1	Old spec.	Experimental	HT	1	167	590	59	200	240	2.46	-			
1HTN2							76	240	240	2.46	-			
1HTN3							57	220	240	2.46	-			
2HTN1				2	334		87	270	350	1.69	-			
2HTN2							98	320	350	1.69	-			
2HTN3							88	330	350	1.69	-			
2HMN1			HM	2	820		170	$> l_b$	710	0.83	0.89			
2HMN2							154	$> l_b$	710	0.83	0.81			
2HMN3							155	$> l_b$	710	0.83	0.82			
4HMN1							4	1640	215	$> l_b$	800	0.74	0.83	
4HMN2									215	$> l_b$	800	0.74	0.83	
4HMN3									229	$> l_b$	800	0.74	0.88	
1HTNF		FEM	HT	1	167	70	240	240	2.46	-				
2HTNF						95	350	350	1.69	-				
2HMNF			HM	2	820	162	$> l_b$	710	0.83	0.79				
4HMNF						220	$> l_b$	800	0.74	0.85				



**Table 5.6(b)** The parameter and results of simulation specimens (FEM analysis) for without soft layer specimen

Series Spec.	Type of spec.	Test	CFRP plate			Bond. Length, $l_b$ (mm)	$P_{max}$ (kN)	$l_e$ (mm)	$l_e$ plate (mm)	$l_b / l_e \text{ plate}$	$\alpha$	Note
			type	$t$ (mm)	$E_p t_p$ (kN/mm)							
FEMN1	New spec.	FEM	HT	1	167	1000	72	240	240	4.17	-	
FEMN2				2	334		95	325	325	3.08	-	
FEMN3				3	501		125	430	430	2.33	-	
FEMN4				4	668		145	550	550	1.82	-	
FEMN5			HT	200	1	167	55	$> l_b$	240	0.83	0.76	
FEMN6					2	334	57	$> l_b$	325	0.62	0.60	
FEMN7					3	501	60	$> l_b$	430	0.47	0.48	
FEMN8					4	668	65	$> l_b$	550	0.36	0.45	
FEMN9			HM	1500	1	410	120	420	420	3.57	-	
FEMN10					2	820	190	585	585	2.56	-	
FEMN11					3	1230	205	710	710	2.11	-	
FEMN12					4	1640	260	800	800	1.88	-	

#### 5.7.4.2 Specimen without polyurea soft layer

For the same purpose with the with soft layer specimen, there were 12 (twelve) new specimens of varying sized there were analyzed by FEM analysis comprises 8 for CFRP plate high tension type and 4 for CFRP high modulus type with the variation of CFRP plate stiffness ( $E_p t_p$ ), bonding length ( $l_b$ ) and polyurea thickness ( $t$ ) for soft layer specimen. Next, these new specimen results were combined with results from experiment. **Table 5.6(a)** and **Table 5.6(b)** show the parameter and the results of both the experiment and the FEM analysis.

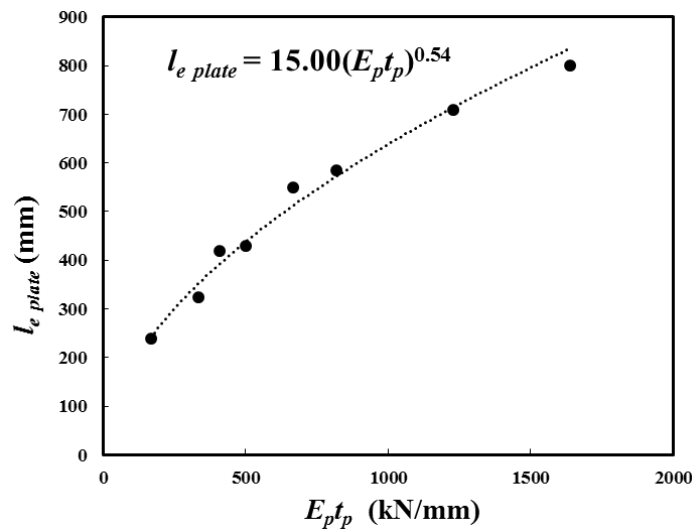


**Fig. 5.22**  $l_e \text{ plate}$  vs  $E_p t_p$

The relationship between effective bonding length ( $l_e \text{ plate}$ ) and plate stiffness ( $E_p t_p$ ) for each specimen can be seen in **Fig. 5.22**. This relationship is for  $l_b/l_e \text{ plate} \geq 1$ . This figure shows that the  $l_e \text{ plate}$  increase with the  $E_p t_p$  increase. Based on this observation the following relationship is proposed as,

$$l_e \text{ plate} = 15.00 (E_p t_p)^{0.54} \quad (5.9)$$

Where,

$l_e \text{ plate}$  = Effective bonding length of each plate stiffness (mm)

$E_p t_p$  = Plate stiffness (kN/mm)

A correlation coefficient,  $R^2$ , of 0.983 was obtained for this equation.

The relationship between maximum load ( $P_{max}$ ) from specimens that have bonding

length ( $l$ ) longer than  $l_e plate$  ( $l / l_e plate \geq 1$ ) and plate stiffness ( $E_p t_p$ ) is shown in **Fig. 5.23**. The  $P_{max}$  increase as the  $E_p t_p$  increase and it can be seen that this relationship is similar to  $l_e plate$  vs  $E_p t_p$  relationship. The relationship is proposed as

$$\bar{P}_{max} = 3.01 (E_p t_p)^{0.60} \quad (5.10)$$

Where,

$\bar{P}_{max}$  = Maximum load of each effective bonding length related the plate stiffness (kN)

A correlation coefficient,  $R^2$ , of 0.969 was obtained for this equation.

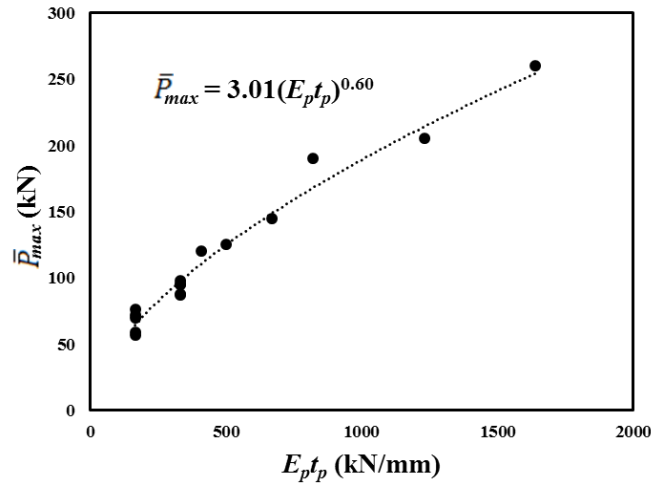


**Fig. 5.23**  $P_{max}$  VS  $E_p t_p$

The Eq. (5.10) can be used only for specimen that have bonding length ( $l$ ) longer than  $l_e plate$  ( $l / l_e plate \geq 1$ ). Then, the factor length ( $\alpha$ ) is needed make a correction for specimen that have bonding length shorter than effective bonding length. The  $\alpha$  is expressed as;

$$\alpha = \frac{P_{max, \text{from specimens have } l / l_e plate < 1}}{P_{max, \text{from specimens have } l / l_e plate \geq 1}}$$

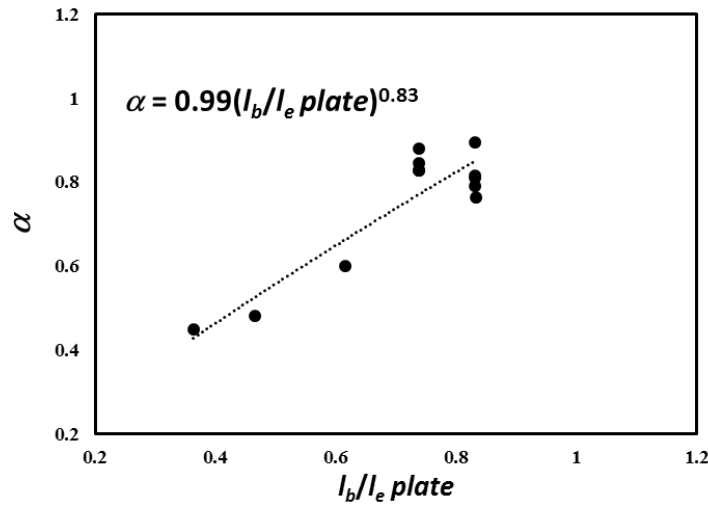


**Fig. 5.24**  $\alpha$  vs  $l_b/l_e$  plate

**Fig. 5.24** shows a relationship between length factor and ratio of bonding length ( $l_b$ ) and effective bonding length ( $l_e$  plate) on related plate stiffness. A correlation coefficient,  $R^2$ , of 0.868 was obtained for this equation. Then, the equation (5.10) can be corrected to,

$$P_{max} = \alpha 3.01 (E_p t_p)^{0.60} \quad (5.11)$$

Where,

$P_{max}$  = Maximum load (kN)

$\alpha = 0.99 (l/l_e \text{ plate})^{0.83} \leq 1$

$l_e \text{ plate} = 15.00 (E_p t_p)^{0.54}$  (mm)

$l_b$  = bonding length (mm)

$E_p t_p$  = plate stiffness (kN/mm)

This proposed relation (Equation (5.11)) is found to predict the maximum load ( $P_{max}$ ) for specimen without soft layer specimen, especially used epoxy as adhesive, with the compressive strength of the concrete is around 50MPa. The maximum load ( $P_{max}$ ) values as calculated by Equation (5.11) and those measured in the experiments and FEM analysis for all specimen are compared in **Fig. 5.25**. It can be seen that a good relationship is shown graphically. The deviation of calculated results value from experimental and FEM analysis value vary from 0.16% to 17.12%. The average of the ratio is 1.01 with the

coefficient of variation of 8.5%

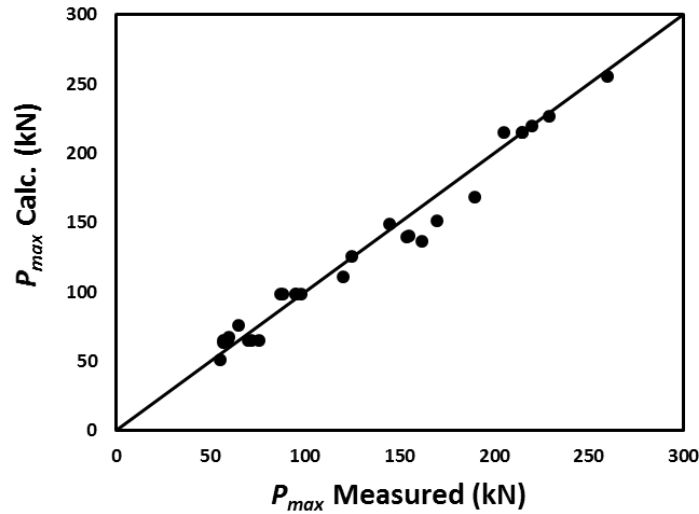


**Fig. 5.25** Calculated prediction vs Experimental and FEM analysis results for specimen without soft layer

## 5.8 Conclusive remarks

This chapter presented the result of polyurea soft layer effect from a testing program of 24 CFRP plate bonding test with a variety of parameter including type of the CFRP plate, thickness of CFRP plate with soft layer and without soft layer condition. Also, FEM analysis of the bonding tests has been described followed by verification study of a prediction method. The conclusion can be drawn up as follows;

1. Specimen with soft layer specimen is experienced fracture on the concrete or the concrete failure. In addition, the interfacial failure and the adhesive failure are dominant for specimen without soft layer.
2. The test results showed that comparison of specimen with and without soft layer in average of maximum load are 2.49, 1.87, 1.06 and 0.87 for 1HT, 2HT, 2HM and 4HM, respectively
3. From the experimental test result, the polyurea soft layer can enhance the performance of bonding behavior on the CFRP high tension type. However, polyurea soft layer does not give effect on the high modulus type.
4. From the bond stress-slip type of high tension type can be seen that soft layer makes a longer slip with a smaller bond stress than without soft layer specimen. Furthermore,

a long slip after the peak in the bond stress-slip curves indicates a ductile bond behavior of soft bond specimen.

5. It is clearly seen that on the soft layer specimens show an increase of interfacial fracture energy with decreasing the plate stiffness. The smaller the CFRP plate stiffness the more effective soft layer can increase the interfacial fracture energy.
6. It can be recommended that the use of soft layer is highly effective for the specimen that have bonding length longer than effective bonding length ( $l_b > l_e$ ). In the case of bonding length shorter or very short than effective bonding length ( $l_b < l_e$ ) produce an equal maximum load or, even, becomes smaller.
7. The results of the experiment can be simulated reasonably well by FEM analysis.
8. To predict the effective bond length of the specimen with soft layer, a proposed equation was found as follows;

$$l_e \text{ plate} = 54.12 (E_p t_p)^{0.48}$$

Then, the effective bond length of the specimen without soft layer can be written as;

$$l_e \text{ plate} = 15.00 (E_p t_p)^{0.54}$$

9. A proposed equation was found to predict the maximum load ( $P_{max}$ ) for specimen with polyurea soft layer, the proposed equation related with the plate stiffness as follows;

$$P_{max} = \alpha 21.93 (E_p t_p)^{0.39}$$

Then, proposed equation for specimen without soft layer can be written as;

$$P_{max} = \alpha 3.01 (E_p t_p)^{0.60}$$

## REFERENCES

- 5.1 Bahsuan R., Hino S., Ohgi T. and Komori A., “Effect of polyurea soft layer on the bonding performance between CFRP plate and concrete” Proc. of 11<sup>th</sup> German Japan Bridge Symposium, Osaka, Japan, Augt 2016
- 5.2 Lu X.Z., Ye L.P., Teng J.G., and Jiang J.J., “Meso-Scale Finite Element Model for FRP Sheets/Plates Bonded to Concrete” Engineering Structures 27, 564-575, 2004
- 5.3 Nakaba K., Kanakubo T., Furuta T. and Yoshizawa H., “Bond Behavior between Fiber-Reinforced Polymer Laminates and Concrete”, ACI Structural Journal, 98 (3): 359-367, 2001
- 5.4 Pelegrino C., and Modena C., “Bond-Slip Relationship between FRP Sheets and Concrete”, 4th International Conference on FRP Composite in Civil Engineering (CICE), 22 - 24 July 2008
- 5.5 Dai J. G., Ueda T., and Sato Y., “Development of the Nonlinear Bond Stress-Slip Model of Fiber Reinforced Plastics Sheet-Concrete Interface with a Simple Method”, Journal of Composite for Construction ASCE, 9 (1): 52-62, 2005
- 5.6 Zhou Y. W., Wu Y. F., and Yun Y. C., “Analytical Modelling of the Bond-Slip Relationship at FRP-Concrete Interfaces for Adhesively-Bonded Joint” Composite: Part B, 41: 423-433, 2010
- 5.7 Ko H., and Sato Y., “Bond Stress-Slip Relationship between FRP Sheet and Concrete under Cyclic Load” Journal of Composite for Construction ASCE, 11 (4): 419-426, 2007
- 5.8 Pham B. H., and Al-Mahaidi R., “Modelling of CFRP-Concrete Shear lap Test”, Construction and Building Materials (21): 727 – 735, 2007
- 5.9 Dai J.G. and Ueda T., “Local Bond Stress Slip Relations for FRP Sheets–Concrete Interface” in Proc. of 6th International Symposium on FRP Reinforcement for Concrete Structure , Singapore : World Scientific Publication; 143-52, 2003
- 5.10 Arazoe M., Kobayashi A., Takahashi Y. and Sato Y., “Bonding and Flexural Behaviors of RC Members with CFRP Strand Sheets–Polyurea Soft Layer Sysytem”, The 7th International Conference on FRP Composite in Civil Engineering (CICE), 22 - 24 August 2014, Vancouver, Canada

- 5.11 Japan Society of Civil Engineering (JSCE), “Standard Specification for Concrete and Structure, Test Method and Specification”, 2007
- 5.12 Dai J.G. and Ueda T., “Interface Bond between FRP Sheets and Concrete Substrate: Properties, Numerical Modelling and Roles in Member Behavior” Prog. Struct. Engng. Mater 7 : John Wiley and Sons, 27-43, 2005
- 5.13 Zhou Y., W., Wu Y., F., and Yun Y., “Analytical Modelling of the Bond-Slip Relationship at FRP-Concrete Interfaces for Adhesively-Bonded Joints” Composite: Part B 41: 423-433, 2010
- 5.14 Lu X.,Z., Teng J.G., Ye L. P. and Jiang J.J. “Bond Slip Models for FRP Sheets/Plates Bonded to Concrete” Engineering Structures 27: 920-937, 2005
- 5.15 Niu H. and Wu Z., “Effects of FRP-Concrete Interface Bond Properties on the Performance of RC Beams Strengthened in Flexure with Externally Bonded FRP Sheets” J. of Materials in Civil Engineering ASCE 18: 723-731, 2006
- 5.16 D. A. Hordijk DA, “ Local Approach to Fatigue Concrete” Delft University of Technology, (1991)
- 5.17 Comite Euro-International du Beton “CEB-FIB Model Code 1990” London, Great Britain, Thomas Telford (1991)
- 5.18 E. Thorenfeldt, A. Tomaszewics, and J. J. Jensen “Mechanical Properties of High-Strength Concrete and Application in Design” Porc. Symposium Utilization of High-Strength Concrete , Stavanger, Norway (1987)



## CHAPTER 6

### CONCLUSION AND RECOMMENDATION

---

#### 6.1 Conclusion

Among the issues that are to still to be taken up in strengthening method in RC members, some issues were address in this research in order to observe the effectiveness of CFRP strand sheet and CFRP plate to improve the bonding behaviour of CFRP strand sheet and CFRP plate strengthening method. Conclusion for each research is concluded in detail as follows.

In **Chapter 3**, the application of CFRP strand sheet strengthening method on the RC beams were examined. A wide variety of adhesive were used in this experiment. The strengthening of CFRP strand sheet used epoxy, MMA (methyl methacrylate) and PCM (polymer cement mortar). The dimensions of RC beams specimen was 200mm x 300mm x 2200mm. The results showed that the strengthening with CFRP strand sheet could improve the capacity of RC beam. The failure mode of specimen with CFRP strand sheet strengthening method was highly dependent with the type of adhesive. Epoxy resin, MMA resin and PCM can be used as adhesive to the CFRP strand sheet strengthening method on RC members. However, the application of PCM adhesive more than one layer of CFRP strand sheet is not recommended.

In **Chapter 4**, the investigation of CFRP strand sheet strengthening method was presented. The bonding test was done based on JSCE-E543-2007, in the size of 100mm x 100 x 620mm with two CFRP strand sheet were bonded on two opposite test (double lap shear pull out test) total bonding length of 280mm on the both sides. Also, this test used two kind of adhesive they are MMA (methyl methacrylate) and PCM (polymer cement mortar). The variation of layers of strand sheet also was considered. The specimen were one, two and three layers of CFRP strand sheet for specimen use MMA as adhesive and then, one and two layers for bonding specimen use PCM as adhesive. The results showed that the typical failure of bonding test was the interfacial bonding failure occurred on only

one side of the prism. From the interfacial fracture energy results showed that MMA and PCM are a fairly good adhesive for CFRP strand sheet strengthening method.

In **Chapter 5**, presentation bonding test of the application of the CFRP plate strengthening method was discussed. The section describe the effect of putting a polyurea soft layer between epoxy and concrete. The comparison of the bonding behavior of specimen with polyurea soft layer and without polyurea soft layer system for both high tension and high modulus type of CFRP plate has been presented. The bonding test was done based on JSCE-E543-2007. By considering a longer the effective bonding length and the limitation of equipment, the size of bonding test specimen was 150mm x 150mm x 1200mm. The specimen was divided into two equal section with the one section area clamped by plate steel. The test results showed that specimen with soft layer has different failure mode than without soft layer specimen. The polyurea soft layer can enhance significantly the performance of bonding behavior on the high modulus type of CFRP plate. However, polyurea soft layer does not give effect on the high modulus type. This is because specimen high modulus type of CFRP plate without soft layer specimen has effective bond length longer than bonding length of specimen itself. At the end of this section, the simple equation has been proposed. To get a complete information of the specimen with soft layer and without soft layer bonding behavior the FEM model was used.

## 6.2 Recommendation

In order to develop the CFRP strand sheet and CFRP plate strengthening, several recommendations are recommended as follows;

1. Regarding to the effective bond length of specimen with polyurea soft layer, it will be considered to use longer bonding test specimen.
2. Need to be considered in future bonding test to use specimen from different modulus elasticity or thickness of CFRP.
3. Important to note that the use of variety of the concrete quality is very influential in the application CFRP strengthening method.
4. In the future, in the application of soft layer need to focus on durability and cyclid load application or fatigue test.

5. Future investigation is necessary the actual test of RC beam or RC slab with the application of CFRP plate with the polyurea soft layer system.